

DRAFT REPORT
Load Distribution on Highway Bridges Based On
Field Test Data: Phase III

Principal investigator
M. AROCKIASAMY, Ph.D., P.E.
Professor and Director

Ahmed Amer, Ph.D., P.E.
Research Associate

Submitted to:
Florida Department of Transportation

under:
WPI No. 0510668, State Job No. 99700-3512-119
Contract No. BA489

Monitored by:
Structural Research Center
Florida Department of Transportation
2007 E. Paul Dirac Drive Tallahassee, FL 32304

Center for Infrastructure and Constructed Facilities
Department of Ocean Engineering
FLORIDA ATLANTIC UNIVERSITY
Boca Raton, Florida-33431

1. Report No.		2. Government Accession No.		3. Recipient's Catalog No.	
4. Title and Subtitle Load Distribution on Highway Bridges Based on Field Test Data : Phase III				5. Report Date July 1998	
				6. Performing Organization Code	
7. Authors M. Arockiasamy and Ahmed Amer				8. Performing Organization Report No.	
9. Performing Organization Name and Address Florida Atlantic University Center for Infrastructure and Constructed Facilities Department of Ocean Engineering Boca Ration, Florida 33731				10. Work Unit No.	
				11. Contract or Grant No. WPI 0510668	
12. Sponsoring Agency Name and Address Florida Department of Transportation 605 Suwannee Street Tallahassee, Florida 32399-0466				13. Type of Report and Period Covered Final Report	
				14. Sponsoring Agency Code 99700-3512-119, BA489	
15. Supplementary Notes Prepared in cooperation with the Federal Highway Administration					
16. Abstract <p>The studies on wheel load distribution are carried out in three phases. Studies in Phase I were focused on straight slab-on-girder, solid slab, voided slab and double Tee bridges. The existing analytical and field load distribution methods were reviewed for different bridge types. The grillage analogy concepts were presented together with the cross sectional properties of different bridge types for grillage analogy idealization, field test procedures and methodologies. Several parameters such as span length, bridge width, slab thickness, edge beam and number of lanes are considered in the parametric studies of solid and voided slab bridges. Hundred and sixty study cases were carried out to evaluate the various parameters affecting load distribution of slab-on-girder bridges. The load distribution factors from the analysis of double Tee simply supported bridges are compared with those based on the AASHTO and LRFD codes.</p> <p>The studies in Phase II were focused on wheel load distribution of the skew slab-on-girder and skew solid slab bridges. The various parameters affecting load distribution of skew simply supported slab-on-girder bridges were studied using finite element method and data from the field tests are used to verify the analytical results. Analytical and field studies on the wheel load distribution of skew simply supported solid slab bridges are presented and compared with those based on the AASHTO and LRFD codes. The finite element method and field test data were used to investigate the continuous skew and straight slab-on-I girder bridges and compute the corresponding wheel load distribution factors.</p> <p>The present studies in Phase III were mainly directed towards the analyses of comprehensive field test data, shear load distribution of continuous slab-on-girder bridges, and effects of diaphragms and shoulders on the wheel load distribution factors. The main parameters that affect shear load distribution are compared for single and multiple span bridges. The study on shear load distribution focuses on five main parameters: spacing between the girders, variation of skew angle, variation in the number of spans, ratio between adjacent two spans, and span length. The effect of diaphragms on wheel load distribution was first evaluated for a field test bridge and compared with a finite element model of the actual bridge. The diaphragm parameters that affect the wheel load distribution were studied to evaluate the effect of each parameter. The main conclusions based on the studies in Phases I, II and III are presented in this report.</p>					
17. Key Words wheel load distribution; effective width; skew bridges; continuous bridges; slab-on-girder; solid slab; slab-on-bulb-tee; finite element method; field test; LRFD code; diaphragms; shoulders				18. Distribution Statement No restrictions. This document is available to the public through the National Technical Information Service, Springfield, Virginia 22161	
19. Security Classif. (of this report) Unclassified		20. Security Classif. (of this page) Unclassified		21. No. of Pages 169	
				22. Price	

UNIT CONVERSION TABLE

To convert from	To	Multiply by
Inch	Centimeter	2.54
square inch	square centimeter	6.4516
Kip	kiloNewton (kN)	4.44747
kip/sq. in. (ksi)	kN/sq. m (kPa)	6,894.28
kip-foot	kN-meter	1.3556

DISCLAIMER

The opinions, findings and conclusions expressed in this publication are those of the authors who are responsible for the facts and accuracy of the data presented herein. The contents do not necessarily reflect the views or the policies of the Florida Department of Transportation or the Federal Highway Administration. This report does not constitute a standard, specification or regulation.

The report is prepared in cooperation with the Florida Department of Transportation and the Federal Highway Administration.

ACKNOWLEDGMENTS

The authors wish to express their sincere thanks to Dr. Mohsen A. Shahawy, Chief Structures Analyst, and Mr. Adnan, Research Engineer, Florida Department of Transportation, for their excellent suggestions, discussions and constructive criticisms throughout the project. They wish to express their appreciation to Dr. S. E. Dunn, Professor and Chairman, Department of Ocean Engineering, and Dr. J. Jurewicz, Dean, College of Engineering, Florida Atlantic University for their continued interest and encouragement.

The valuable assistance in the preparation of the report from Mr. Nathaniel Bell, Graduate Student, Florida Atlantic University, is gratefully acknowledged.

SUMMARY

The studies on wheel load distribution are carried out in three phases. Studies in Phase I was focused on straight slab-on-girder, solid slab, voided slab and double Tee bridges. The existing analytical and field load distribution methods were reviewed for different bridge types. The grillage analogy concepts were presented together with the cross sectional properties of different bridge types for grillage analogy idealization, field test procedures and methodologies. Several parameters such as, span length, bridge width, slab thickness, edge beam and number of lanes are considered in the parametric studies of solid and voided slab bridges. Hundred and sixty study cases were carried out to evaluate the various parameters affecting wheel load distribution of slab-on-girder bridges. The load distribution factors from the analysis of double Tee simply supported bridges are compared with those based on the AASHTO and LRFD codes.

The studies in Phase II were focused on wheel load distribution of the skew slab-on-girder and skew solid slab bridges. The various parameters affecting load distribution of skew simply supported slab-on-girder bridges were studied using finite element method and data from the field tests are used to verify the analytical results. Analytical and field studies on the wheel load distribution of skew simply supported solid slab bridges are presented and compared with those based on the AASHTO and LRFD codes. The finite element method

and field test data were used to investigate the continuous skew and straight slab-on-I girder bridges and compute the corresponding wheel load distribution factors.

The present studies in Phase III were mainly directed towards the analyses of comprehensive field test data, shear load distribution of continuous slab-on-girder bridges, and effects of diaphragms and shoulders on the wheel load distribution factors. The main parameters that affect shear load distribution are compared for single and multiple span bridges. The study on shear load distribution focuses on five main parameters: spacing between the girders, variation of skew angle, variation in the number of spans, ratio between adjacent two spans, and span length. The effect of diaphragms on wheel load distribution was first evaluated for a field test bridge and compared with a finite element model of the actual bridge. The diaphragm parameters that affect the wheel load distribution were studied to evaluate the effect of each parameter. The main conclusions based on the studies in Phases I, II and III are presented in this report.

TABLE OF CONTENTS

Acknowledgments	iii
Summary	iv
List of Figures	xi
List of Tables	xx

CHAPTER 1 INTRODUCTION

1.1 INTRODUCTION	1-1
1.2 OBJECTIVES AND SCOPE	1-3

CHAPTER 2 REVIEW OF WORK ON WHEEL LOAD DISTRIBUTION CARRIED OUT IN PHASES I AND II

2.1 INTRODUCTION	2-1
2.2 METHODS OF ANALYSIS.....	2-2
2.2.1 Grillage Analogy Method.....	2-2
2.2.2 Finite Element Method.....	2-3
2.3 LOAD DISTRIBUTION FACTORS BASED ON FIELD TESTS	2-5
2.3.1 Field Load Testing	2-5
2.3.2 Measured Distribution Factors	2-6
2.4 REVIEW ON LOAD DISTRIBUTION STUDIES IN PHASE I.....	2-11

2.4.1 Solid and Voided Slab Bridges.....	2-11
2.4.1.1 Solid slab bridges	2-11
2.4.1.2 Voided slab bridges	2-14
2.4.2 Slab-on-Girder Bridges	2-14
2.4.3 Double Tee Bridges	2-17
2.5 REVIEW ON LOAD DISTRIBUTION STUDIES IN PHASE II	2-20
2.5.1 Skew Slab-on-Girder bridges	2-20
2.5.2 Skew Solid Slab Bridges	2-24
2.5.3 Continuous Slab-on-Girder Bridges	2-25

CHAPTER 3 LOAD DISTRIBUTION FACTORS BASED ON

COMPREHENSIVE FIELD BRIDGE TESTING

3.1 INTRODUCTION	3-1
3.2 FIELD TESTS ON SKEW BRIDGES.....	3-2
3.2.1 Skew Slab-on-Girder Bridge (Bridge # 940115).....	3-2
3.2.2 Continuous skew slab-on-steel girder bridges #100477 and #100478	3-11

CHAPTER 4 SHEAR LOAD DISTRIBUTION OF CONTINUOUS SLAB-ON GIRDER

BRIDGES

4.1 INTRODUCTION	4-1
4.2 SHEAR LOAD DISTRIBUTION FACTORS.....	4-2
4.2.1 Finite Element Method.....	4-4

4.2.2 AASHTO and LRFD Shear Distribution Factors	4-5
4.3 PARAMETRIC STUDY	4-7
4.3.1 Introduction	4-7
4.3.2 Truck Load Position	4-11
4.3.3 Case Studies.....	4-13
4.3.3.1 Skew Angle	4-14
4.3.3.2 Number of spans	4-20
4.3.3.3 Number of Girders per Lane	4-28
4.3.3.4 Ratio of Adjacent Two Spans.....	4-33
4.3.3.5 Span Lengths	4-38
 CHAPTER 5 DIAPHRAGM AND SHOULDER EFFECTS ON WHEEL LOAD DISTRIBUTION	
5.1 INTRODUCTION	5-1
5.2 DIAPHRAGMS.....	5-1
5.2.1 FEM Modeling of Slab-on-Girder Bridge With and Without Diaphragms...	5-3
5.2.2 Diaphragm Parametric Study	5-4
5.3 SHOULDER EFFECT ON LOAD DISTRIBUTION.....	5-11
 CHAPTER 6 DISCUSSIONS ON WHEEL LOAD DISTRIBUTIONS OF SKEW SLAB- ON-I-GIRDER BRIDGES BASED ON FIELD TESTS AND BRIDGE RATING	
6.1 INTRODUCTION	6-1

6.2 SKEW SLAB-ON-I-GIRDER BRIDGE FIELD TESTS	6-2
6.3 FINITE ELEMENT ANALYSES OF SLAB-ON-I-GIRDER BRIDGES.....	6-8
6.4 LOAD DISTRIBUTION FACTORS OF SLAB-ON-I-GIRDER BRIDGES BASED ON STRAIN AND DEFLECTION MEASUREMENTS.....	6-9
6.5 FIELD TEST RESULTS AND DISCUSSIONS.....	6-11
6.6 SLAB-ON-I-GIRDER BRIDGE RATING BASED ON DIFFERENT WIMEL LOAD DISTRIBUTION FACTORS.....	6-16
 CHAPTER 7 SUMMASUMMARY AND CONCLUSIONS	
7.1 SUMMARY	7-1
7.2 CONCLUSIONS	7-2
7.2.1 Straight Solid and Voided Slab Bridges.....	7-2
7.2.2 Straight Slab-on-Girder Bridges	7-4
7.2.3 Straight Double-Tee Bridges	7-5
7.2.4 Skew Solid Slab Bridges.....	7-6
7.2.5 Skew Slab-on-Girder Bridges.....	7-7
7.2.6 Continuous Slab-on-Girder Bridges.....	7-8
7.2.6.1 Parametric Study on Flexural Load Distribution Factors	7-9
7.2.6.2 Parametric Study on Shear Load Distribution Factors.....	7-9
7.2.7 Diaphragm and Shoulder Effects on Wheel Load Distribution	7-11
7.2.7.1 Diaphragms.....	7-11
7.2.7.2 Shoulder.....	7-12
7.2.8 Field Tests.....	7-13

7.2.9 Comments on the Load Distribution Factors Based on Measured Strains.... 7-14

REFERENCES R-1

LIST OF FIGURES

Fig. 2.1	Grillage idealization of slab element	2-3
Fig. 2.2	Details of finite element model.....	2-5
Fig. 2.3	Typical FDOT test vehicle.....	2-8
Fig. 2.4	Typical truck loads for spans larger than 55 ft.....	2-9
Fig. 2.5	Typical truck loads for spans less than 55 ft.....	2-10
Fig. 2.6	Effective width variations for different edge beam depths	2-13
Fig. 2.7	Effective width variation based on the grillage analogy and the proposed formula	2-13
Fig. 2.8	Effect of girder spacing variations on load distribution of slab-on-girder bridges.....	2-16
Fig. 2.9	Longitudinal stiffness parameter, K_g effect on load distribution based on grillage analogy, AASHTO and LRFD codes (interior girders)	2-16
Fig 2.10	Span length variation effect on load distribution based on grillage analogy, AASHTO and LRFD codes (interior girders).....	2-18
Fig 2.11	Shear load distribution simplified formula (interior girder)	2-19
Fig 2.12	Shear load distribution simplified formula (exterior girder).....	2-19
Fig. 2.13	Load distribution factor variation with skew angle for slab-on-girder bridges (interior girders)	2-22

Fig. 2.14	Load distribution factor variation with girder spacing for slab-on-girder bridges (interior girders)	2-23
Fig. 2.15	Load distribution factor variation with thickness for slab-on-girder bridges (interior girders)	2-23
Fig. 2.16	Effective width variation with skew angle for solid slab bridges	2-25
Fig. 2.17	Strain distribution at midspan for two span bridges with different.....	2-27
Fig. 3.1	Over view of bridge # 940115	3-1
Fig. 3.2	Plan view of bridge # 940115	3-5
Fig 3.3	Cross section of bridge #940115.....	3-6
Fig 3.4	Longitudinal View of Bridge #940115.	3-6
Fig 3.5	Load position for bridge #940115	3-7
Fig 3.6	FDOT test vehicles on bridge #940115	3-7
Fig 3.7	Location of strain and deflection gauges for bridge #940115.....	3-8
Figs 3.8	Measured and FEM strains for St. Lucie County Bridge #940115.....	3-10
Fig. 3.9	Bridge # 100477 (Southbound 1-75 over U.S. 301)	3-13
Fig 3.10	Longitudinal <i>view</i> of bridge #100477	3-13
Fig. 3.11	Bridge # 100478 (Northbound 1-75 over U.S. 301)	3-14
Fig 3.12	Longitudinal view of bridge #100477	3-14
Fig. 3.13	<i>Plan</i> view of bridge # 100477	3-16
Fig 3.14	Cross section of bridge #100477.....	3-16
Fig 3.15	Typical built-up steel plate girder in bridge #100477.....	3-17
Fig. 3.16	Finite element model of bridge # 100477	3-18
Fig 3.17	Test truck positions and strain gage locations for positive moment	3-19

Fig 3.18	Test truck positions and strain gage locations for negative moment...	3-19
Fig 3.19	Transverse strain distribution at mid-span for trucks positioned at maximum positive moment location.	3-20
Fig 3.20	Transverse strain distribution over the support for trucks positioned at maximum positive moment location..	3-20
Fig. 3.21	Transverse strain distribution at mid-span for trucks positioned at negative moment location.....	3-21
Fig. 3.22	Transverse strain distribution over the support for trucks at negative moment location.....	3-21
Fig 4.1	Typical continuous slab-on-girder bridge	4-8
Fig. 4.2	AASHTO type IV girder details	4-9
Fig. 4.3	Typical FEM model for shear load distribution parametric study	4-10
Fig. 4.4	Truck loading positions in the transverse direction for interior and exterior girders.....	4-12
Fig 4.5	Shear distributions at exterior support for different skew angles (Interior Girder Loading).....	4-16
Fig. 4.6	Shear load distribution factors for different skew angles close to the exterior support (interior girder).....	4-16
Fig 4.7	Shear distributions at interior support for different skew angles (interior girder loading)	4-17
Fig. 4.8	Shear load distribution factors for different skew angles close to the interior support (interior girder).....	4-17

Fig 4.9	Shear distributions at exterior support for different skew angles (exterior girder loading)	4-18
Fig. 4.10	Shear load distribution factors for different skew angles close to the exterior support (exterior girder)	4-18
Fig 4.11	Shear distributions at interior support for different skew angles (exterior girder loading).....	4-19
Fig. 4.12	Shear load distribution factors for different skew angles close to the interior support (exterior girder).....	4-19
Fig. 4.13	Shear distributions at exterior support for straight bridges with different number of spans (interior girder loading)	4-22
Fig. 4.14	Shear load distribution factors at exterior support for straight bridges with different number of spans (interior girder).....	4-22
Fig. 4.15	Shear distributions at interior support for straight bridges with different number of spans (interior girder loading)	4-23
Fig. 4.16	Shear load distribution factors at interior support for straight bridges with different number of spans (interior girder).....	4-23
Fig. 4.17	Shear distributions at exterior support for straight bridges with different number of spans (exterior girder loading).....	4-24
Fig. 4.18	Shear load distribution factors at exterior support for straight bridges with different number of spans (exterior girder)	4-24
Fig. 4.19	Shear distributions at interior support for straight bridges with different number of spans (exterior girder loading).....	4-25

Fig. 4.20	Shear load distribution factors at interior support for straight bridges with different number of spans (exterior girder)	4-25
Fig. 4.21	Shear distributions at interior support for skew bridges with different number of spans (interior girder loading)	4-26
Fig. 4.22	Shear load distribution factors at interior support for skew bridges with different number of spans (interior girder)	4-26
Fig. 4.23	Shear distributions at interior support for skew bridges with different number of spans (exterior girder loading).....	4-27
Fig. 4.24	Shear load distribution, factors at interior support for skew bridges with different number of spans (exterior girder)	4-27
Fig. 4.25	Shear distributions at interior support for straight bridges with different girder spacing (interior girder loading).....	4-29
Fig. 4.26	Shear load distribution factors at interior support for straight bridges with different girder spacing (interior girder loading)	4-29
Fig. 4.27	Shear distributions at interior support for straight bridges with different girder spacing (exterior girder loading).....	4-30
Fig. 4.28	Shear load distribution factors at interior support for straight bridges with different girder spacing (exterior girder loading)	4-30
Fig. 4.29	Shear distributions at interior support for skew bridges with different girder spacing (interior girder loading)	4-31
Fig. 4.30	Shear load distribution factors at interior support for skew bridges with different girder spacing (interior girder loading)	4-31

Fig. 4.31	Shear distributions at interior support for skew bridges with different girder spacing (exterior girder loading)	4-32
Fig. 4.32	Shear load distribution factors at interior support for skew bridges with different girder spacing (exterior girder loading)	4-32
Fig. 4.33	Shear distributions at interior support for straight bridges with different span ratios (interior girder)	4-34
Fig. 4.34	Shear load distribution factors close to the interior support for straight bridges with different span ratios (interior girder)	4-34
Fig. 4.35	Shear' distributions at interior support for straight bridges with different span ratios (exterior girder)	4-35
Fig. 4.36	Shear load distribution factors at interior support for straight bridges with different span ratios (exterior girder)	4-35
Fig. 4.37	Shear distributions at interior support for skew bridges with different span ratios (interior girder).....	4-36
Fig. 4.38	Shear load distribution factors at interior support for skew bridges with different span ratios (interior girder)	4-36
Fig. 4.39	Shear distributions at interior support for skew bridges with different span ratios (exterior girder)	4-37
Fig. 4.40	Shear load distribution factors at interior support for skew bridges with different span ratios (exterior girder)	4-37
Fig. 4.41	Shear distributions at interior support for straight bridges with different span lengths (interior girder).....	4-39

Fig. 4.42	Shear load distribution factors at interior support for straight bridges with different span lengths (interior girder).....	4-39
Fig. 4.43	Shear distributions at interior support for straight bridges with different span lengths (exterior girder)	4-40
Fig. 4.44	Shear load distribution factors at interior support for straight bridges with different span lengths (exterior girder)	4-40
Fig. 4.45	Shear distributions at interior support for skew bridges with different span lengths (interior girder).....	4-41
Fig. 4.46	Shear load distribution factors at interior support for skew bridges with different span lengths (interior girder)	4-40
Fig. 4.47	Shear distributions at interior support for skew bridges with different span lengths (exterior girder)	4-42
Fig. 4.48	Shear load distribution factors at interior support for skew bridges with different span lengths (exterior girder)	4-42
Fig 5.1	Transverse strain distributions at mid-span of straight bridges with different location of diaphragms (interior girder loading)	5-7
Fig 5.2	Load distribution factors at mid-span of straight bridges with different location of diaphragms (interior girders)	5-7
Fig 5.3	Transverse strain distributions at mid-span of straight bridges with different location of diaphragms (exterior girder loading).....	5-8
Fig 5.4	Load distribution factors at mid-span of straight bridges with different location of diaphragms (exterior girders)	5-8

Fig 5.5	Transverse strain distributions at mid-span of skew bridges with different location of diaphragms (interior girder loading)	5-9
Fig 5.6	Load distribution factors at mid-span of skew bridges with different location of diaphragms (interior girders)	5-9
Fig 5.7	Transverse strain distribution at mid-span of skew bridges with different location of diaphragms (exterior girder Loading)	5-10
Fig 5.8	Load distribution factors at mid-span of skew bridges with different location of diaphragms (exterior girders)	5-10
Fig 5.9	Typical slab-on-girder bridges: (a) without shoulder: (b) with one shoulder and (c) with two shoulders	5-12
Fig. 5.10	Transverse strain distributions at mid-span for bridge with both traffic lanes loaded (no shoulders)	5-14
Fig. 5.11	Transverse strain distributions at mid-span for bridge with both traffic lanes loaded (one shoulder).....	5-15
Fig. 5.12	Transverse strain distributions at mid-span for bridge with both traffic lanes and shoulder loaded (one shoulder) ..	5-16
Fig. 5.13	Transverse strain distribution at mid-span for bridge with both traffic lanes loaded (two shoulders)	5-16
Fig. 5.14	Transverse strain distribution at mid-span for bridge with both traffic lanes and shoulders loaded (two shoulders)	5-17
Fig. 6.1	Details of bridge - field test # 1.....	6-5
Fig. 6.2	Details of bridge - field test # 2.....	6-6
Fig. 6.3	Details of bridge - field test # 3	6-7

Fig. 6.4	Details of bridge - field test # 4	6-8
Fig. 6.5	Transverse strain variations (field test # 1).....	6-13
Fig. 6.6	Transverse strain variations (field test # 2).....	6-13
Fig. -6.7	Transverse deflection variations (field test # 3)	6-14
Fig. 6.8	Transverse strain variations (one truck)(field test # 4).....	6-14

LIST OF TABLES

Table 3.1	Deflection measurements for various loads (bridge #940115).....	3-8
Table 3.2	Material and sectional properties for bridge #940115	3-9
Table 3.3	FEM deflections for various loads (Bridge #940115)	3-9
Table 3.4	Measured and FEM strains for St. Lucie County Bridge #940115	3-10
Table 3.5	Summary of Bridge #940115 load distribution factors (Interior Girders)	3-11
Table 3.6	Material and sectional properties for bridges	3-15
Table 3.7	Load distribution factors for bridge #100477.....	3-22
Table 4.1	Material and sectional properties for typical continuous slab-on-girder bridge	4-8
Table 4.2	Summary of parametric studies for shear load distribution on continuous slab-on-girder bridges.....	4-14
Table 5.1	Summary of parametric studies for diaphragms.....	5-5
Table 5.2	Load distribution factors for bridges with or without shoulders.....	5-14
Table 6.1	Skew slab-on-I girder bridge field tests	6-2
Table 6.2	Truck Wheel Loads for the Skew Bridge Field Tests	6-4
Table 6.3	Summary of load distribution factors (interior girders)	6-15
Table 6.4	Summary of slab-on-I-girder bridge rating factors.....	6-18

CHAPTER 1

INTRODUCTION

1.1 INTRODUCTION

Analysis of the highway bridges to vehicular live loads is the key element in designing new bridges and evaluating existing bridges for their load-carrying capacities. The American Association of State Highways and Transportation Officials (AASHTO) method of load distribution reduces the complex analysis of a bridge subjected to one or more vehicles to simple analysis of a beam. According to the AASHTO method, the maximum load effects in a girder can be obtained by treating a girder as a one dimensional beam subject to a loading, which is obtained by multiplying one line of wheels of the design vehicle by a load fraction (Wheel Load Distribution Factor). The AASHTO load distribution factor is defined as S/D , where D is a constant and has the units of length and S is the girder spacing. The constant D is given by the AASHTO specifications for different bridge types.

Recent research has produced a substantial amount of information on various bridge types indicating a need for revisions of the AASHTO bridge specifications. The conservative load distribution factors may be acceptable for the design of new bridges, but are unacceptable for reviewing existing bridges. The conservative load distribution factors, that are used to evaluate an old bridge, may give the impression that the bridge is unsafe, while the bridge may be safe, if more accurate distribution factors are used. The science of bridge analysis and design has undergone major changes

and a number of available powerful analytical tools include: i) the grillage analogy method, ii) the orthotropic plate method, iii) the articulated plate method, and iv) the finite element method including finite strip formulation. The results from the refined methods of analysis could be used to improve the existing simplified approaches.

NCHRP project 12-26 (1992) was initiated to develop comprehensive specification provisions for distribution of wheel loads in highway bridges. The formulae developed in the NCHRP research project form the basis for the current LRFD bridge design specifications and commentary. Interest in the field load testing of highway bridges has increased significantly in recent years. The increased interest has resulted in part from large number of older bridges across the country with posted load limits that are below the normal legal truck weights. Field load testing frequently offers a means of illustrating that the safe load capacity of a bridge, or bridge rating, is greater than the capacity determined from standard rating calculations based on the AASHTO method.

The studies carried out in Phase I (Arockiasamy and Amer, 1995) present the load distribution on certain bridge types viz., straight slab-on-girder, solid slab, voided slab and doubletee bridges. The existing analytical and field load distribution methods for different bridge types are reviewed in this study. Grillage analogy was used as an analytical tool to study the various parameters affecting wheel-load distribution. The results from the analytical studies are compared with those based on the field test data.

The primary aim of the studies in Phase II (Arockiasamy and Amer, 1997) was to investigate the wheel load distribution of different bridge types - solid slab bridges and slab-on-girder bridges with varying skew angles and multiple continuous spans. The study reviewed the existing analytical and field load distribution methods for different bridge types. Finite element method was used to carry out the detailed analyses to study the various parameters affecting wheel load distribution. The data from field tests were collected and analyzed to evaluate the LRFD specifications and the results from the finite element method.

1.2 OBJECTIVES AND SCOPE

The objectives of the research in Phase III are the following:

- i) Evaluation of load distribution factors of typical bridges based on comprehensive field testing.
- ii) Determination of shear load distribution factors of continuous straight and skew slab-on-girder-bridges.
- iii) Investigation of the effects of diaphragms and shoulders on the wheel load distribution factors.
- iv) Evaluation of methods for determining the load distribution factors based on measured strains and deflections.

Chapter 2 reviews the work carried out in Phases I and II on wheel load distribution factors for different bridge types. Chapter 3 presents comprehensive field tests of skew slab-on-girder and

continuous skew slab-on-steel-girder bridges. Chapter 4 summarizes the results of the finite element method for shear load distribution of skew single and multiple span slab-on-girder bridges. Chapter 5 presents the studies on the effects of diaphragms and shoulders on the wheel load distribution of simply supported slab-on-girder bridges. The discussions on wheel load distribution of skew slab-on-girder bridges based on field tests and bridge rating are presented in Chapter 6. The summary and conclusions of the work carried out in Phases I, II,

CHAPTER 2
REVIEW OF WORK ON WHEEL LOAD DISTRIBUTION
CARRIED OUT IN PHASES I AND II

2.1 INTRODUCTION

This chapter presents the summary of the wheel load distribution studies carried out in Phases I and II [Arockiasamy and Amer, 1995 and 1997]. This summary will include the grillage analogy and the finite element methods used in these investigations, the parametric studies and comparisons with the field test data. The analyses of the bridges, which have been subjected to field load -testing as well as the parametric studies carried out in Phase III are based on the finite element method.

The studies in Phase I are focused on the wheel load distribution on the more commonly used bridge types in Florida viz., slab-on-girder, solid slab, voided slab and double Tee bridges. The existing analytical and field load distribution methods for different bridge types are reviewed and grillage analogy used as an analytical tool to study the various parameters affecting wheel load distribution.

The primary aim of the studies in Phase II was to investigate the wheel load distribution of different skew and continuous bridges. The study reviewed the existing analytical and field load distribution methods for skew and continuous bridges. Finite

element method was used to carry out the detailed analyses to study the various parameters affecting wheel load distribution. The data from field tests were collected and analyzed to evaluate the AASHTO and LRFD specifications and the results from the finite element method.

2.2 METHODS OF ANALYSIS

2.2.1 Grillage Analogy Method

The grillage analogy is essentially an assembly of one-dimensional beams subjected to loads acting in the direction perpendicular to the plane of the assembly. The deformation characteristics of a rectangular element of an isotropic plate subjected to out of--plane load can be represented by an equivalent frame work model with a distribution of stiffness that represents, as accurately as possible the properties of the real structure. The rectangular model consists of an assembly of four side and two diagonal beams. This idealization is shown in Fig. 2.1 and the expressions for the properties of the various beams are as follows:

$$\begin{aligned}
 I_x &= \left(L_y - \frac{\nu L_x^2}{L_y} \right) \frac{t^3}{24(1-\nu^2)} \\
 I_y &= \left(L_x - \frac{\nu L_y^2}{L_x} \right) \frac{t^3}{24(1-\nu^2)} \\
 J_x &= \left(\frac{EL_y(1-3\nu)}{G} \right) \frac{t^3}{24(1-\nu^2)} \\
 J_y &= \left(\frac{EL_x(1-3\nu)}{G} \right) \frac{t^3}{24(1-\nu^2)}
 \end{aligned} \tag{2.1}$$

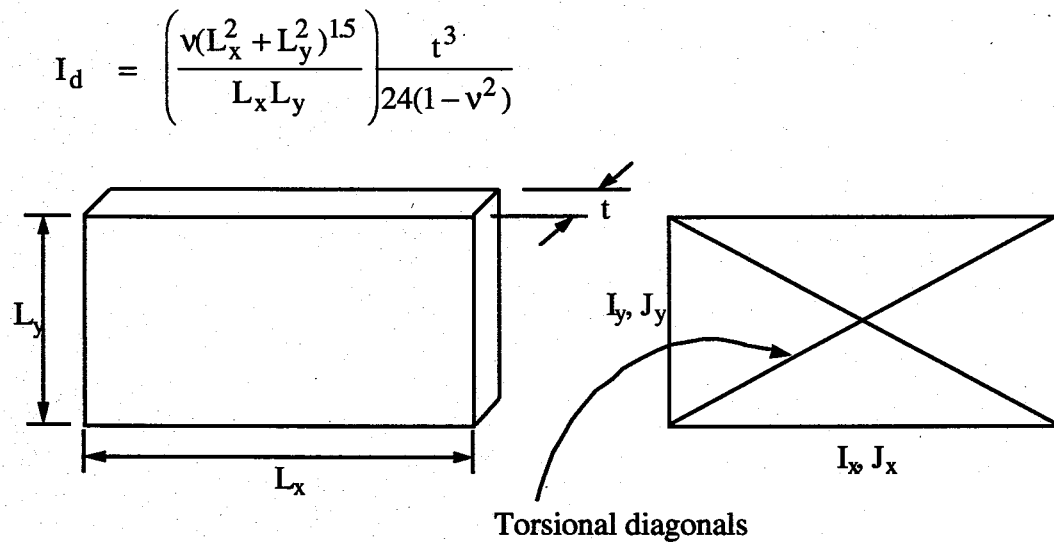


Figure 2.1 Grillage idealization of slab element

where I and J refer to the second moment of area and torsional inertia respectively, and v is the Poisson's ratio of the material of the plate. By making the Poisson's ratio zero, the diagonal beams can be eliminated, and the grillage reduced to an orthogonal assembly of beams. The expressions for various beam properties appropriate to the different types of bridge girders, corresponding to zero Poisson's ratio are given in Chapter 3, Phase I Final Report [Arockiasamy and Amer, 1995]. The matrix displacement method is used in the analysis of the bridge structure idealized with longitudinal and transverse beams.

2.2.2 Finite Element Method

The finite element method is more versatile and flexible for the analyses of highly skewed bridges (bridge skew $> 45^\circ$). In this study (Phases II and III), the bridge is modeled as a three dimensional system using a generalized discretization scheme using ANSYS 5.2 finite element program. The shell elements coupling bending with

membrane action were used to model the bridge deck / slab. Also, beam elements were used to model the top or bottom flanges of the girder.

Linear elastic material properties are used in the modeling. The reinforced concrete slab is modeled using an 8 or 4 node shell element. Each I-girder is divided into three parts: the two flanges and the web. Each flange was modeled by a beam element with its properties lumped at the centroid of the flange. The web was modeled by shell elements with four or eight mid-surface nodes. Each mid-surface node has six degrees of freedom. To satisfy the compatibility of composite behavior, a rigid element was assumed between the top beam elements and the centroids of the top deck slab shell elements (Fig.2.2). Each bearing support was assumed to be located at the centroid of the beam element representing the bottom flange of the girder. Under linear elastic conditions, strains are proportional to the bending moments in the girders. Hence, maximum strains at the extreme fiber of the bottom flanges obtained from finite element results were used to compute the wheel load distribution factors of the girders, which are compared with those based on the AASHTO and LRFD specifications.

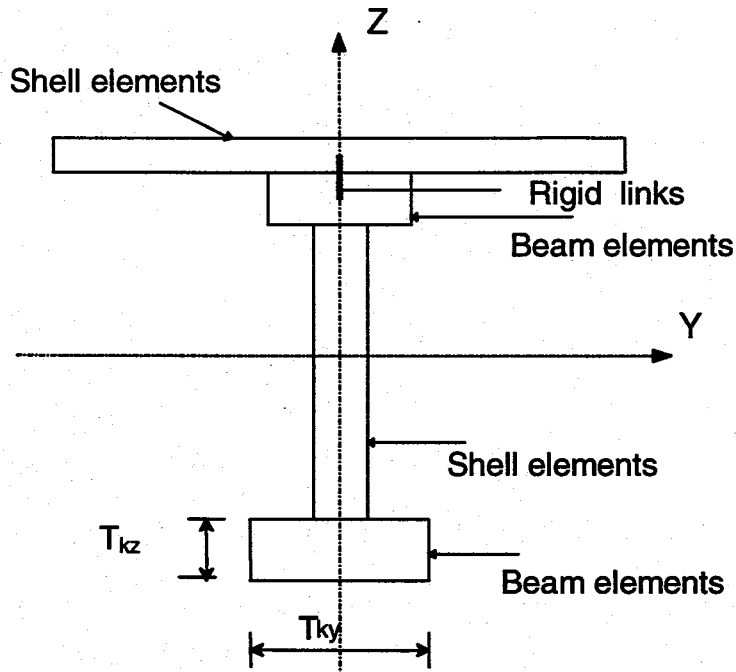


Fig. 2.2 Details of finite element model

2.3 LOAD DISTRIBUTION FACTORS BASED ON FIELD TESTS

2.3.1 Field Load Testing

Field load testing frequently offers a means of determining the load capacity of a bridge. The strength of a bridge can also be determined from standard rating calculation based on the AASHTO and LRFD methods. In some cases, the field tests indicate a higher load capacity since the AASHTO wheel load distribution factors tend to overestimate the loads carried by the individual girders. Florida Department of Transportation (FDOT) have been testing many bridges to check the strengths and establish bridge ratings. The strength of bridge elements is generally determined by first placing strain or deflection transducer gages at the bridge critical locations along the elements, and then incrementally loading

them to induce maximum effects. The data collected can then be analyzed and used to establish the strength of each component as well as the load distribution factors.

The FDOT's bridge load testing system consists of test vehicles and a mobile data acquisition system. Each test vehicle is a specially designed tractor-trailer combination, weighing in excess of 200 kips when fully loaded with concrete blocks. Detailed dimensions of the test vehicles are shown in Figure 2.3. Each vehicle can carry a maximum of 72 concrete blocks, each weighing approximately 2,150 pounds. Incremental loading is achieved by adding blocks with a self-contained hydraulic crane mounted on each truck. Figs. 2.4 and 2.5 show the wheel loads for each load increment.

Data from some bridge testing reports were used for load distribution analyses in Phases I and II. The typical report contains transverse strain distributions in the maximum bending moment section for several loading stages. The report also contains the applied moment vs. strain curves for several loading stages.

2.3.2 Measured Distribution Factors

This measured wheel load distribution factor can be used in bridge rating calculations in place of wheel load distribution defined by the AASHTO. The AASHTO (Guide specifications 1989) has also presented a refined bridge rating methodology in which measured wheel load distribution factors can be used. A load distribution factor may be calculated from the strains of each girder determined from the finite element analyses or field tests. The distribution factor, DF is equal to the ratio of maximum girder

bending moment obtained from the finite element method or field test to the total bending moment in the bridge idealized as a one-dimensional beam subjected to one set of wheels." The sum of internal bending moments is equivalent to externally applied bending, moments due to the wheel loads for a straight bridge. Assuming all traffic lanes are; loaded with equal-weight trucks, the wheel load distribution factor for the i th girder in a straight bridge is calculated from the strains as follows (Stalling and Yoo 1993):

$$DF_i = \frac{n\varepsilon_i}{\sum_{j=1 \rightarrow k} \varepsilon_j W_j} \quad (2.2)$$

where

ε_i = the bottom flange strain at the i th girder

W_j = ratio of the section modulus of the j th girder to the section modulus of a typical interior girder

n = number of wheel lines of applied loading

Eqn. 2.2 is based on the assumption that the sum of the internal moments or the total area under the moment distribution curve should be equal to the externally applied moment. However, this assumption is not realistic to yield the actual moment distribution in skew bridges. The sum of the girder strains in a straight bridge will be used to take into account the total external load effects in skew bridges. Eq. 2.2 can, therefore, be modified as follows:

$$DF_{i\theta} = \frac{n\varepsilon_{i\theta}}{\left(\sum_{j=1 \rightarrow k} \varepsilon_j W_j\right)_{\theta=0}} \quad (2.3)$$

where $\varepsilon_{i\theta}$ = the bottom flange strain at the i th girder of the skew bridge

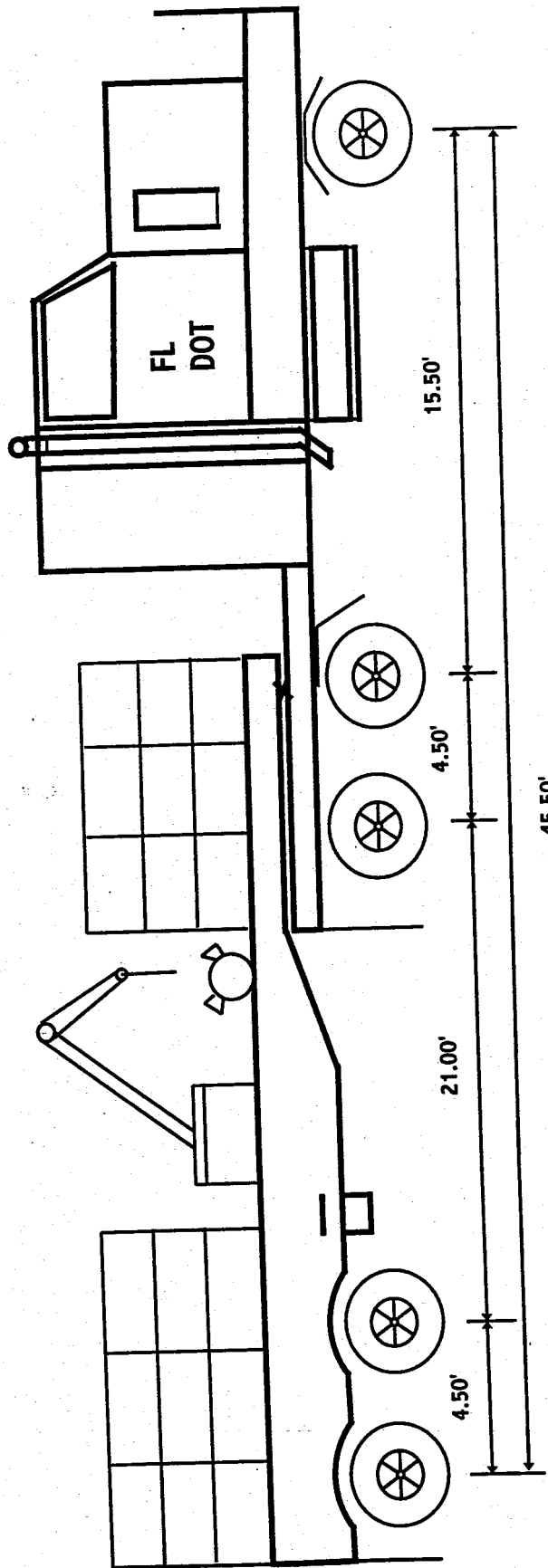
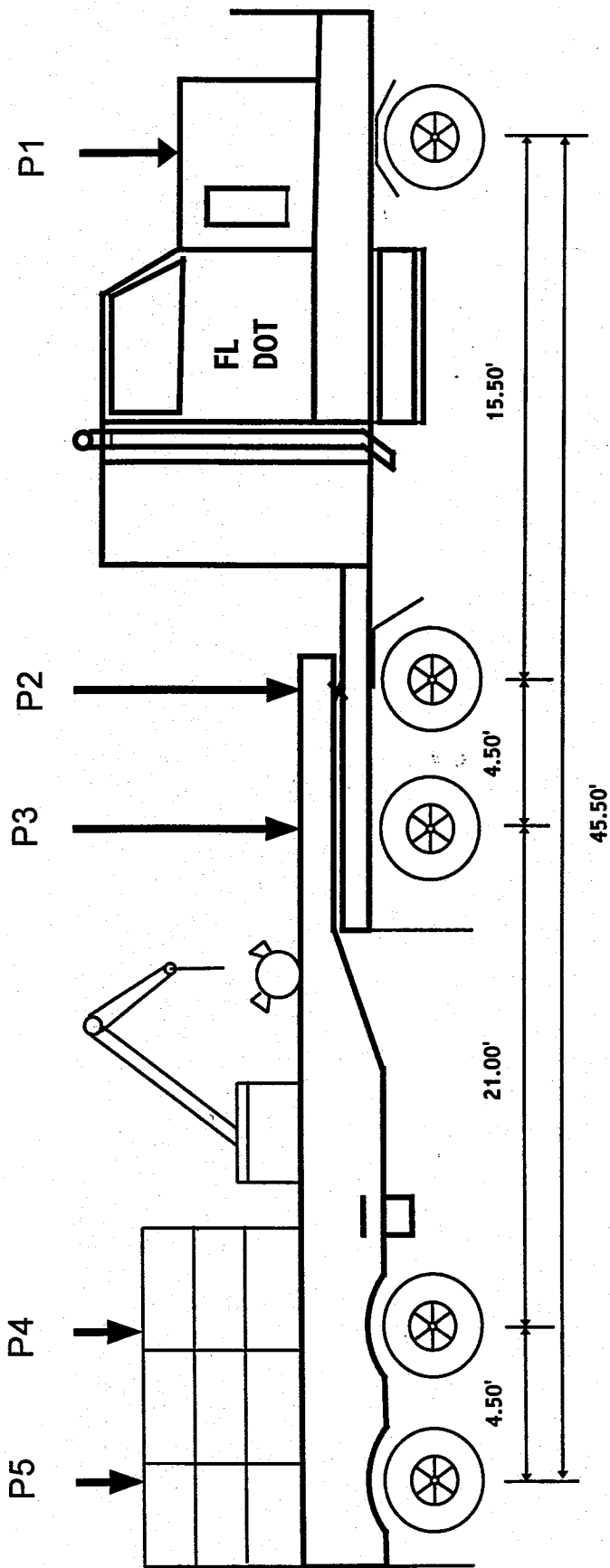
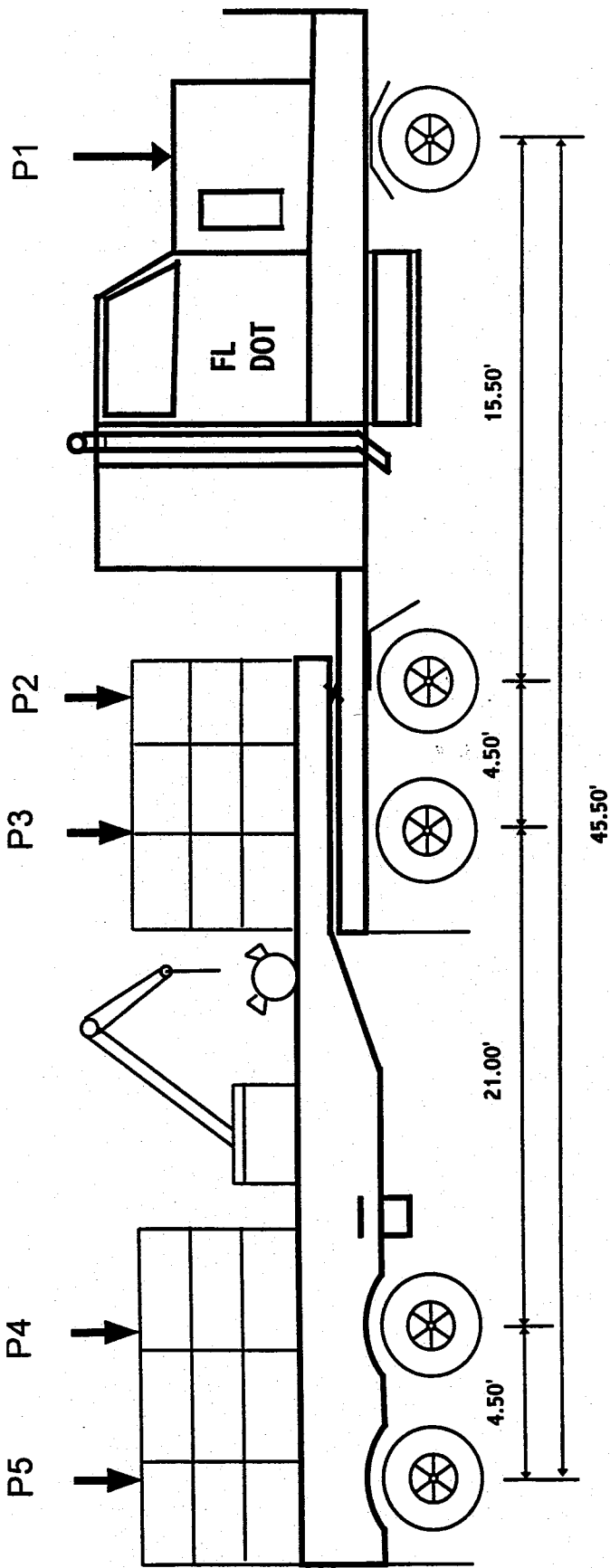


Fig. 2.3 Typical FDOT test vehicle



# A Block	P5	P4	P3	P2	P1
24	30.61	30.61	11.01	11.01	11.26
30	35.48	35.48	11.68	11.68	11.26
36	41.78	41.78	11.95	11.95	11.26
42	46.60	46.60	12.67	12.67	11.26

Fig. 2.4 Typical truck loads for spans less than 55 ft.



# A Block	P5	P4	P3	P2	P1
24	22.40	22.40	18.66	18.66	11.49
36	29.21	29.21	24.95	24.95	11.66
48	36.03	36.03	28.23	28.23	11.83
72	49.66	49.66	37.80	37.80	12.17

Fig. 2.5 Typical truck loads for spans larger than 55 ft.

2.4 REVIEW ON LOAD DISTRIBUTION STUDIES IN PHASE I

2.4.1 Solid and Voided Slab Bridges

The slab bridges are solid or voided sections that span between supports in the longitudinal direction, i.e., traffic direction. The slab bridges are practical for shorter spans up to 45 ft. for voided sections and up to 30 ft. for solid sections [Heins and Lawrie, 1984]. Wheel load distribution analyses of slab bridges based on both grillage analogy and field tests were carried out in Phase I. The effects of span length, bridge width, slab thickness, edge beam and other parameters on effective width were investigated using grillage analogy method. The AASHTO and LRFD load distribution factors were compared with the results of solid and voided slab bridge field tests. A simple design criteria for load distribution was derived as an alternative to current design methods.

2.4.1.1 Solid slab bridges

The effective widths calculated using grillage analogy are larger than those calculated using AASHTO and LRFD codes, which indicate that both AASHTO and LRFD codes give conservative estimate of effective width, E for solid slab bridges. Based on this limited study, the bridge width can be neglected as a parameter in calculating the effective widths of solid slab bridges. The variation of slab thickness has very little effect in the effective width. This finding confirms the approaches specified by the AASHTO and LRFD codes in neglecting the thickness as a parameter in effective width calculation.

The edge beam moment increases with increase in moment of inertia, i.e. increase in edge beam depth or width. The edge beam depth significantly affects the value of effective

width (Fig. 2.6). Slab bridges without edge beams or with hidden edge beams have greater maximum moment than similar slab bridges with edge beam and hence the resulting effective width is smaller. These results suggest that the edge beam size should be taken into account in wheel load distribution. Neither AASHTO specifications nor the LRFD code considers the edge beam effect in the effective width calculations. Based on the solid slab parametric studies, the span length and the edge beam depth are the main parameters, which significantly affect the effective width -calculations. Effective width equations are proposed for solid slab bridges without edge beams and with edge beams. For solid slab bridges without edge beams or with hidden edge beams, the following equation based on the least square fit of the grillage analogy results for the effective width could be used for spans up to 40 ft. and slab. thickness up to 14 in. (Fig. 2.7):

$$E = 6.89 + 0.23 L \quad (2.4)$$

where

E = Effective width over which truck load is assumed to be uniformly distributed, ft.

L =Span length, ft.

The effect of edge beam depth above the slab thickness can be taken into consideration by multiplying eq. 2.4 by a factor C_{edge} given by

$$C_{edge} = 1.0 + 0.0125 (d_1 - 6.0) \quad (2.5)$$

where d_1 = Edge beam depth above the slab thickness, in.

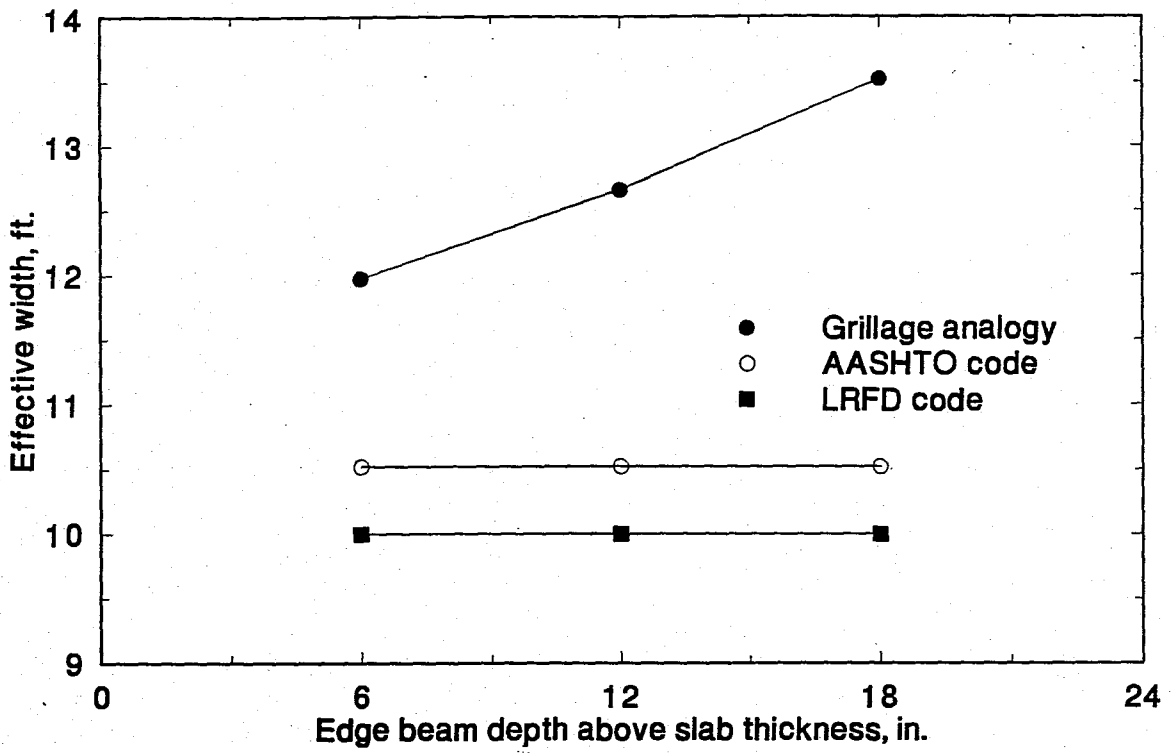


Fig. 2.6 Effective width variations for different edge beam depths

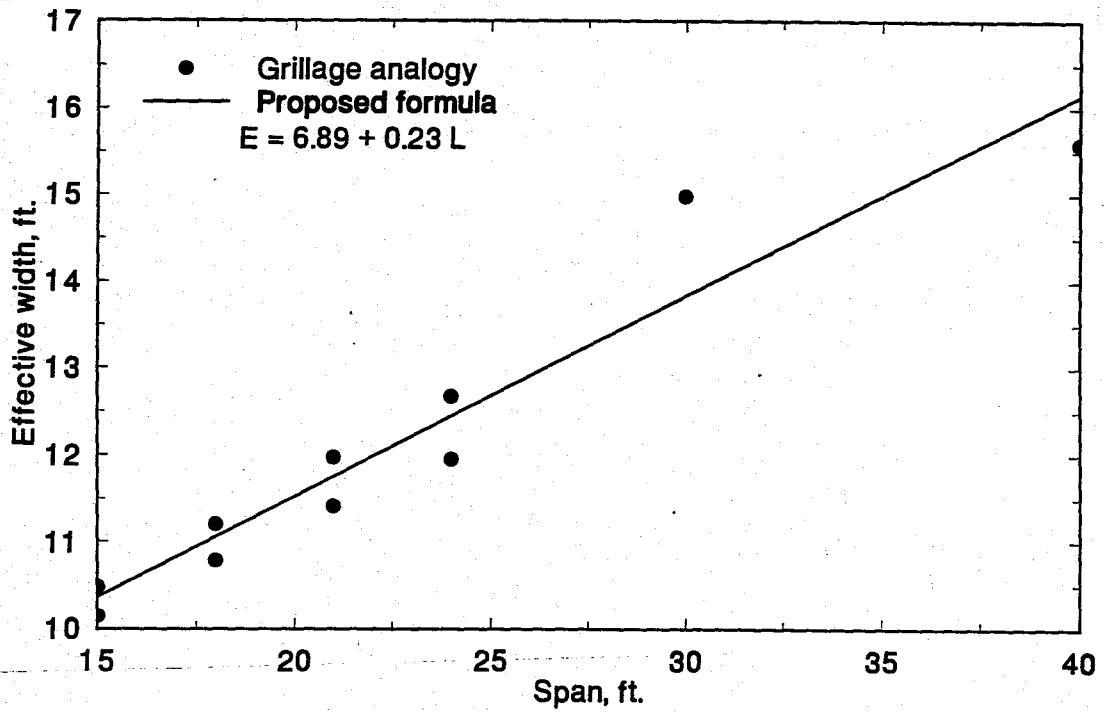


Fig. 2.7 Effective width variation based on the grillage analogy and the proposed formula

2.4.1.2 Voided slab bridges

Comparisons between similar solid and voided slab bridges were made to examine the assumption that both solid and voided slab bridges have the same effective width. The maximum bending moment for solid slab is smaller than that for voided slab, which means the solid slab has larger effective width than an identical voided slab bridge. The difference in effective widths of solid and voided slab bridges may be attributed to the relative vertical movements between the voided slab precast units.

2.4.2 Slab-on-Girder Bridges

The slab-on-girder bridges are the most common type of bridges in Florida. The precast concrete girders such as standard precast AASHTO I-girders and precast bulb-Tee sections are efficient and very economical. The slab-on-girder bridges are practical for spans up to 120 ft. for AASHTO I-girders, whereas the bulb-Tee girders are ideal for spans up to 150 ft.

Wheel load distributions of slab-on-girder bridges based on grillage analogy and field tests are investigated in Phase I. The effects of girder spacing, span length, bridge width, slab thickness, exterior and interior girders and other parameters on wheel load distribution are studied using grillage analogy. The measured load distribution factors from the field tests are compared with the AASHTO and the LRFD load distribution factors.

Girder spacing is a very important factor in determining flexural and shear wheel load distributions of slab-on-girder bridges. The flexural distribution factors for interior girders based on LRFD are generally smaller than those calculated using grillage analogy

particularly for larger girder spacing (Fig. 2.8). It is shown that the distribution factors based on LRFD code are in better agreement with those calculated using grillage analogy for smaller girder spacing, which is more commonly used. For a given girder spacing, the LRFD load distribution equation overestimates the effect of longitudinal stiffness parameter, K_g on wheel load distribution (Fig. 2.9) and this is more evident for exterior girders.

The distribution factor calculated using grillage analogy is larger than those based on AASHTO and LRFD codes particularly for shorter spans. However, the AASHTO and LRFD load distribution factors compare well for longer spans (90 and 100 ft), which are commonly used in bridges (Fig. 2.10). The distribution factor for the 54 ft. wide bridge is slightly higher than that for the 36 ft. wide bridge (2% to 4%) and this can be considered to be insignificant. This establishes that AASHTO and LRFD codes are realistic in neglecting the bridge width as a parameter in load distribution.

The detailed parametric studies on shear load distribution indicate that the girder spacing is a dominant parameter in shear load distribution. Parameters such as span length, bridge width and girder stiffness have little effect on shear load distribution for AASHTO girders. Simplified equation for shear load distribution of slab-on-AASHTO girders is suggested for interior and exterior girders. Fig. 2.11 shows the effect of girder spacing variation on load distribution factors for all the cases calculated using grillage analogy method for interior girders. The best linear fit for shear load distribution of AASHTO interior girders is given by

$$\text{Shear DF} = 0.04 + 0.1 S \quad (2.6)$$

Where S= girder spacing.

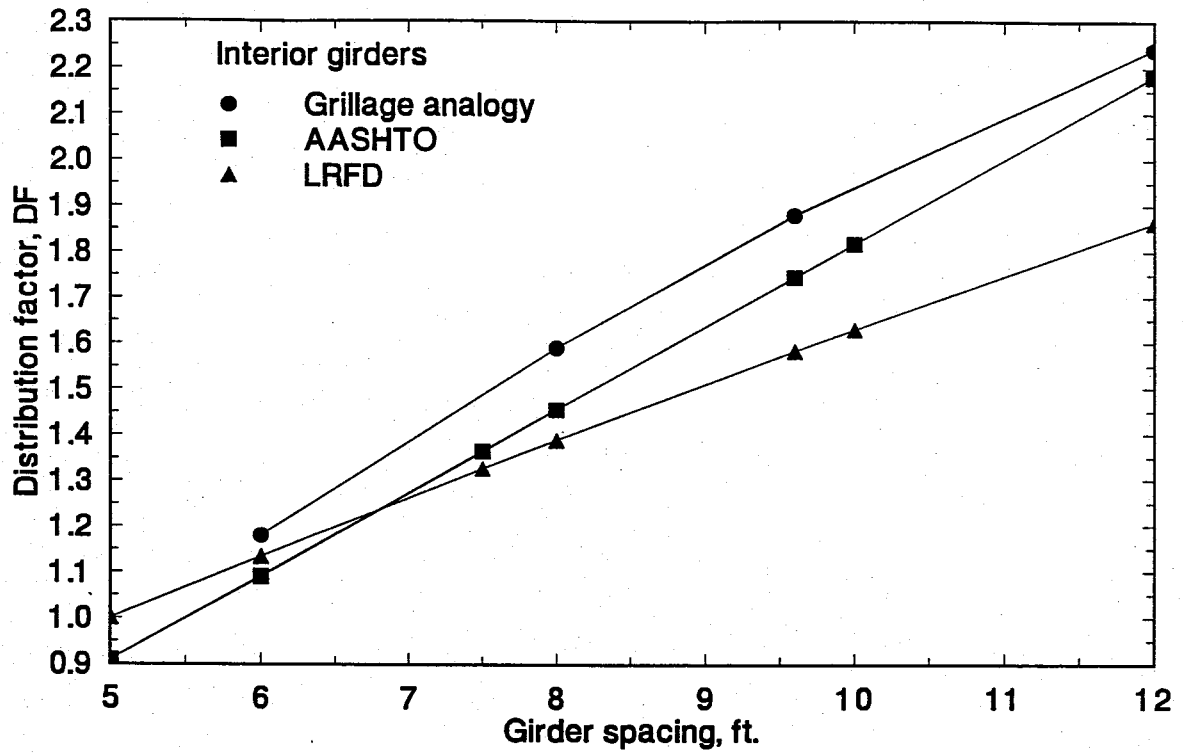


Fig. 2.8 Effect of girder spacing variations on load distribution of slab-on-girder bridges

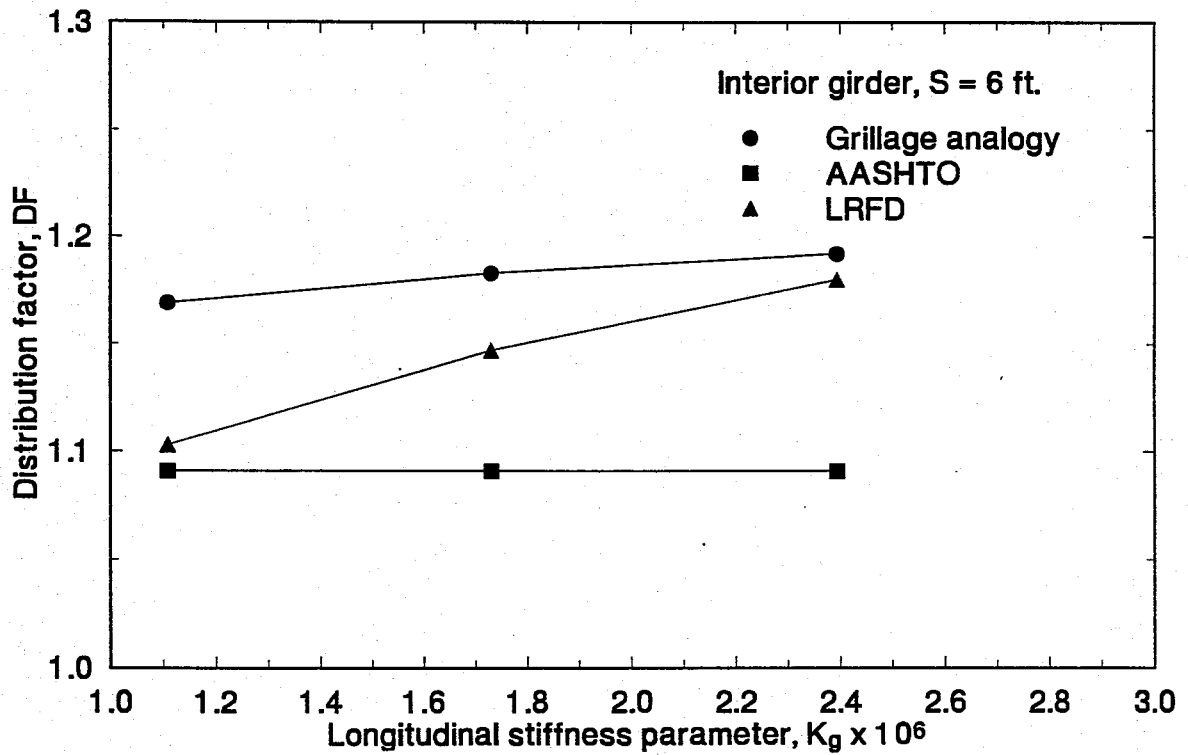


Fig. 2.9 Longitudinal stiffness parameter, K_g effect on load distribution based on grillage analogy, AASHTO and LRFD codes (interior girders)

Fig. 2.12 shows the effect of girder spacing variation on load distribution factors for all the cases calculated using grillage analogy method for exterior girders. The best linear fit for shear load distribution of AASHTO exterior girders is given as

$$\text{Shear DF} = 0.21 + 0.055 S \quad (2.7)$$

Eqns. 2.6 and 2.7 are simple, and for smaller girder spacings, give results comparable to those based on LRFD code.

In general the load distribution factor decreases with increasing span for interior and exterior bulb-tee girders; but this decrease is more than that for AASHTO girders. The effect of span length on distribution factors of bulb-Tee girder requires more studies including field test data to quantify its importance. The girder stiffness effect was insignificant in bulb-Tee flexural load distribution. The grillage analogy method gives larger moment load distribution factors than the LRFD and AASHTO codes, but smaller shear load distribution factors compared to the LRFD and AASHTO codes

2.4.3 Double Tee Bridges

Double tee beams have been used in the past for rural and secondary roads; however they can be used at state and interstate highways with spans up to 80 ft. The precast doubleTee beams are arranged longitudinally side by side forming a simple "V" joint and tied together by transverse post-tensioning. The elimination of cast-in-place elements is associated with speed of construction and reduction in labor costs. The grillage analogy method is used in Phase I to analyze a double tee simply supported bridge and calculate the corresponding load distribution factors. The results obtained are compared with those based on AASHTO and LRFD codes. Field tests of double tee bridges performed by FDOT are analyzed to investigate the load distribution factors of double tee bridges.

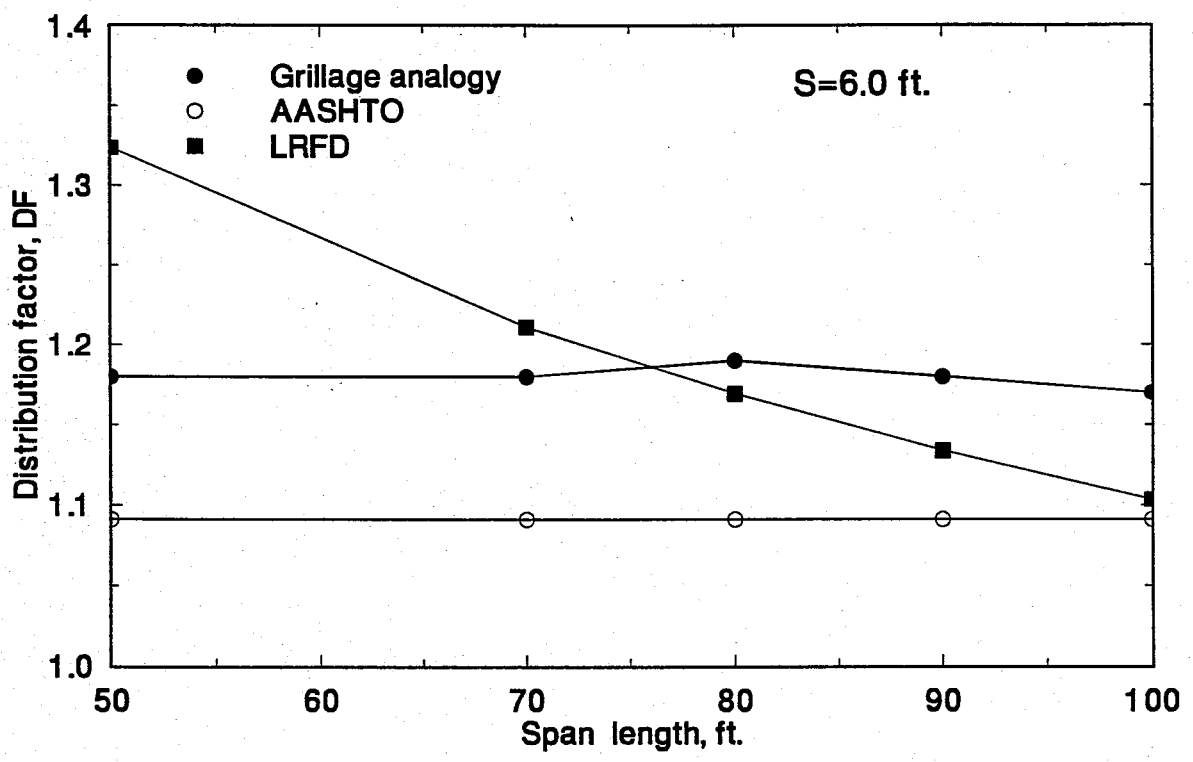


Fig. 2.10 Span length variation effect on load distribution based on grillage analogy, AASHTO and LRFD codes (interior girders)

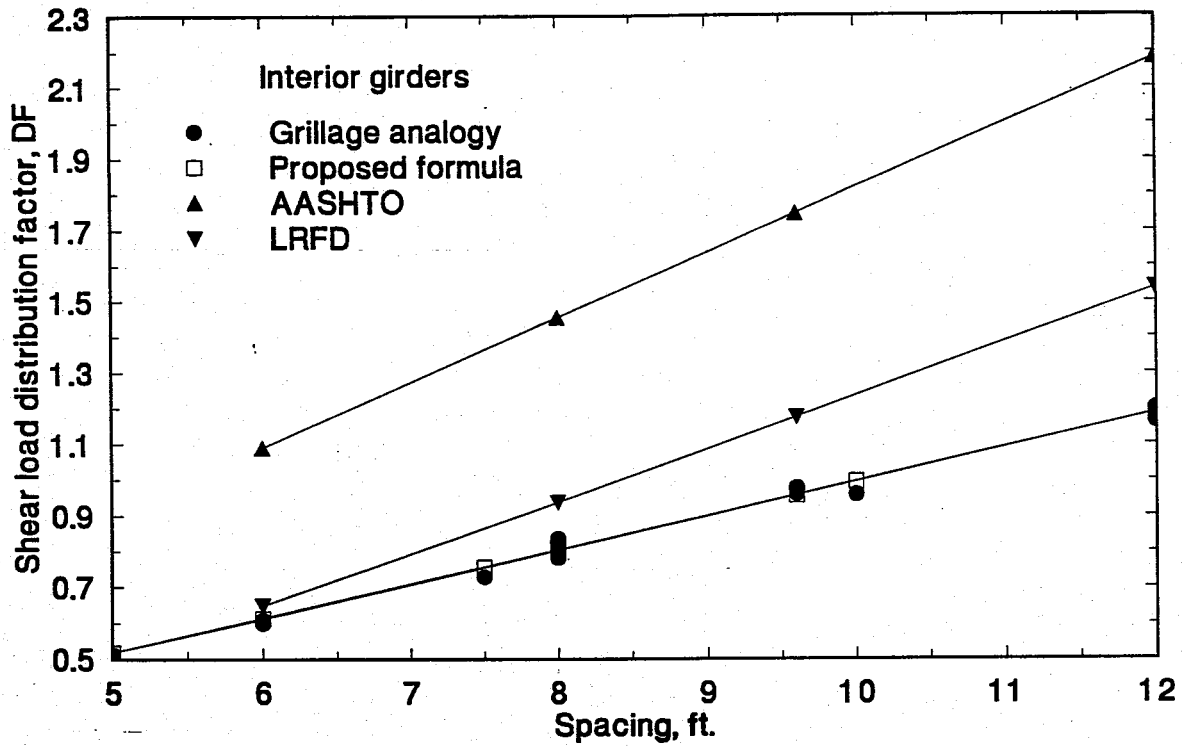


Fig. 2.11 Shear load distribution simplified formula (interior girder)

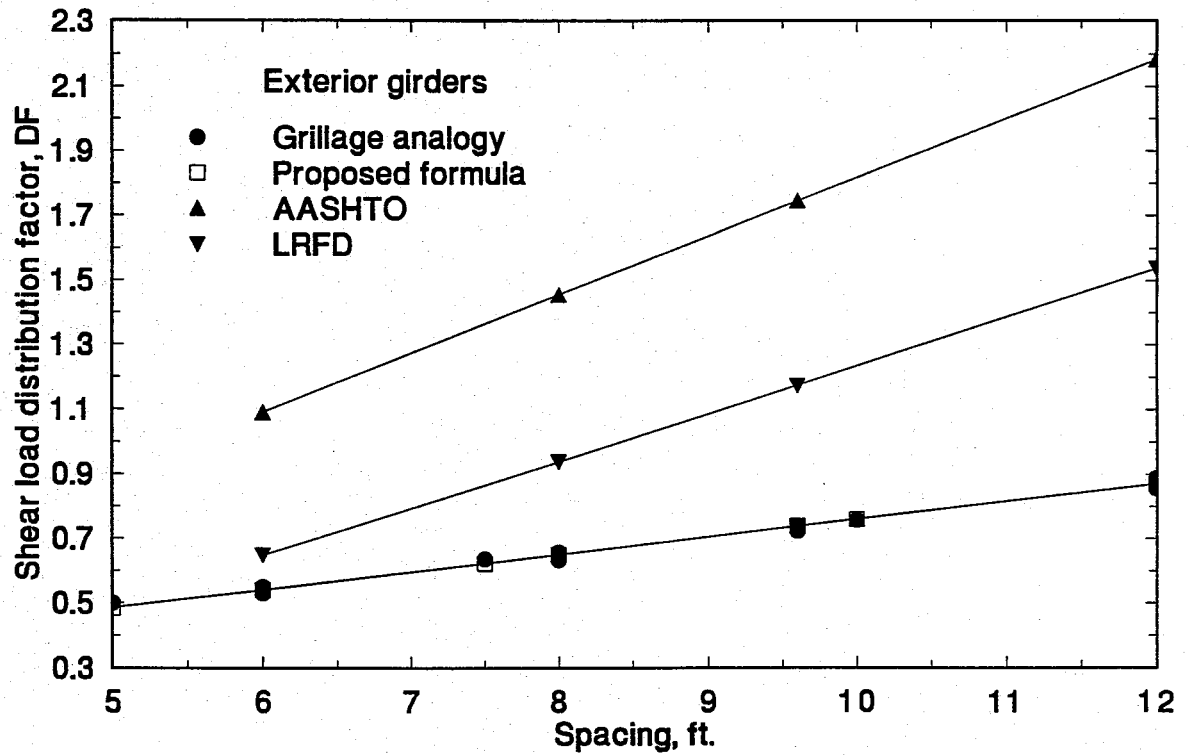


Fig. 2.12 Shear load distribution simplified formula (exterior girder)

The load distribution factors for the interior girders decrease with increasing span and the load distribution factors of exterior girders increase with span increase. It is clear that the load distribution factor of the exterior girders is more dependent on the span than the interior girders. This is consistent with the results of analysis of slab-on-AASHTO girders. The LRFD code does not consider that exterior girders are more dependent on span length than interior girders. This observation needs further research on more double tee cross section types. The measured DF was smaller than that based on grillage analogy, LRFD and AASHTO codes.

2.5 REVIEW ON LOAD DISTRIBUTION STUDIES IN PHASE II

2.5.1 Skew Slab -on-Girder Bridges

Wheel load distributions of skew slab-on-girder bridges based on finite element method and field tests are investigated in Phase II. The effects of skew angle, span length, girder spacing and slab thickness, exterior and interior girders and other parameters on wheel load distribution are determined using finite element method. The measured wheel load distribution factors based on field tests on skew slab-on girder bridges are compared with the AASHTO and the LRFD values.

Increase in skew angle reduces load distribution factors for the interior girders. The results from finite element analyses compare reasonably with the LRFD code particularly for skew angles higher than 30 degrees (Fig. 2.13). Skew angle effect on load distribution for exterior girders is similar to that of the interior girders. The finite element results show

decrease in the load distribution factor with the increase in skew angles. Girder spacing is a very important factor in determining flexural wheel load distributions of skew slab-on-girder bridges. The flexural load distribution factors based on LRFD code are in better agreement with those calculated using finite element method for smaller girder spacing, which are more commonly used (Fig. 2.14).

The interior girder distribution factor based on finite element method shows smaller decreases with increasing span length. However, the load distribution for exterior girders based on finite element analyses increases with increasing span length. For a given skew angle, girder spacing and span length, the LRFD load distribution equation overestimates the effect of slab thickness on wheel load distribution (Fig. 2.15). The finite element results show little effect on load distribution for the variation of slab thickness between 3.85 in to 7 in., which corresponds to a variation of stiffness ratio, H between 5 to 30. ($H = E_g I_{gx} / a D$, $D =$ flexural stiffness of slab per unit width).

The data from three field tests conducted on skew slab-on-girder bridges were used to validate the finite element model. In addition, the wheel load distribution factors based on the field test data were compared with those based on finite element analyses and AASHTO and LRFD codes. The load distribution factors based on finite element analyses were greater by 30 % of the measured values. This difference may be attributed to the variations in concrete strength and section modulus, which are used in calculating the measured load distribution factor. The distribution factors based on AASHTO codes and LRFD were higher than those calculated using the measured strains and finite element method. This may, be: attributed to the fact that both AASHTO code and to a lesser extent, the LRFD, code

do not take into account the additional stiffness contribution of the shoulder and parapets to the bridge stiffness. The effect of the shoulders in the load distribution is investigated in phase III of this study.

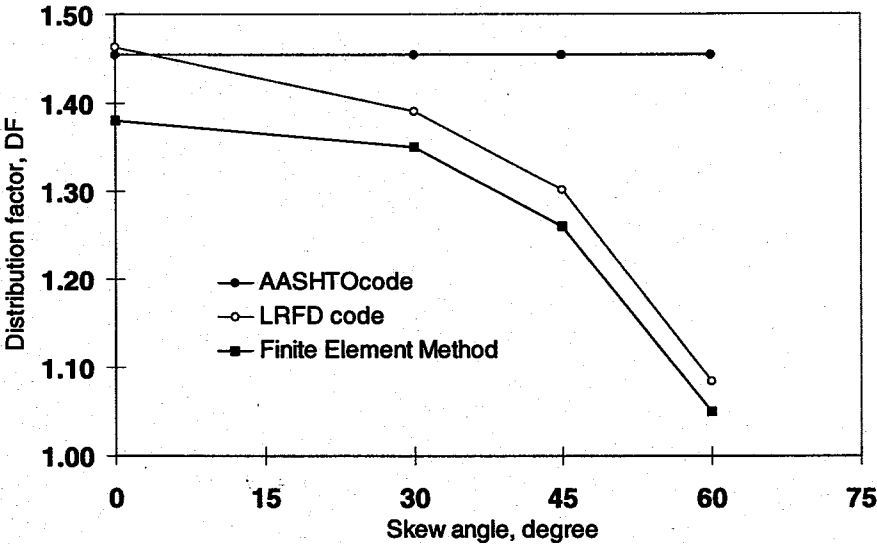


Fig. 2.13 Load distribution factor variation with skew angle for slab-on-girder bridges (Interior girders)

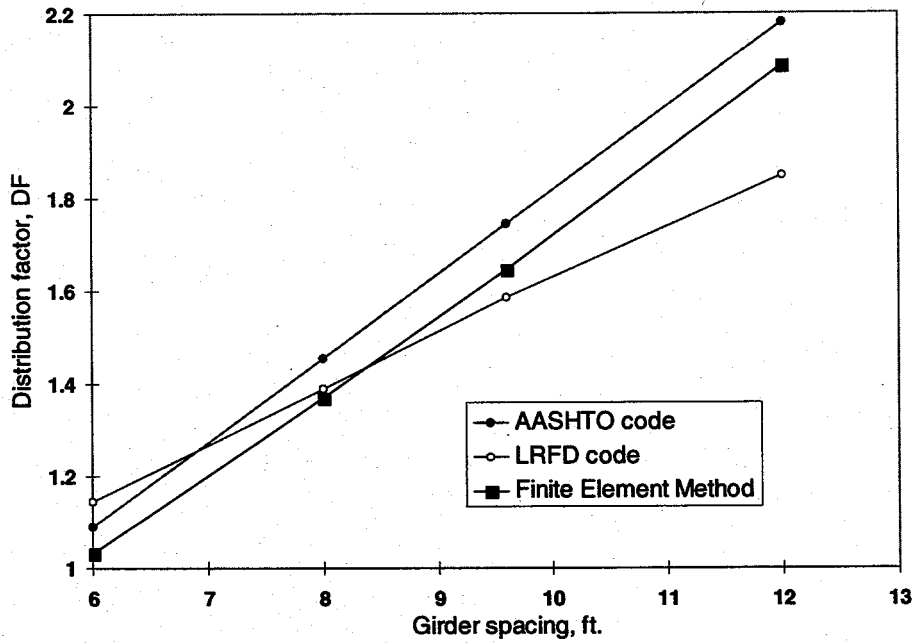


Fig. 2.14 Load distribution factor variation with girder spacing for slab-on-girder bridges (Interior girders)

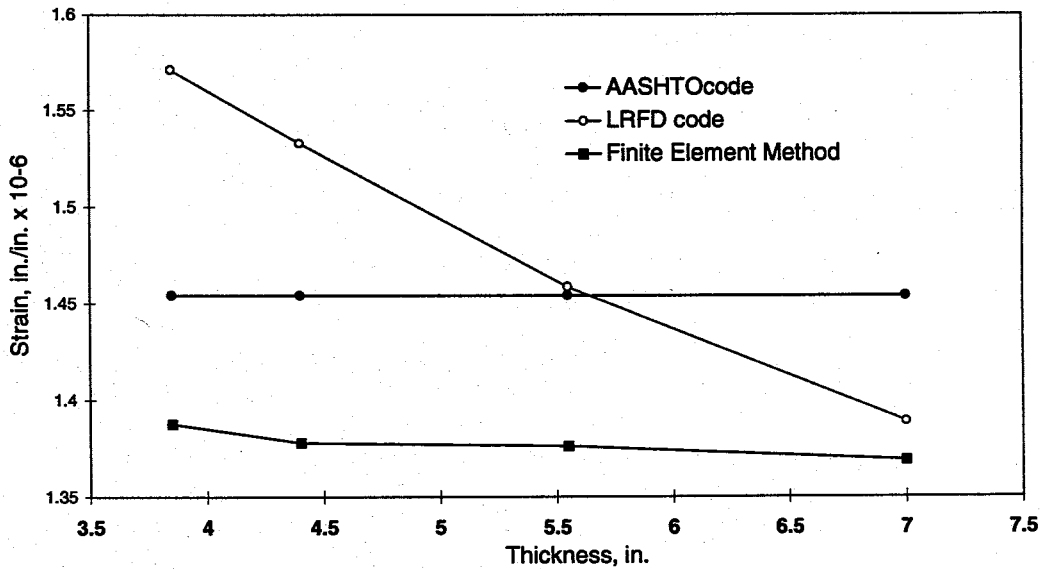


Fig. 2.15 Load distribution factor variation with thickness for slab-on-girder bridges (Interior girders)

2.5.2 Skew Solid Slab Bridges

Wheel load distribution factors of skew solid slab bridges are determined based on finite element method and field tests. The finite element method is used to determine the effective width and study the effects of skew angle, span length, edge beam depth and other parameters on wheel load distribution. The effective widths based on the AASHTO and the LRFD codes are compared with the measured values of simply supported skew slab bridges.

The effective widths calculated using finite element method are larger than those calculated using AASHTO and LRFD codes, which indicate that both AASHTO and LRFD codes give conservative estimate of effective width, E for skew solid slab bridges. The effective width increases with increase in the skew angle for solid slab bridges. This agrees with the LRFD codes in considering the skew angle as a parameter in effective width calculation. The finite element results show that for skew angles higher than 30° , the effective width is governed by the lane width (Fig. 2.16).

The span length is an important factor ineffective width calculation. The effective width tends to increase as the span length increases. The edge beam moment increases with increase in moment of inertia, i.e. increase in edge beam depth or width. The edge beam depth significantly affects the value of effective width, E . Based on the skew solid slab parametric studies, the skew angle, span length and the edge beam depth are the main parameters, which significantly affect the effective width calculations.

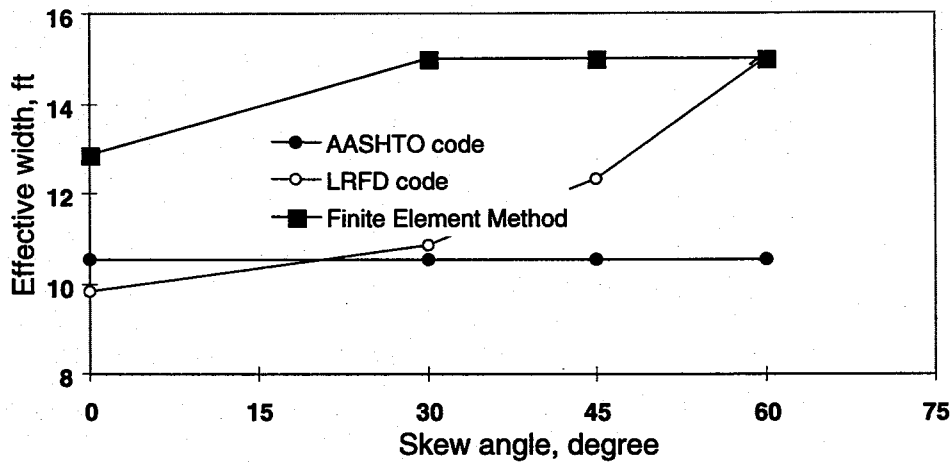


Fig. 2.16 Effective width variation with skew angle for solid slab bridges

2.5.3 Continuous Slab-on-Girder Bridges

The AASHTO and LRFD codes do not specify any modification for computing the distribution factors for continuous bridges as they do for single span skew bridges. The LRFD code commentary gives the following for deleting the correction factors: the value of the correction factors were within 5%, which is less than the level of the accuracy for the approximate distribution factor method; also the increase in the distribution coefficient for negative moments tends to cancel out when the distribution of reaction force over the bearing is considered. Other publications have recognized the need for more research to examine the importance of the correction factor for continuity [Khaleel, Itani 1990]. Alternative designs for continuous bridges have taken a direction in which computer models using finite element method (FEM) accurately predict the bridge behavior for various loading cases. The effects of bridge skew angles, number of spans, span ratio between two spans, and other parameters on flexural load distribution

factors were studied using FEM, AASHTO, and LRFD. The flexural load distribution factors based on FEM are compared with those based on field tests on continuous bridges.

In continuous bridges, the strains are generally higher at the interior supports than at mid-spans. The strain distributions in the transverse direction are similar for both positive and negative moment load cases. The FEM analyses show strain distributions become less uniform as skew angle increases (Fig. 2.17). Based on the parametric studies, the effect of the number of spans on the load distribution factors is small and can be neglected. In general, the FEM load distribution factors are smaller than those based on the LRFD code.

The interior girder load distribution factors show little variation as the ratios between the spans increase for both positive and negative moments. However, the exterior girder load distribution factors show a small increase (10%-13%) as the ratios between the spans increase. Comparisons between continuous and single span slab-on-girder bridges show that there is little change in the flexural load distribution factor with increase in the number of spans.

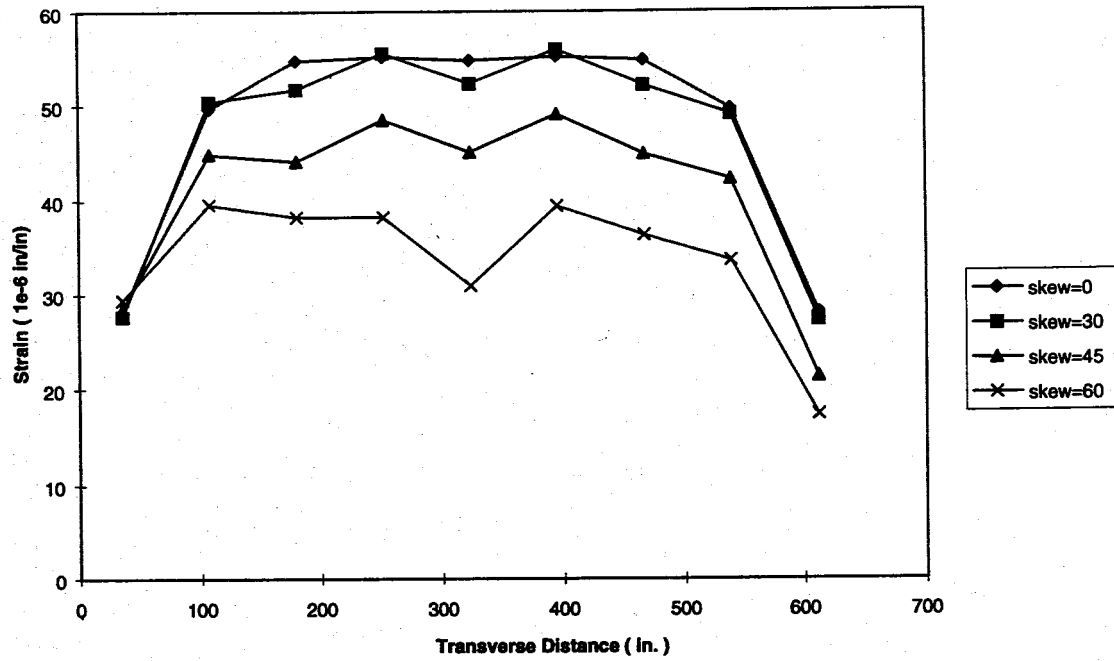


Fig. 2.17 Strain distribution at midspan for two span bridges with different skew angles (interior girder loading)

CHAPTER 3
LOAD DISTRIBUTION FACTORS BASED ON
COMPREHENSIVE FIELD BRIDGE TESTING

3.1 INTRODUCTION

The non-destructive testing of bridges can be used as an efficient tool for evaluating new design concepts and construction practices. The studies carried out in Phases I and II were focused on wheel load distribution factors of different bridge types. This chapter presents comprehensive field tests of typical bridge types. The load testing procedure and the type of instrumentation were designed based on the preliminary analysis to obtain the structural parameters and the maximum bridge response.

The typical bridge types for load testing include i) skew slab-on-girder and ii) continuous skew slab-on-steel girder bridges. The instrumentation was designed to measure strains and deflections at critical sections of the test bridges. The members of the research team from the Center for Infrastructure and Constructed Facilities participated in the comprehensive field-testing carried out by the Structural Research Center, Florida Department of Transportation, Tallahassee.

3.2 FIELD TESTS ON SKEW BRIDGES

3.2.1 Skew Slab-on-Girder Bridge (Bridge # 940115)



Fig. 3.1 Over view of bridge # 940115

The bridge is located on I-95 over Glades Road in St. Lucie County, Florida. It consists of six simply supported spans with span lengths of 64.08, 73.33, 73.33, 73.33, 125.08, and 68.17 ft. respectively. The length of the test span is 125.08 ft with a skew angle of 45 degrees. The span consists of nine AASHTO type V prestressed concrete girders, spaced at 6 ft. 7 ½ in. center to center and slab thickness of 7.0 in. The bridge carries three lanes of traffic with curb-to-curb width of 56.0 ft.

Fig. 3.1 shows the bridge on 1-95 over Glades Road (Bridge #940115). Fig. 3.2 shows the plan view of the bridge with the spacing of the girders and the location of the diaphragms. Diaphragms of 8 in. width are provided at four transverse sections along the bridge span. The bridge cross section is shown in Fig. 3.3 with a total width of 58 ft. 9 in. The longitudinal view of the bridge is shown in Fig. 3.4. Figs. 3.5 and 3.6 show respectively the schematic of truckload positions and general view of FDOT test vehicles on' the bridge. The trucks were positioned at 62 ft. from the edge of the span to front tire of the rear axle in the direction of traffic. The trucks are offset by 45 degrees corresponding to the skew angle of the bridge (Figs. 3.5 & 3.6). Fig. 3.7 shows the location of the instrumentation, which includes six deflection gages, electrical and vibrating wire strain gages. Two deflection gages were positioned on each girder (G5, 6, 7) at 30 feet from each end of the span on the bottom of the girder. Electrical and vibrating wire strain gauges are placed on the bottom of the each girder at 3.5 feet from the centerline of the bridge. Additional electrical and vibrating wire strain gauges are placed at the centerline of girders 5 and 6 on the bottom of the girder (Fig.3.7).

The two test vehicles are initially loaded with twenty four concrete blocks and driven to position on the critical locations of the bridge. The data acquisition system was used to monitor the deformations. The data are immediately analyzed, displayed and compared with the theoretical predictions to assure the safety of the bridge, equipment and testing personnel. Additional blocks were then added to the test vehicles and the test repeated until the design load is applied. The wheel loads corresponding to the number of concrete blocks are given in Figs. 2.4 and 2.5.

The measured deflections of girders G-5, G-6, and G-7 for different load cases are presented in Table 3.1. A maximum deflection of 0.43 in. was measured under the girder G-6 (30 ft. from the end of the span in the direction of traffic). The measured transverse strain distributions in the bottom of the girders of bridge #940115 are shown in Fig. 3.8. A maximum strain of 155 micro-strains was measured in girder G-6 corresponding to the maximum moment of 4057 ft-kips (equivalent to 60 blocks).

The finite element model shown in Fig. 2.2 was used to analyze the test bridge. Table 3.2 summarizes the material and sectional properties used in the finite element analyses of the bridge. Table 3.3 presents the deflections based on the finite element method for various load cases. In general, the calculated deflections are larger (about 24%) than the measured values. Fig. 3.8 and Table 3.4 show the comparisons of the measured and calculated strain distributions along the bridge width. The measured and calculated strains show a better agreement than the corresponding deflections. This indicates that the finite element model used in the analysis is more accurate in predicating the strains. Table 3.5 summarizes the load distribution factors based on measured and calculated strains, AASHTO and LRFD methods. The load distribution factors based on measured and calculated strains were determined using Eqn. 2.2.

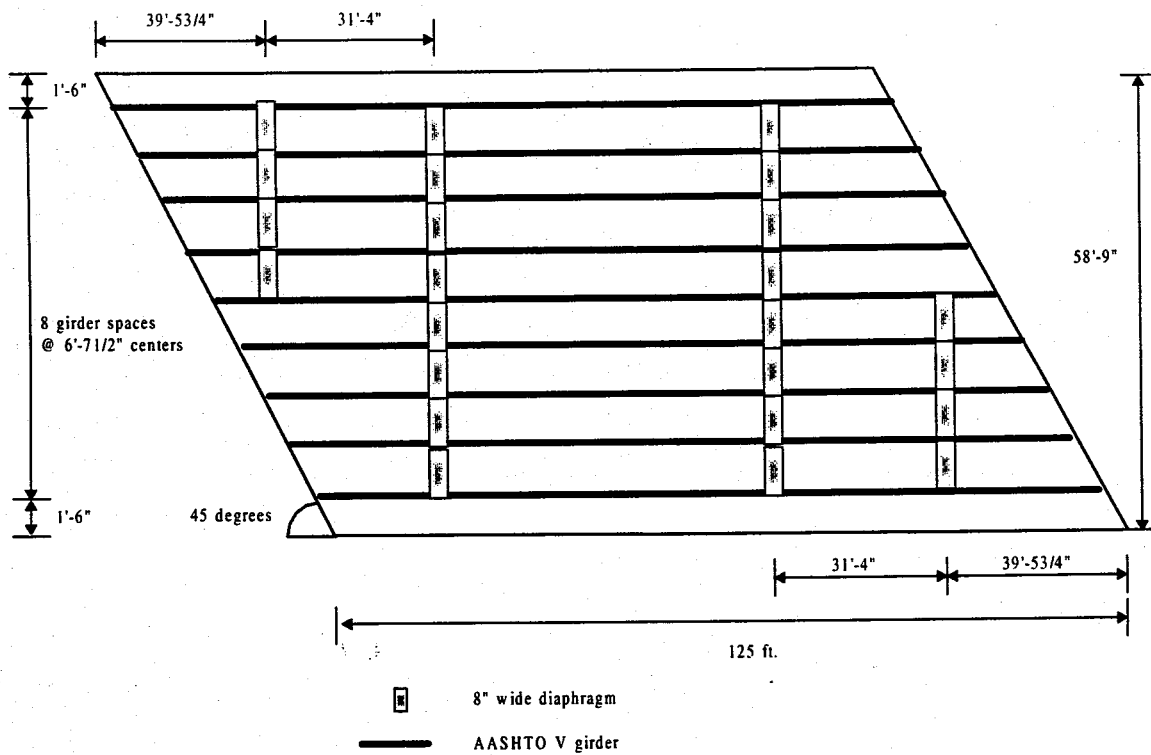


Fig. 3.2 Plan view of bridge # 940115

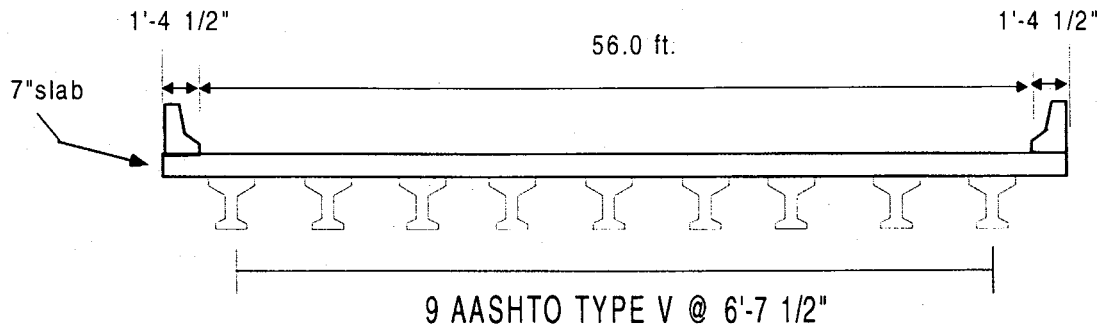


Fig 3.3 Cross section of bridge #940115

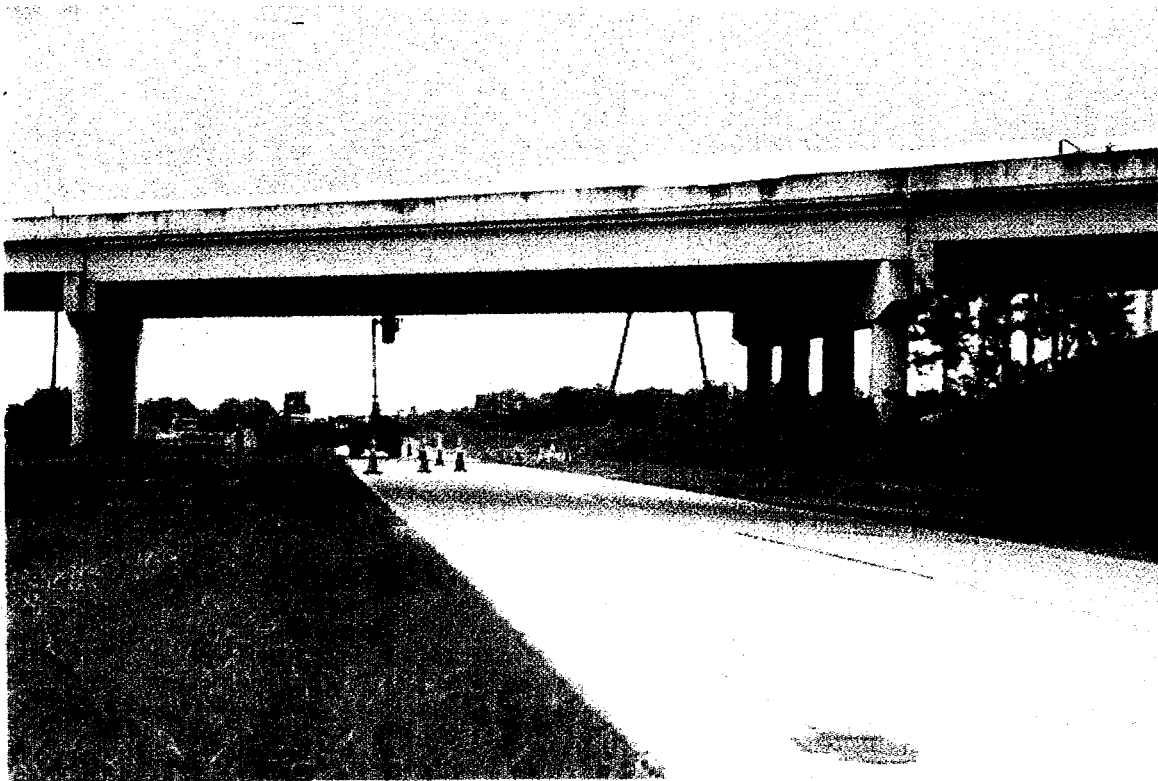


Fig 3.4 Longitudinal View of Bridge #940115

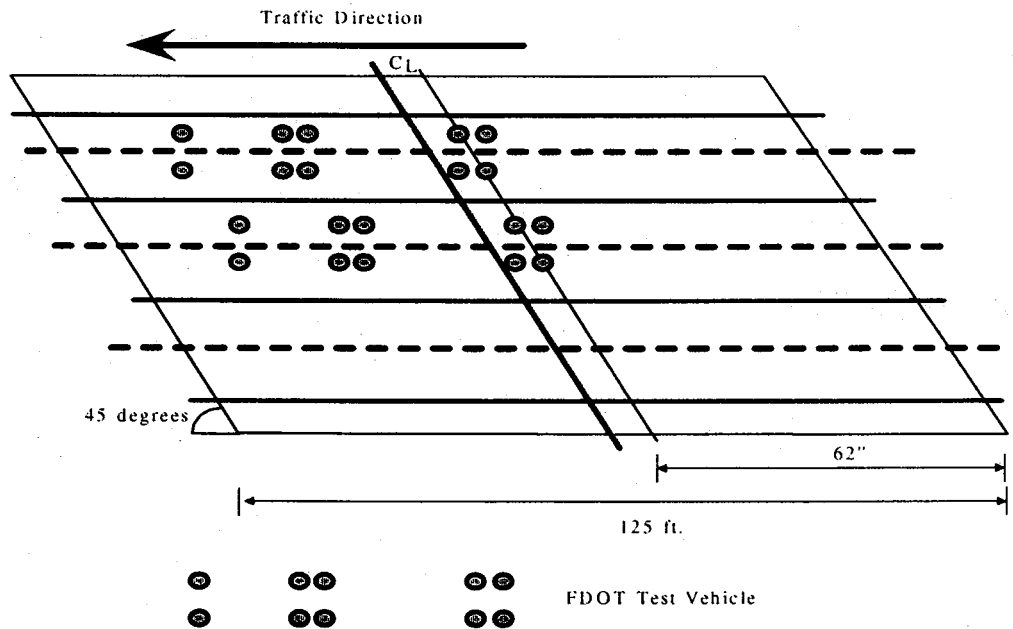


Fig 3.5 Load position for bridge #940115



Fig 3.6 FDOT test vehicles on bridge #940115

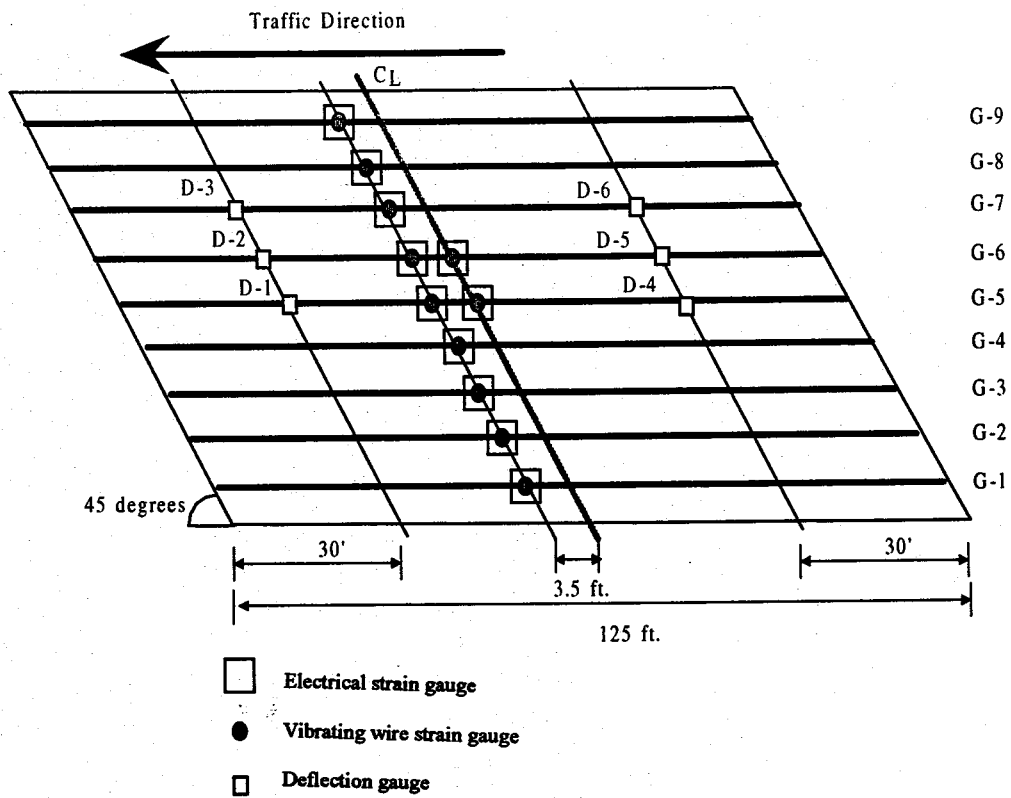


Fig 3.7 Location of strain and deflection gauges for bridge #940115

Table 3.1 Deflection measurements for various loads (bridge #940115)

Deflection gage	D-1 (in.)	D-2 (in.)	D-3 (in.)	D-4 (in.)	D-5 (in.)	D-6 (in.)
24 Blocks	0.161	0.040	0.190	0.210	0.240	0.240
36 Blocks	0.273	0.200	0.250	0.310	0.320	0.290
48 Blocks	0.294	0.230	0.290	0.350	0.360	0.320
60 Blocks	0.300	0.280	0.350	0.410	0.430	0.370

Table 3.2 Material and sectional properties for bridge #940115

Material Properties	E_{deck} (ksi)	E_{beam} (ksi)	Poisson's Ratio, ν	G (ksi)
	4031	4031	0.2	1679

Section Properties	Slab	Thickness = 7 in.				
	Top Flange	A (in ²)	I_y (in ⁴)	I_z (in ⁴)	T_{ky} (in)	T_{kz} (in)
		294	1201	43218	42	7
AASHTO type V girder	Web	Thickness = 8 in.				
	Bottom Flange	A (in ²)	I_y (in ⁴)	I_z (in ⁴)	T_{ky} (in)	T_{kz} (in)
		364	5126	23781	28	13

* E_{deck} , E_{girder} = Elastic modulus of the deck slab and girder respectively,

G = Modulus of rigidity,

A = Area of cross section of the girder,

I_y , I_z = Moment of inertia of the girder in y and z directions respectively,

T_{ky} , T_{kz} = Thickness and width of the beam elements respectively.

Table 3.3 FEM deflections for various loads (Bridge #940115)

Deflection Gage	D-1 (in.)	D-2 (in.)	D-3 (in.)	D-4 (in.)	D-5 (in.)	D-6 (in.)
24 Blocks	0.200	0.221	0.196	0.245	0.289	0.275
36 Blocks	0.254	0.281	0.249	0.315	0.370	0.352
48 Blocks	0.309	0.341	0.301	0.384	0.452	0.429
60 Blocks	0.362	0.400	0.354	0.453	0.533	0.506

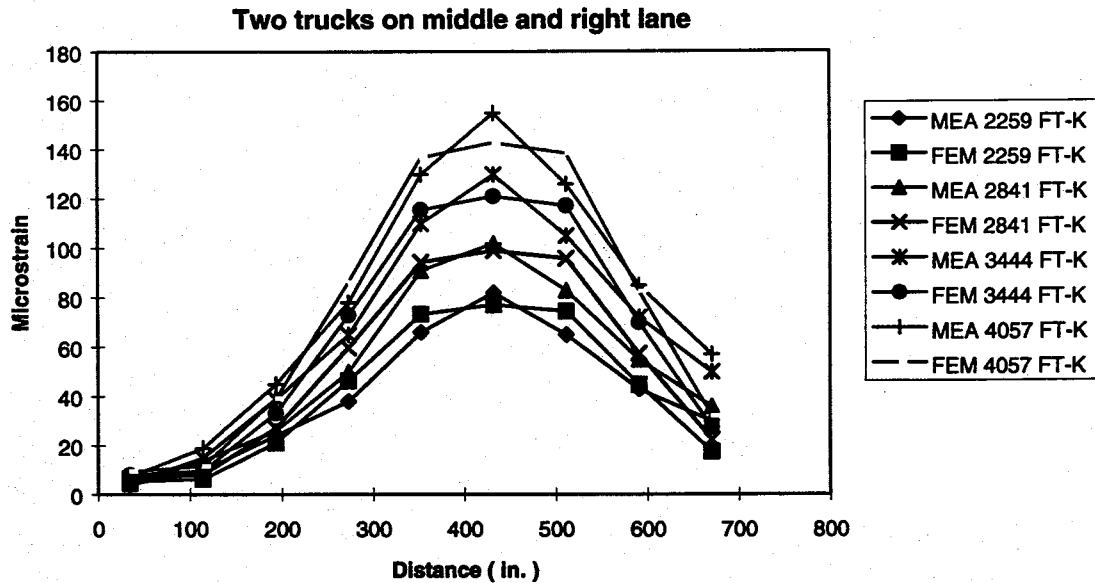


Fig. 3.8 Measured and FEM strains for St. Lucie County Bridge #940115

Table 3.4 Measured and FEM strains for St. Lucie County Bridge #940115

Girder number	Measured 2259 ft-k (24 block)	FEM 2259 ft-k (24 block)	Measured 2841 ft-k (36 block)	FEM 2841 ft-k (36 block)	Measured 3444 ft-k (48 block)	FEM 3444 ft-k (48 block)	Measured 4057 ft-k (60 block)	FEM 4057 ft-k (60 block)
G-1	4	5.2	4.5	6.7	5	8.1	7.5	9.6
G-2	10	6.3	14	8.1	15	9.8	19	11.6
G-3	24	21.2	26	27.2	39	33.2	45	39.2
G-4	38	46.4	50	59.7	65	73	78	86.3
G-5	66	73.3	91	94.4	110	115.5	130	136.7
G-6	82	77.1	102	99	130	121	155	143
G-7	65	74.5	83	95.8	105	117.2	126	138.5
G-8	43	44.8	55	57.4	72	70	85	82.6
G-9	30	17.7	36	22.5	50	27.4	57	32.2

**Note: All strains are in micro-strain units
(): Number of blocks**

Table 3.5 Summary of Bridge #940115 load distribution factors (Interior Girders)

AASHTO	LRFD	Measured 4057 ft-k (60 blocks)	FEM 4057 ft-k (60 blocks)
1.200	0.973	0.883	0.842

3.2.2 Continuous skew slab-on-steel girder bridges #100477 and #100478

The bridges are located on I-75 over U.S. 301 in Hillsborough County, Florida (Figs. 3.9-3.12). The bridge # 100477 on southbound I-75 consists of four continuous spans with span lengths of 65'-2-5/16", 165'-3-3/4", 172'-8-13/16", and 77'-4-7/16". The bridge # 100478 on northbound I-75 also consists of four continuous spans with span lengths of 73'-5-1/2", 165'-3-3/4", 172'-8-13/16", and 84'-10-3/4". The length of the tested spans is 172'-8-13/16" with a skew angle of 45°. Eight A36 steel plate girders are spaced at 7'-7" center-to-center with a deck slab thickness of 7 in. The bridge carries three lanes of traffic with curb-to-curb width of 56.0 ft.

The plan view of Bridge #100477 is shown in Fig. 3.13. The bridge has a small horizontal curve of eleven degrees, which is neglected in the finite element modeling. Fig. 3.14 shows the cross section of the bridge with the concrete deck, steel girders, and diaphragms in place. Fig. 3.15 shows atypical continuous steel plate girder in the bridge. Different plate sections and lengths are used in the built-up plate girder.

Table 3.6 shows the material and sectional properties of the bridges used in the finite element modeling. The plan view of the finite element model is shown in Fig. 3.16. There are 125 elements at 4 ft in the longitudinal direction and 16 elements in the

transverse direction. Although span 3 was the test span in the bridge, the entire bridge was modeled in the finite element analysis since the bridge is continuous. Figs 3.17 and 3.18 show the MOT test trucks for two positions, one for maximum positive bending moment and the other for maximum negative bending moment. There are three lanes on the bridge and two trucks were used for each strength test. The trucks were placed in the two right lanes in the directions of traffic. Figs 3.17 and 3.18 also show the locations of the strain gages for positive and negative moments.

The transverse strain distributions from the FEM analysis are compared with the measured field test data for Bridge #100477 in Figs. 3.19 to 3.22. The difference between the measured and computed maximum strains at mid-span is in the range of 11% when diaphragms are not considered in the FEM analysis (Fig 3.19). However, this difference reduces to only 3% when diaphragms are taken into account in the FEM analysis. Similar trend is observed for maximum strains over the support corresponding to the truck positions at the positive moment locations (Fig. 3.20). Fig. 3.22 shows the strain distributions over the supports for the trucks positioned at the maximum negative moment location. The FEM analysis considering the diaphragms resulted in an 11% difference from the maximum measured strains over the supports and the difference increases to 17% when diaphragms are not considered in the analysis. Table 3.7 shows the load distribution factors for Bridge #100477 based on AASHTO, LRFD, FEM and the measured strains. The AASHTO and LRFD load distribution factors are higher than the FEM values and the FEM results are closer to the measured load distribution factors.

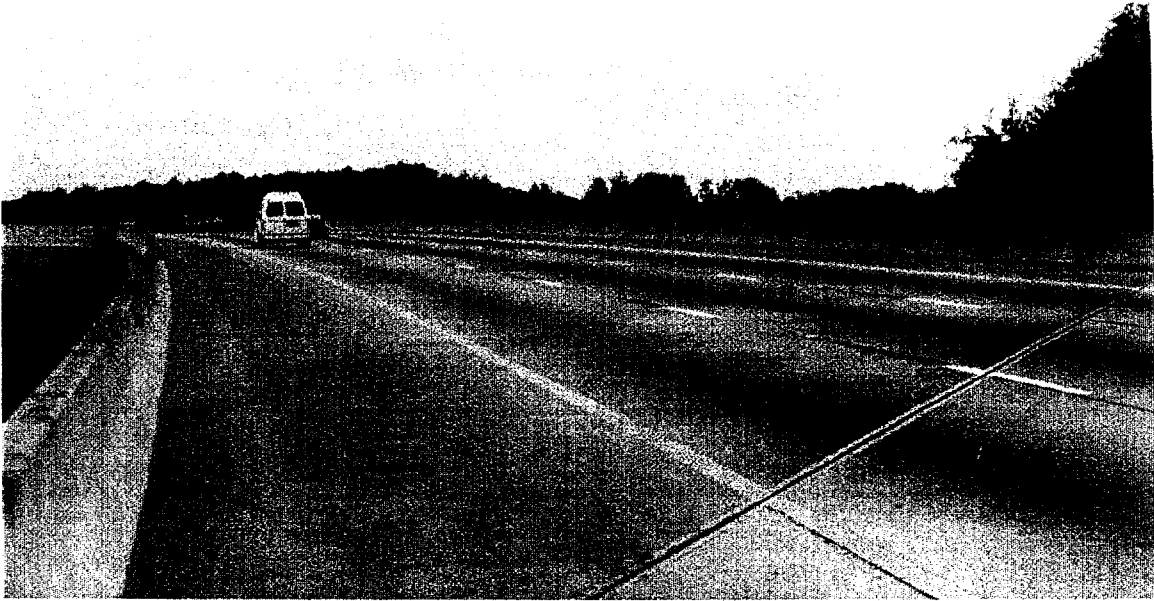


Fig. 3.9 Bridge # 100477 (Southbound I-75 over U.S. 301)



Fig 3.10 Longitudinal view of bridge #100477



Fig. 3.11 Bridge # 100478 (Northbound I-75 over U.S. 301)



Fig 3.12 Longitudinal view of bridge #100477

Table 3.6 Material and sectional properties for bridges

Material properties		E (ksi)		Poisson's Ratio, ν	G (ksi)	
Concrete deck slab		4031		0.2	1679	
Steel plate girders		29,000		0.3	11,154	
Section Properties	Slab	Thickness = 7.0 in.				
	Grade	A (in ²)	I _y (in ⁴)	I _z (in ⁴)	T _{ky} (in)	T _{kz} (in)
Flanges (in inches)						
PI 5/8 x 12	A36	7.5	0.244	90	12	5/8
PL 1-1/2 x 16	A588	24	4.5	512	16	1.5
PL 3/4 x 12	A36	9	0.422	108	12	0.75
PL 1-1/8 x 20	A588	22.5	2.37	750	20	1.125
PL 2-1/8 x 22	A588	46.75	18	1886	22	2.125
PL 1-5/8 x 16	A36	26	5.72	555	16	1.625
Web (in inches)						
PL 5/8 x 60	A36				5/8	60
Diaphragms (in inches)						
L 3 x 3 x 5/16	A36	1.78	1.51	1.51	5/16	5/16
L 4 x 4 x 5/16	A36	2.4	3.71	3.71	5/16	5/16

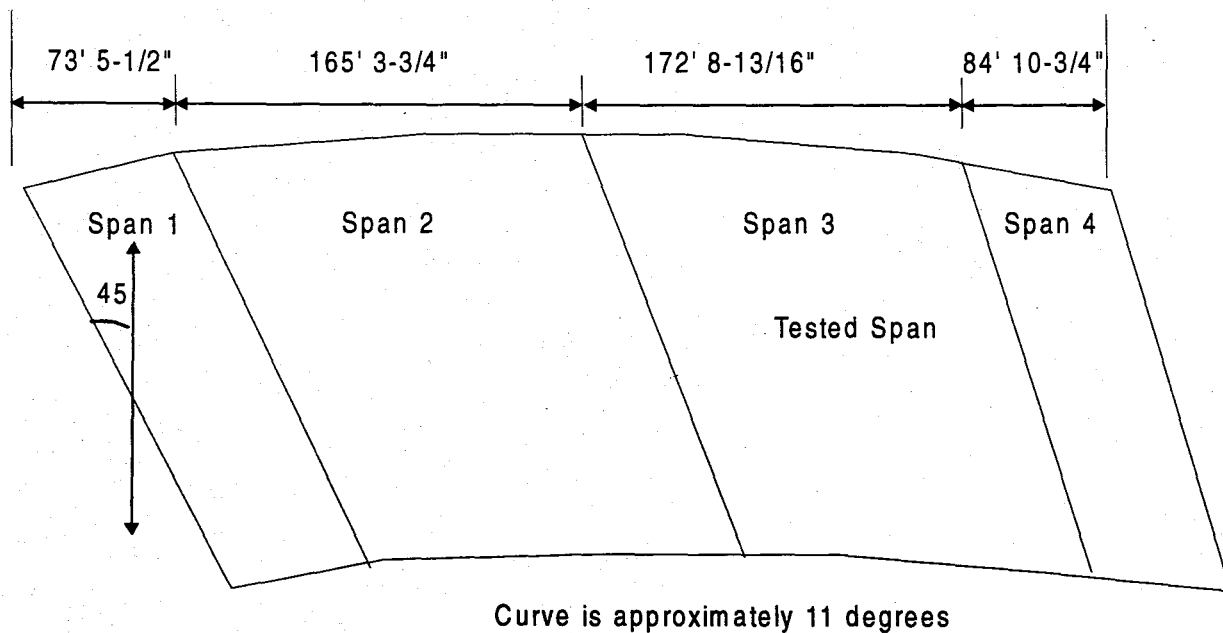


Fig. 3.13 Plan view of bridge # 100477

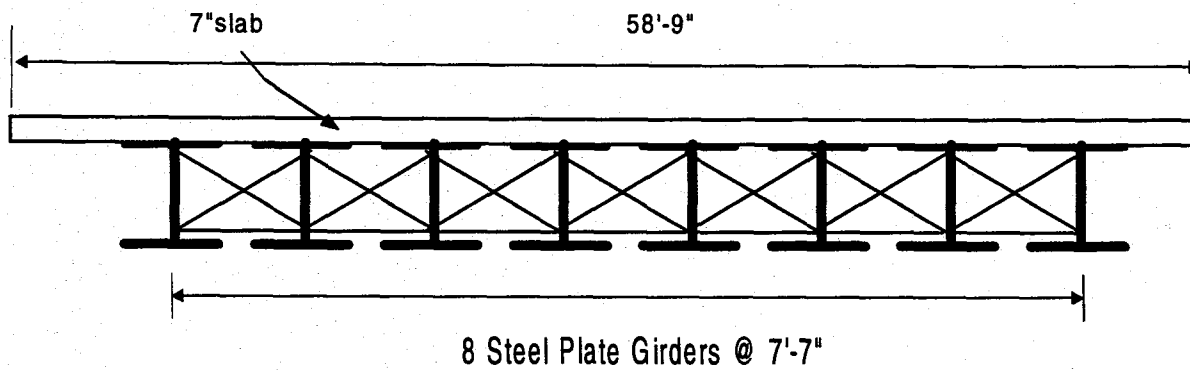


Fig 3.14 Cross section of bridge #100477

- PL 5/8 x 12
- PL 3/4 x 12
- PL 2-1/8 x 22
- PL 5/8 x 60
- PL 1-1/2 x 16
- PL 1-1/8 x 20
- PL 1-5/8 x 16

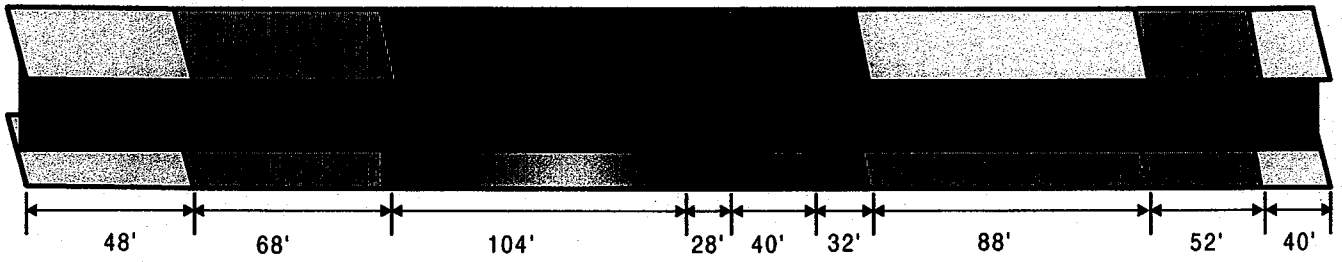


Fig 3.15 Typical built-up steel plate girder in bridge #100477

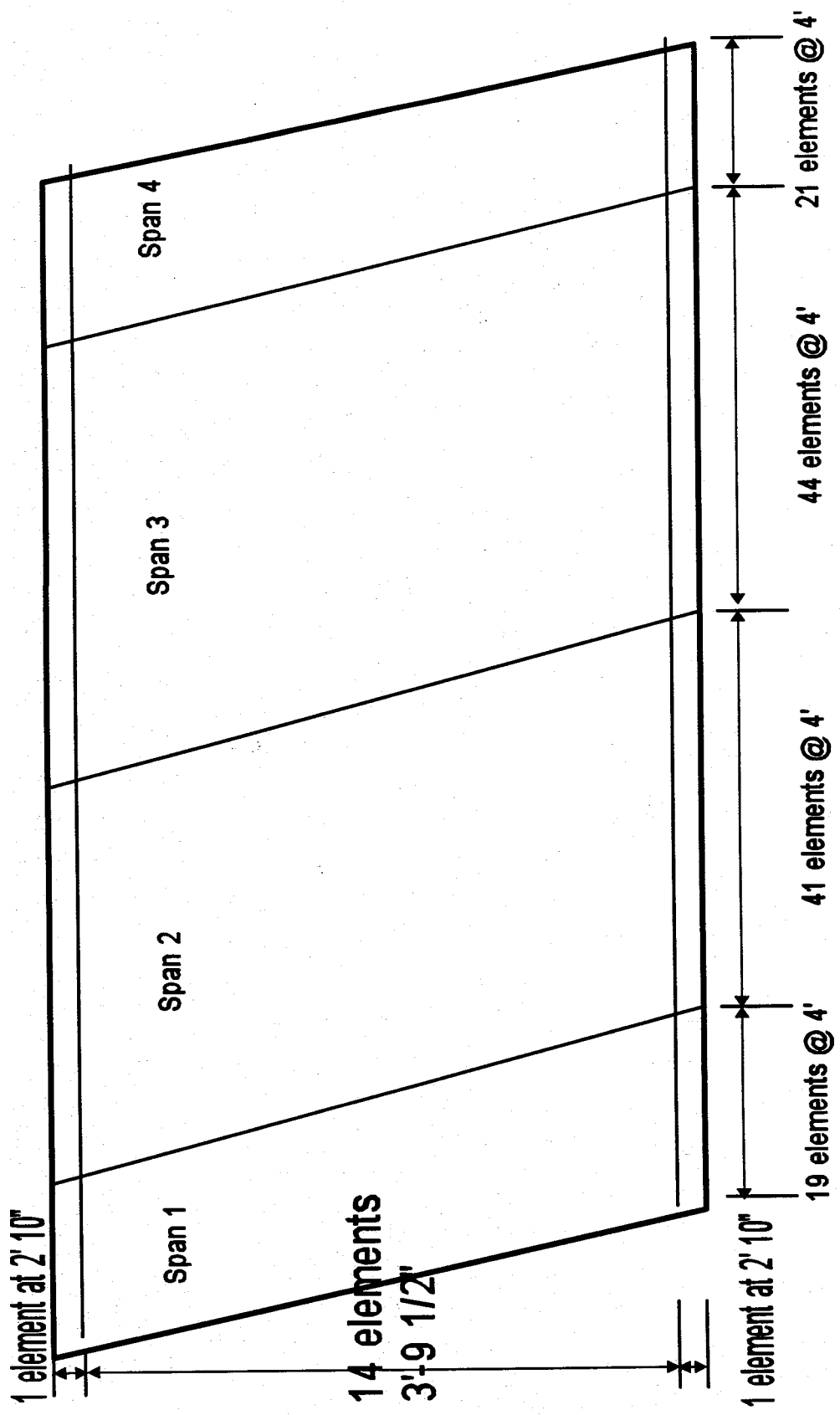


Fig. 3.16 Finite element model of bridge # 100477

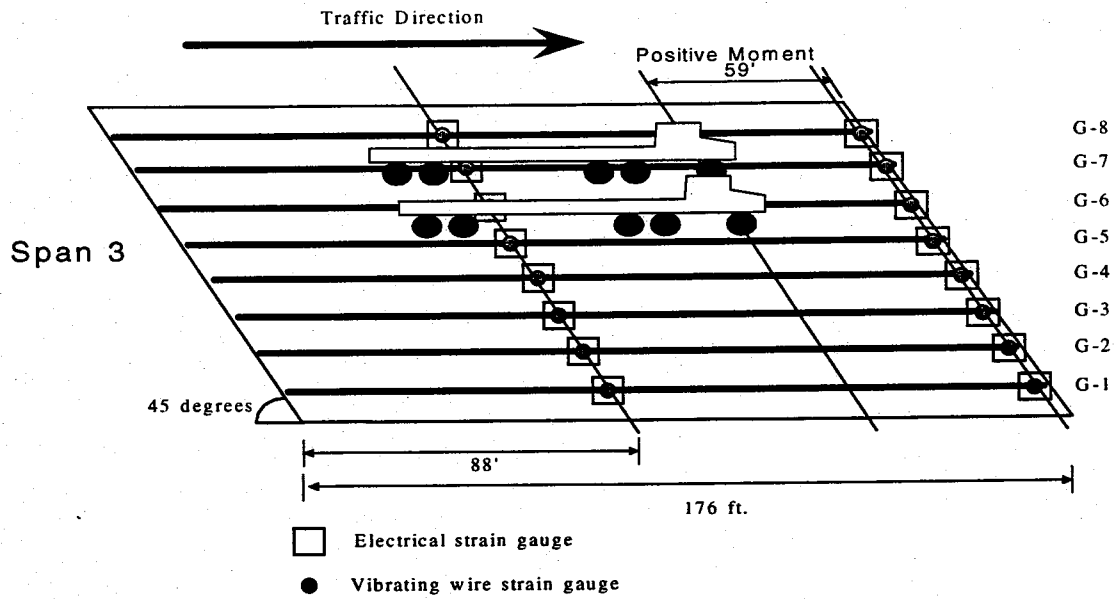


Fig 3.17 Test truck positions and strain gage locations for positive moment

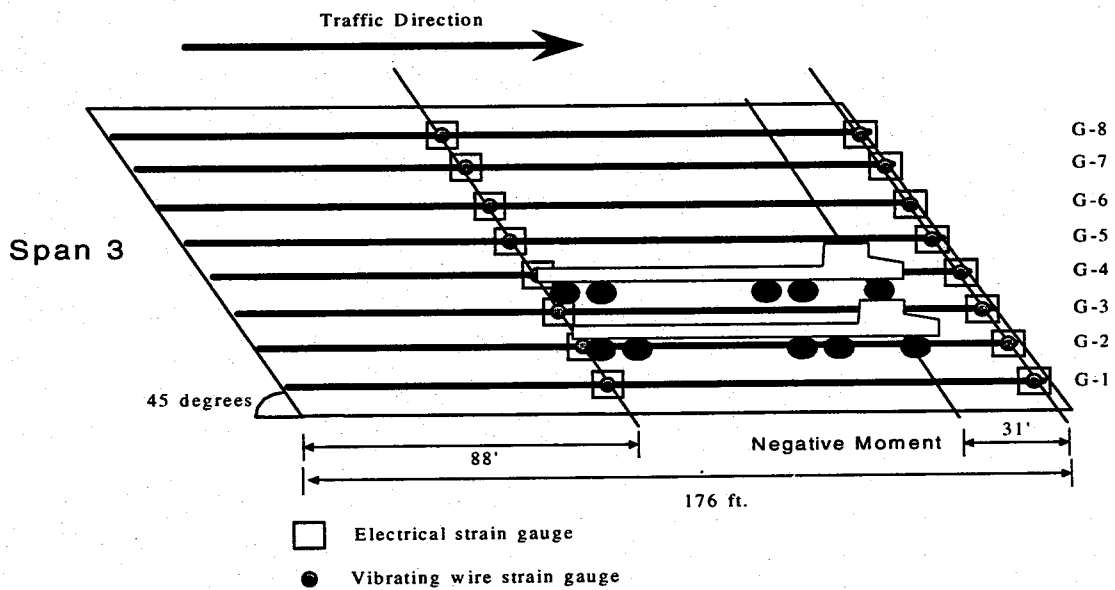


Fig 3.18 Test truck positions and strain gage locations for negative moment

BRIDGE # 100477

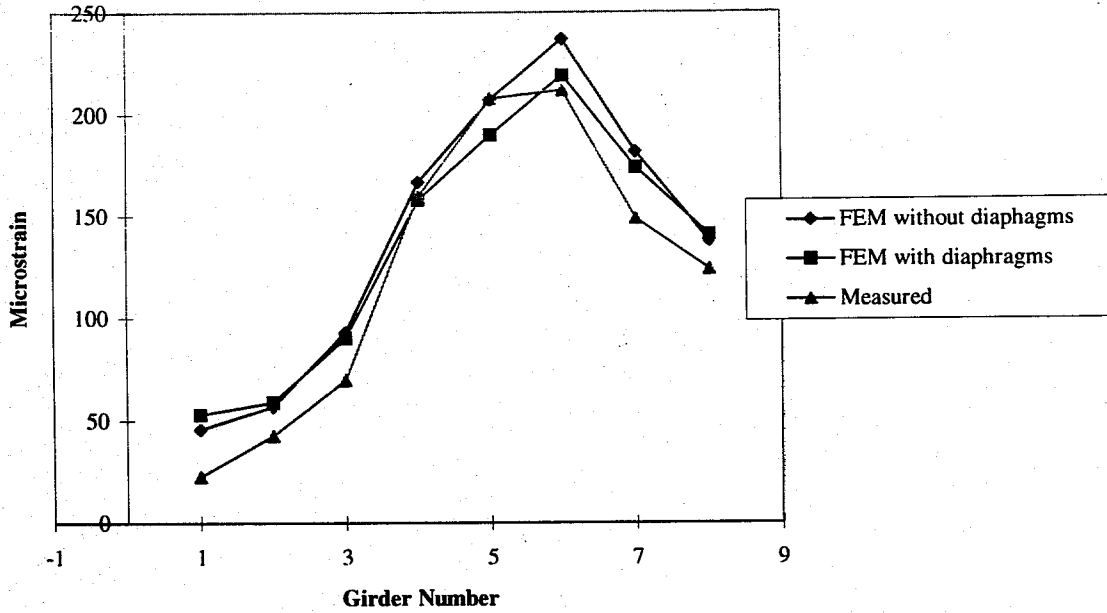


Fig 3.19 Transverse strain distribution at mid-span for trucks positioned at maximum positive moment location

BRIDGE # 100477

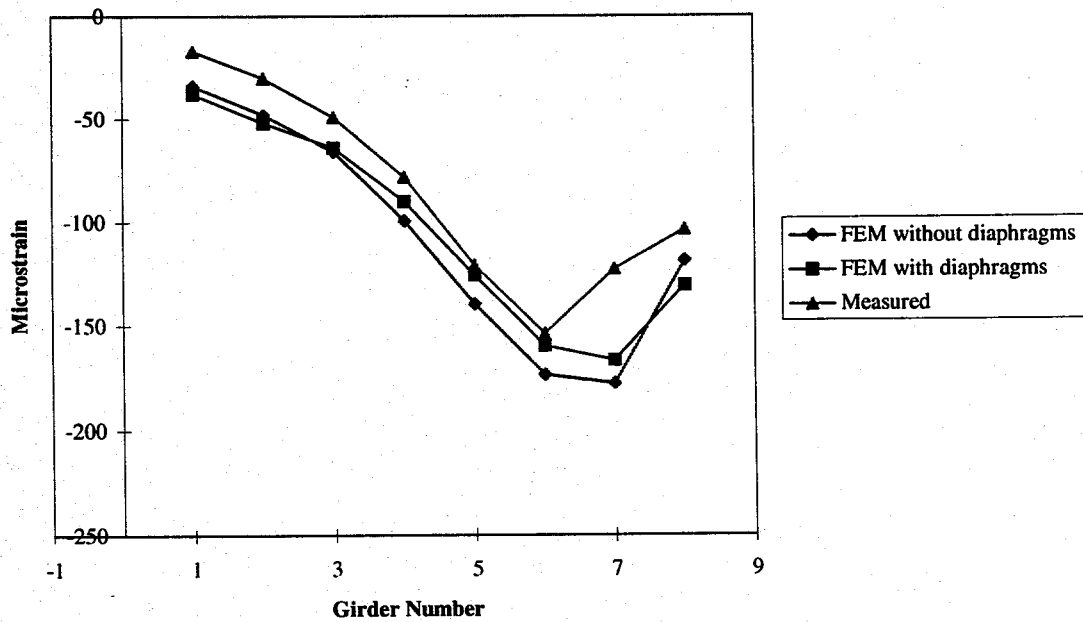


Fig 3.20 Transverse strain distribution over the support for trucks positioned at maximum positive moment location

BRIDGE # 100477 (trucks at max. -ve)

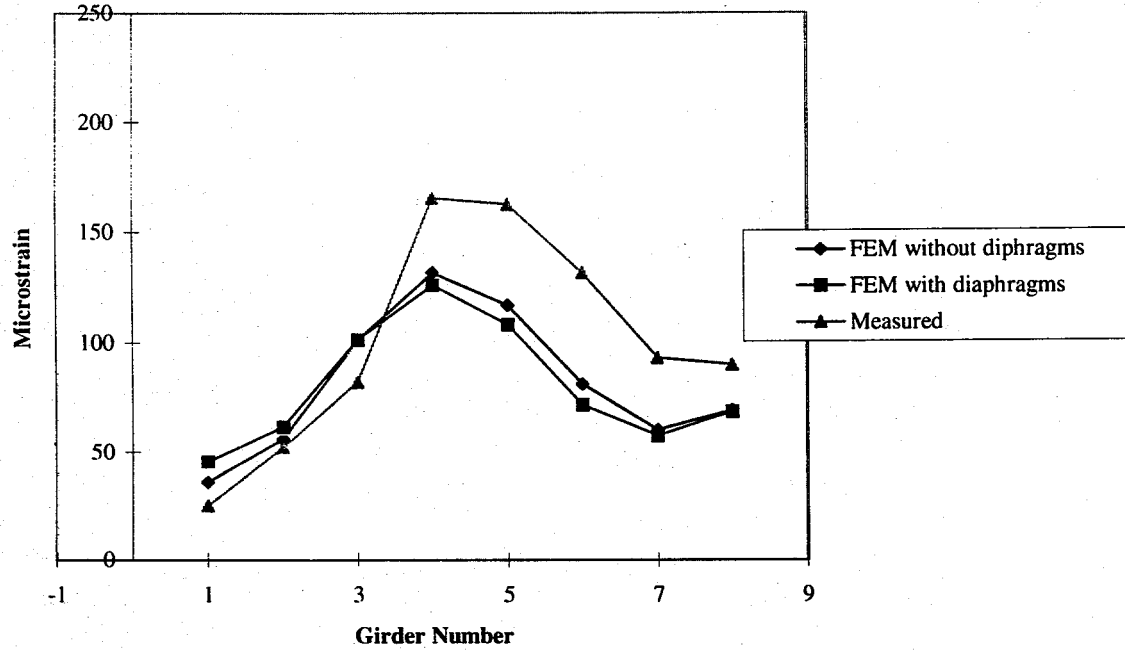


Fig. 3.21 Transverse strain distribution at mid-span for trucks positioned at negative moment location

BRIDGE # 100477 (trucks at max. -ve)

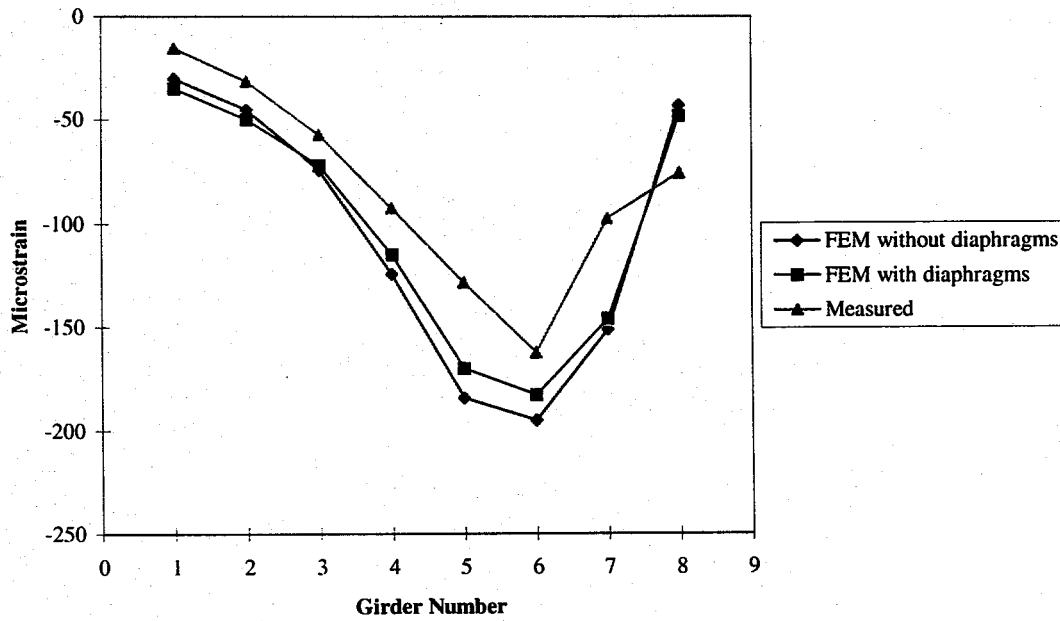


Fig. 3.22 Transverse strain distribution over the support for trucks at negative moment location

Table 3.7 Load distribution factors for bridge #100477

	AASHTO	LRFD	FEM without diaphragms	FEM with diaphragms	Measured
Max. positive moment	1.38	1.06	0.841171	0.808118	0.857432
Max. negativ moment	1.38	1.06	0.921986	0.893773	0.986301

CHAPTER 4

SHEAR LOAD DISTRIBUTION OF CONTINUOUS SLAB-ON-GIRDER BRIDGES

4.1 INTRODUCTION

The AASHTO code assumes that the transverse distribution patterns of various load effects (moment, shear, etc.) are similar. This means the load distribution factors for bending moment and shear are the same along the span. This assumption is difficult to justify and the difference between the distribution factors for moments and shears can sometimes become so large that special attention has to be given for shear distribution factors. Therefore, the LRFD code has two different sets of equations for flexural and shear load distribution factors. The AASHTO and LRFD codes do not specify special provisions for load distribution factors for continuous bridges.

It is important to understand the effect of various parameters on shear load distribution of continuous slab-on-girder bridges. The studies on: the flexural load distribution factors were carried out in Phase II. The main parameters that affect load distribution are compared for single and multiple span bridges. This study focuses on five main parameters: spacing between the girders, variation of skew angle, variation in the number of spans, ratio between adjacent two spans, and span length. The parametric study includes a total of 116 cases that have been investigated and presented in this chapter. The shear distribution factors are determined using FEM analyses and compared with the AASHTO and LRFD codes.

4.2 SHEAR LOAD DISTRIBUTION FACTORS

The AASHTO method of load distribution reduces the complex analysis of a bridge subjected to one or more vehicles to the simple analysis of a beam. According to this method, the maximum moment or shear in a girder can be obtained by treating a girder as a one-dimensional beam subjected to a loading, which is obtained by multiplying one line of wheels of the design vehicle by a load distribution factor. The LRFD approach is similar to AASHTO method, but considers more parameters such as span length, bridge width, slab thickness and number of lanes. The LRFD distribution factors for live load moment and shear are defined for a truck in a lane instead of a single line of wheels. The load distribution factors are presented in this study in the AASHTO format based on a single line of wheels. The LRFD load distribution factors are multiplied by two for comparison with the corresponding AASHTO values.

The proposed method of calculating the shear load distribution factor (DF) based on the Finite Element Method (FEM) and the field tests is shown here:

$$DF = V_{\text{girder}}/V_{\text{bridge}} \quad (4.1)$$

Where:

V_{girder} = the maximum girder shear in the bridge obtained from FEM or field test.

V_{bridge} = the maximum shear in the bridge idealized as one dimensional beam
subjected to a single line of wheels

Since the external shear in the bridge equals the total internal shear in all the girders (field test or FEM),

$$V_{bridge} \times n = \sum_{i=1}^{n_1} V_{ith_girder} \quad (4.2a)$$

Where=

n = number of wheel loads across the width of the bridge

i = girder number

n₁ = number of girders

The shear in the bridge, V_{bridge} due to a single line of wheels can be written as

$$\therefore V_{bridge} = \frac{\sum_{i=1}^{n_1} V_{ith_girder}}{n} \quad (4.2b)$$

Substituting Eqn. 4.2b in Eqn. 4.1, the distribution factor for shear is given by

$$DF = \frac{\left(\frac{V_{girder}}{\sum_{i=1}^{n_1} V_{ith_girder}} \right)}{n} = \frac{n \times V_{girder}}{\sum_{i=1}^{n_1} V_{ith_girder}} \quad (4.3a)$$

Eqn: 4:3 is used to calculate the distribution factor of the interior girder. When calculating the distribution factor for exterior girders, the exterior girder shears replace the maximum shears as follows:

$$DF = \frac{n \times V_{girder,ext}}{\sum_{i=1}^{n_1} V_{ith_girder}} \quad (4.3b)$$

4.2.1 Finite Element Method

The ANSYS finite element program (Swanson Analysis Systems, Inc. 1995) was used in the analysis of the continuous slab-on-girder bridges. The finite element modeling presented in section 2.2.2 (Fig. 2.2) consists of solid slab and girder elements. The deck slab was modeled using a 4-node quadrilateral shell element (SHELL 63) with six degrees of freedom (u_x u_y u_z rot_x rot_y rot_z) at each node. The girder was modeled using a 4-node quadrilateral shell element (SHELL 63) for the web and two elastic frame elements (BEAM 4) for the top and bottom flanges. The frame element is a 3-D 2-node element with six degrees of freedom (u_x u_y u_z rot_x rot_y rot_z). Composite action between the deck slab and the girder is achieved by coupling vertically the nodes in the deck slab and the nodes in the top flange of the girder. Identical translations in vertical direction for both deck and girder are prescribed in the coupling. The deck slab finite element mesh was selected with an aspect ratio less than 1: 2. The boundary conditions imposed on the model were selected to represent the actual behavior of the continuous bridges. The nodes at each end of the bridge were prevented from translating in x, y, and z directions. The bottom flange nodes at the interior supports of the continuous bridges were prevented from vertical movements. The output results from the ANSYS program provide the shear stresses for the element. The maximum shear stress in the girder is approximately close to the center of the web. The maximum shear forces were

4.2.2 AASHTO and LRFD Shear Distribution Factors

There are no special provisions for calculating shear load distribution factors for multiple span (continuous) bridges in AASHTO and LRFD specifications. The AASHTO Specifications (1992) and the LRFD bridge design specifications (1994) for simply supported bridges were used in the comparisons with the finite element results. The AASHTO Specifications (1992) take into account only the spacing, S between the girders:

Distribution Factor	
One lane	Two or more lanes
$S/7.0$	$S/5.5$ (4.4)
(S less than 10 ft.)	(S less than 14 ft.)

The LRFD specifications recommend the following for the shear load distribution factor per lane for interior beams:

One lane loaded

$$g = 0.36 + \frac{S}{7600} \quad (4.5 \text{ SI})$$

$$g = 0.36 + \frac{S}{25.0} \quad (4.5 \text{ US})$$

Two or more lanes loaded

$$g = 0.2 + \frac{S}{3600} - \left(\frac{S}{10700} \right)^{2.0} \quad (4.6 \text{ SI})$$

$$g = 0.5 * \left(0.4 + \frac{S}{6} - \left(\frac{S}{25} \right)^{0.2} \right) \quad (4.6 \text{ u s})$$

When the supports are skewed, the shear in the beams may be reduced using the following skew factor:

$$\text{skew factor} = 1.0 + 0.20 \left(\frac{L t_s^3}{K_g} \right)^{0.3} \tan \theta \quad (4.7 \text{ SI})$$

$$\text{skew factor} = 1.0 + 0.20 \left(\frac{12.0 L t_s^3}{K_g} \right)^{0.3} \tan \theta \quad (4.7 \text{ US})$$

where

g	=	distribution factor
S	=	spacing of supporting component (mm or ft.)
L	=	span length (mm or ft.)
K_g	=	longitudinal stiffness parameter (mm^4 or in^4)
t_s	=	depth of concrete slab (mm or in)
K_g	=	$n (I + A e_g^2)$
n	=	modular ratio between beam and deck
I	=	second moment of inertia of beam (mm^4 or in^4)
A	=	area of the beam (mm^2 or in^2)
e_g	=	distance between centers of gravity of the basic beam and deck (mm or in.)

The distribution factors for exterior beams should be determined by applying the lane fraction (g) as specified below:

$$g_{ext} = e(g) \quad (4.8)$$

$$e = 0.6 + \frac{d_e}{3000} \quad (4.9 \text{ SI})$$

$$e = \frac{6 + d_e}{10} \quad (4.9 \text{ US})$$

where

d_e = distance between the center of exterior beam and the interior edge of curb or traffic barrier (mm or ft.)

4.3 PARAMETRIC STUDY

4.3.1 Introduction

The important design variables such as number of spans, skew angle variation, adjacent span length ratios, girder spacing and span length are selected to study their effects on the continuous bridges. Fig. 4.1 shows the typical continuous slab-on-girder bridge used in the analysis. The typical two span slab-on-girder bridge has a slab thickness of 7 in., span lengths of 70 ft., and bridge width of 54 ft. The bridge has nine AASHTO type IV girders spaced at 6 ft. center to center (Fig. 4.2). The concrete strength of the girder and the slab is taken as 5000 psi in the study.

The continuous slab-on-girder bridge is divided longitudinally into twenty elements for each span and the slab deck is divided in the transverse direction into two elements between each girder (Fig. 4.3). The material properties (Elastic modulus, E , Poisson's ratio, ν , and modulus of rigidity, G) used in the FEM analysis are presented in Table 4.1 along with the sectional properties of the AASHTO type IV girder (Area, A and moments of inertia, I_y and I_z).

Table 4.1 Material and sectional properties for typical continuous slab-on-girder bridge

Material Properties		E_{deck} (ksi)	E_{girder} (ksi)	Poisson's ratio, ν	G (ksi)	
		4031	4031	0.2	1679	
Section properties	Slab	Thickness = 7 in.				
	Top Flange	A (in ²)	I_y (in ⁴)	I_z (in ⁴)	T_{ky} (in)	T_{kz} (in)
AASHTO IV girder	Web	Thickness = 8 in.				
	Bottom Flange	A (in ²)	I_y (in ⁴)	I_z (in ⁴)	T_{ky} (in)	T_{kz} (in)
		312	3744	17576	26	12

* E_{deck} , E_{girder} = Elastic modulus of the deck slab and girder respectively,
 G = Modulus of rigidity,
 A = Area of cross section of the girder,
 I_y , I_z = Moment of inertia of the girder in y and z direction respectively,
 T_{ky} , T_{kz} = Thickness and width of the beam elements respectively.

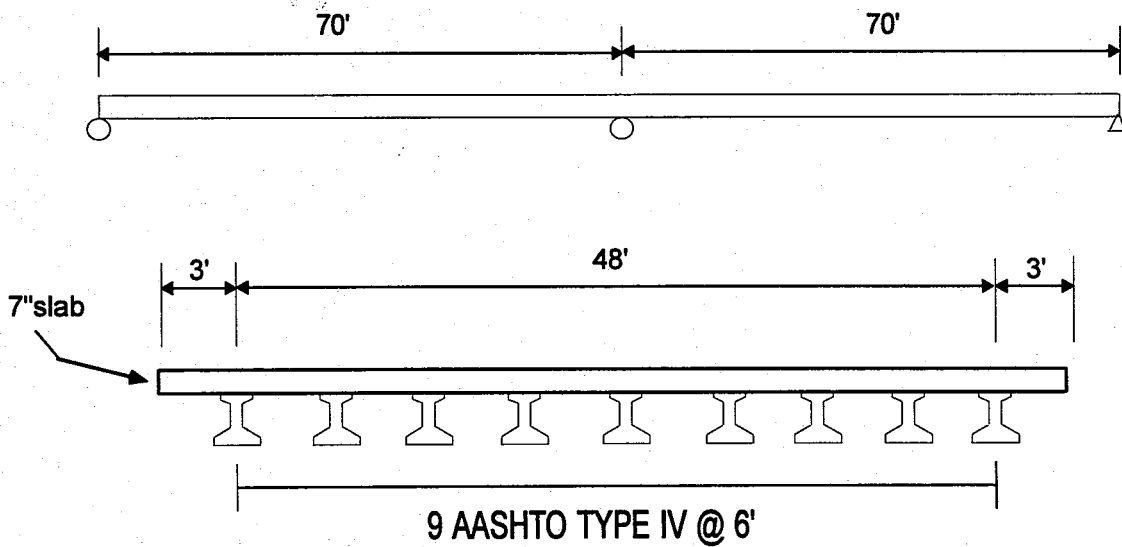


Fig. 4.1 Typical continuous slab-on-girder bridge

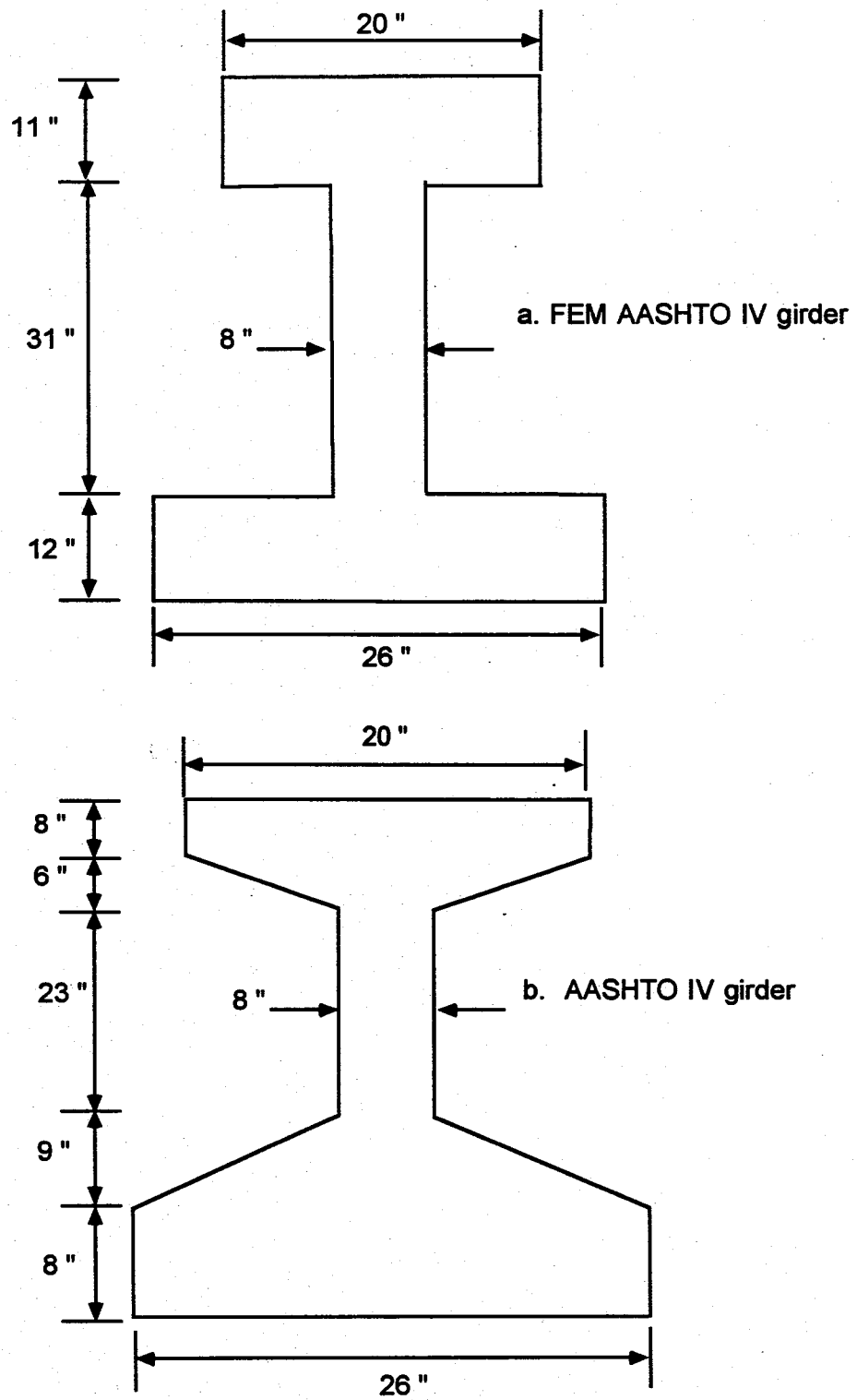


Fig. 4.2 AASHTO type IV girder details

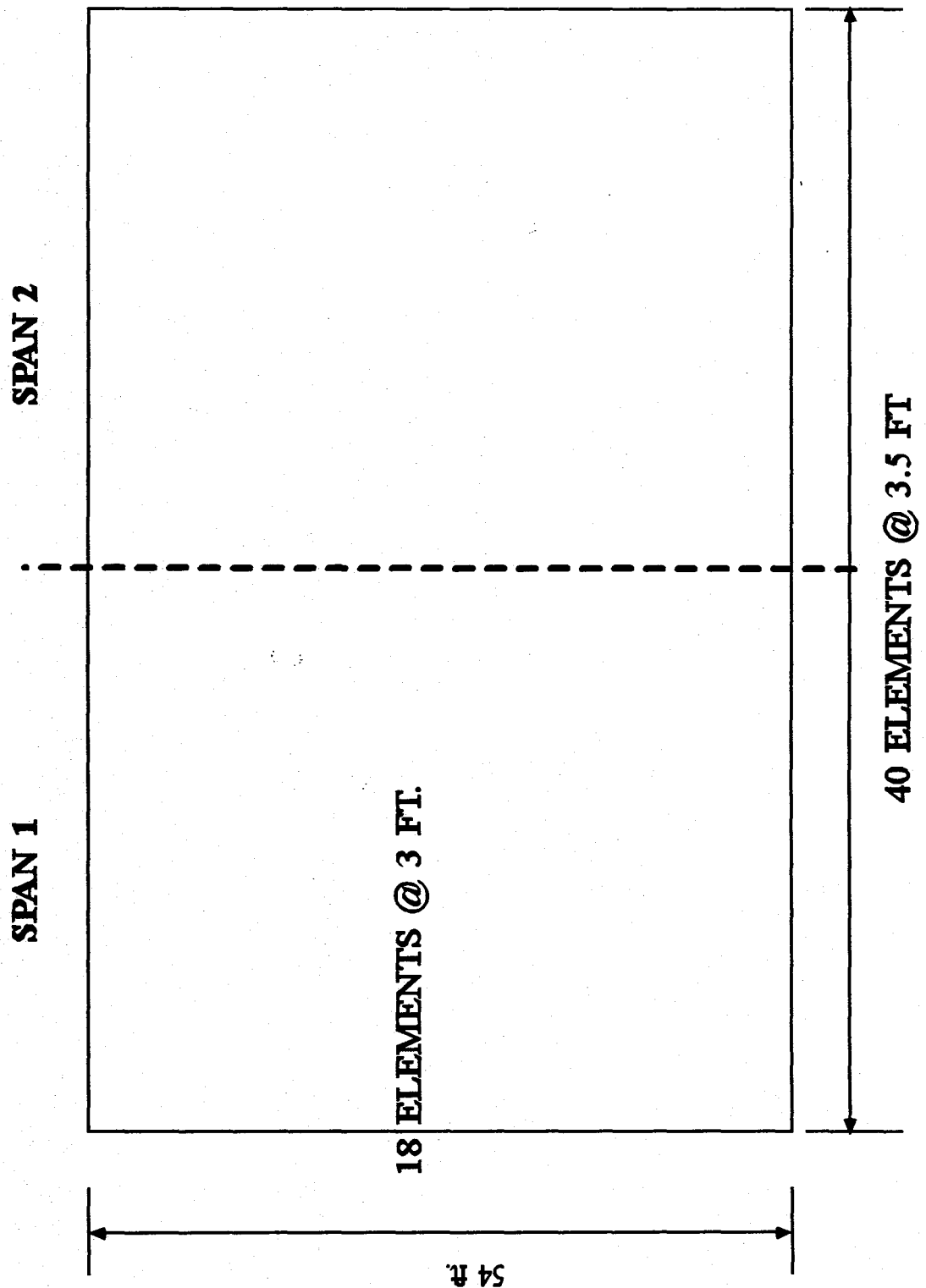
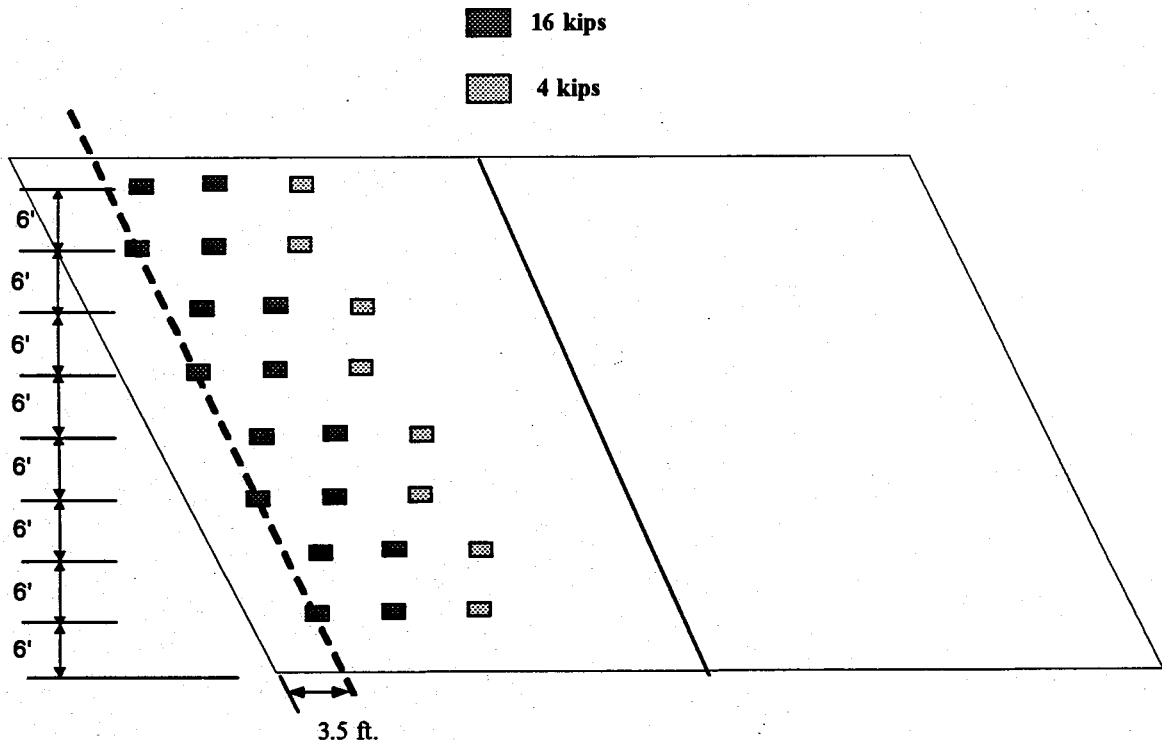


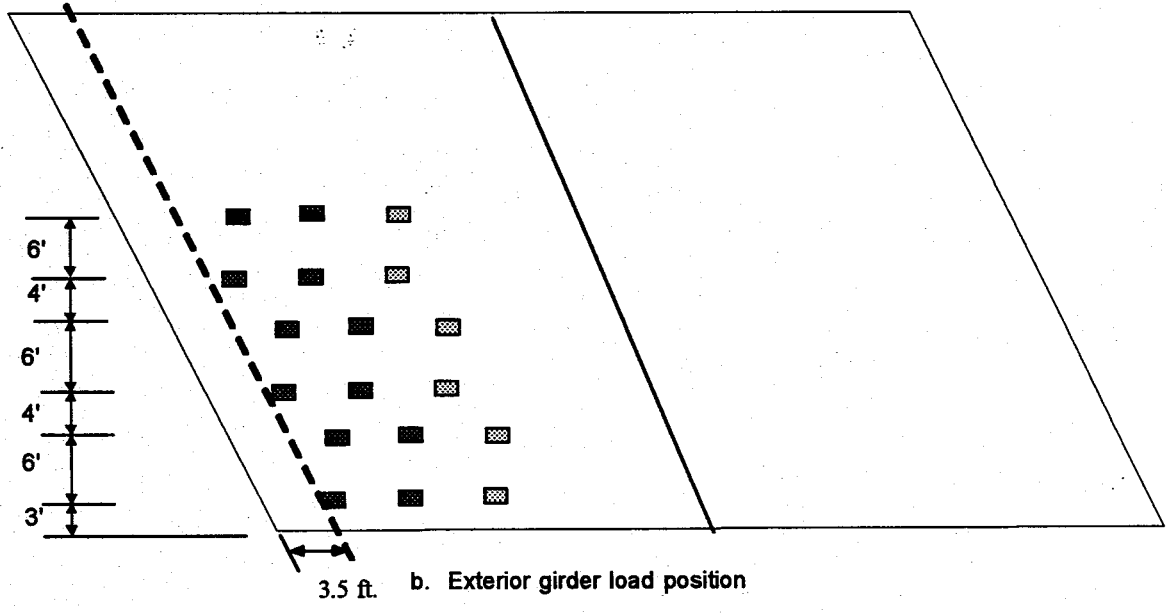
Fig. 4.3 Typical FEM model for shear load distribution parametric study

4.32 Truck Load Position

The AASHTO HS20-44 trucks were used with a minimum spacing of 14 ft. between axles to produce the maximum shear. Based on the analyses carried out in Phase II, three trucks loaded transversely were used in this study for determination of load distribution factors for the exterior girders. Four trucks were also used in calculating the load distribution factors of interior girders. Typical truck loading positions for interior and exterior girders are shown in Fig. 4.4. The truck loading positions in the longitudinal direction were determined so as to obtain the maximum shear in the continuous bridge. The longitudinal positions of the trucks for maximum shear are close to the supports. Therefore, the trucks were placed with the back tandem at 3.5 ft from the supports corresponding to the first node on the deck slab element.



a. Interior girder load position



b. Exterior girder load position

Fig. 4.4 Truck loading positions in the transverse direction for interior and exterior girders

4.3.3 Case Studies

The parametric study is focused on five main parameters: skew angle, number of spans, number of girders per lane, ratio between two adjacent spans, and span length. A total of 116 cases have been investigated in this parametric study (Table 4.2). The effects of varying the skew angle of a two-span continuous bridge were studied in the first section, 4.3.3.1. For a certain skew angle, the bridges were analyzed for four truck loading positions to determine the shear load distribution factors for the interior and exterior girders at the exterior and interior supports.

The second section, 4.3.3.2 involves changing the number of spans with two different skew angles. The third section, 4.3.3.3 focuses on the effect of varying the number of girders per lane. The effects of varying the length of continuous spans for two different skew angles are studied in the fifth section, 4.3.3.5. Each bridge in the above cases as analyzed for four truck loading positions to determine the shear load distribution factors for the interior and exterior girders at the exterior and interior supports.

The effects of varying the ratios between the adjacent spans for two different skew angles are investigated in the fourth section, 4.3.3.4. Each bridge in the fourth section was analyzed for six truck loading positions to calculate the shear load distribution factors for the interior and exterior girders at the three supports.

Table 4.2 Summary of parametric studies for shear load distribution on continuous slab-on-girder bridges*

Parameter	Span lengths (ft.)			Skew angles (degrees)	Cases	Comments
Skew angle (2 spans)	70, 70			0	4	Cases:Interior 1st support Exterior 1st support Interior 2 nd support Exterior 2 nd support
	70, 70			30	4	
	70, 70			45	4	
	70, 70			60	4	
Number of spans (1-3)	70			0	4	Cases:Interior 1st support Exterior 1st support Interior 2 nd support Exterior 2 nd support
	70, 70			0	4	
	70,70,70			0	4	
	70			30	4	
	70, 70			30	4	
	70,70,70			30	4	
Number of girders per lane (length, spacing ft., # girders)	70,70	6	9	0	4	Cases:Interior 1st support Exterior 1st support Interior 2 nd support Exterior 2 nd support
	70,70	8	7	0	4	
	70,70	12	5	0	4	
	70,70	6	9	30	4	
	70,70	8	7	30	4	
	70,70	12	5	30	4	
Ratio between two spans	70,70			0	6	Cases:Interior 1st support Exterior 1st support Interior 2 nd support Exterior 2 nd support Interior 3 rd support Exterior 3 rd support
	70, 105			0	6	
	70, 140			0	6	
	70,70			30	6	
	70, 105			30	6	
	70, 140			30	6	
Span length	70,70			0	4	Cases:Interior 1st support Exterior 1st support Interior 2 nd support Exterior 2 nd support
	105,105			0	4	
	70,70			30	4	
	105,105			30	4	
Total					116	

(*All cases have a bridge width of 54 ft. and a slab thickness of 7 in.)

4.3.3.1 Skew angle

Skew angle is an important factor in the bridge design. The LRFD code provides formulae for adjusting the load distribution factors for different skew angles. The code, however, does not specify special recommendations for continuous bridges. The results from FEM analyses of the continuous bridges are compared with LRFD load distribution factors based on single span skew bridges.

Eqns. 4.3a and 4.3b are used to calculate the distribution factors of the interior and exterior girders respectively. Fig. 4.5 shows that the shears increase with increase in skew angles for interior girders at the exterior support. The increase in skew angle results in non-uniform transverse shear distributions in the girders. The shear load distribution factors at the exterior support for interior girders are shown in Fig. 4.6. The shear load distribution factors based on FEM analysis are smaller than those based on LRFD code and generally the trend remains the same. The FEM shear load distribution factors are smaller than the AASHTO values for straight bridges and greater for skew bridges. Fig. 4.7 shows the transverse shear distributions for interior girders close to the interior support. In general, the maximum shear forces in the bridge tend to increase with the increase in skew angle. The shear load distribution factors are shown in Fig. 4.8, which shows the same trend as that shown in Fig. 4.6 for the exterior support. The transverse shear distributions for exterior girders close to the exterior support are shown in Fig. 4.9. The graph shows the effect of asymmetric truck loading with respect to the width of the bridge. The shear load distribution factors for the exterior girders close to the exterior support are shown in Fig. 4.10, which shows the same trend as that for the interior girders. Fig. 4.11 shows the transverse shear distributions for exterior girders close to the interior support for different skew angles. Generally, for skew angles of 30 and 45 degrees, a small increase in shears is seen in the exterior girder. Fig. 4.12 shows the shear load distribution factors for the exterior girder close to the interior support. There is a slight increase in the factors based on LRFD specifications, whereas the factors determined from FEM analyses are lower than those based on LRFD and AASHTO nodes.

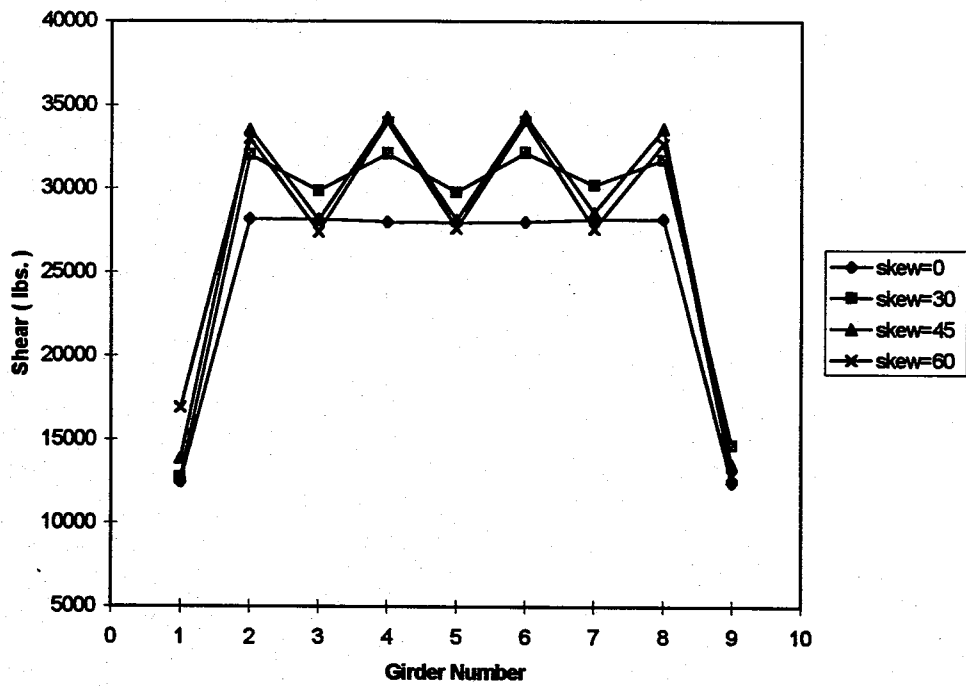


Fig 4.5 Shear distributions at exterior support for different skew angles (Interior Girder Loading)

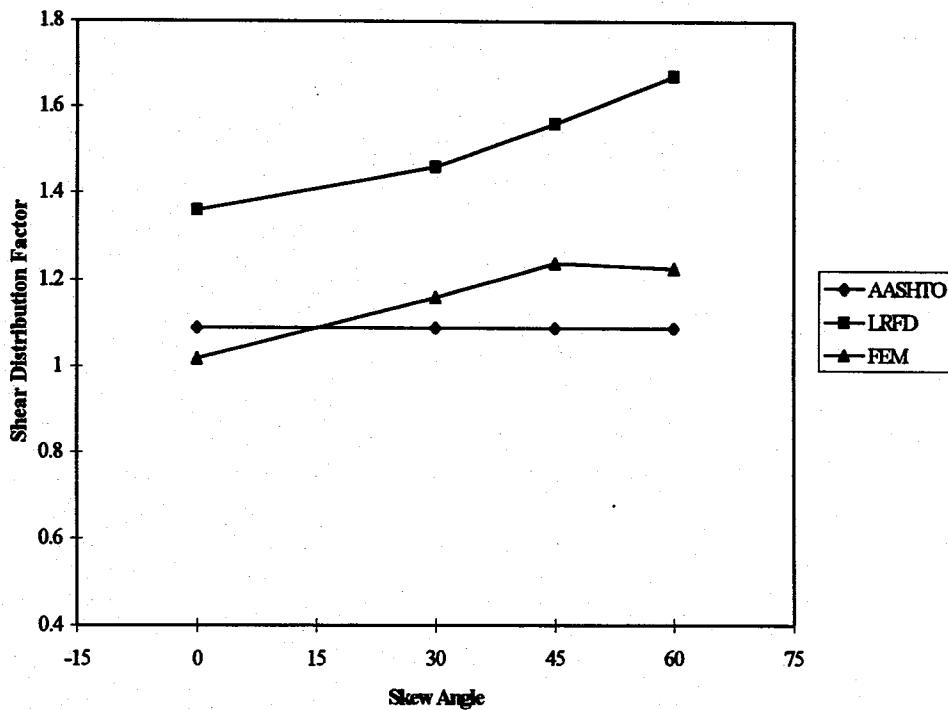


Fig. 4.6 Shear load distribution factors for different skew angles close to the exterior support (interior girder)

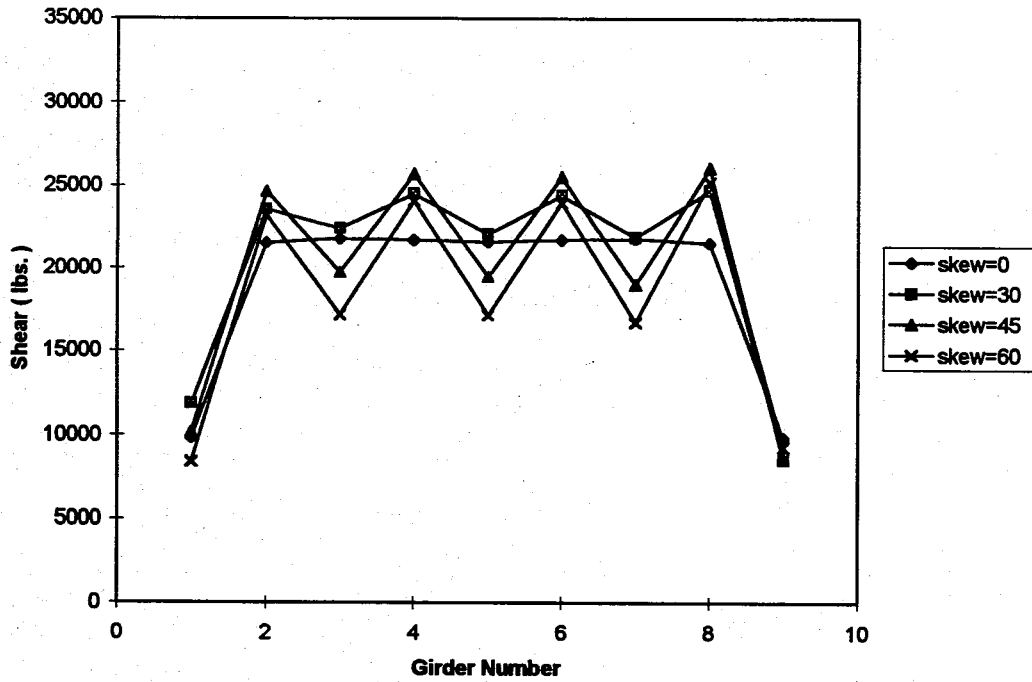


Fig 4.7 Shear distributions at interior support for different skew angles (interior girder loading)

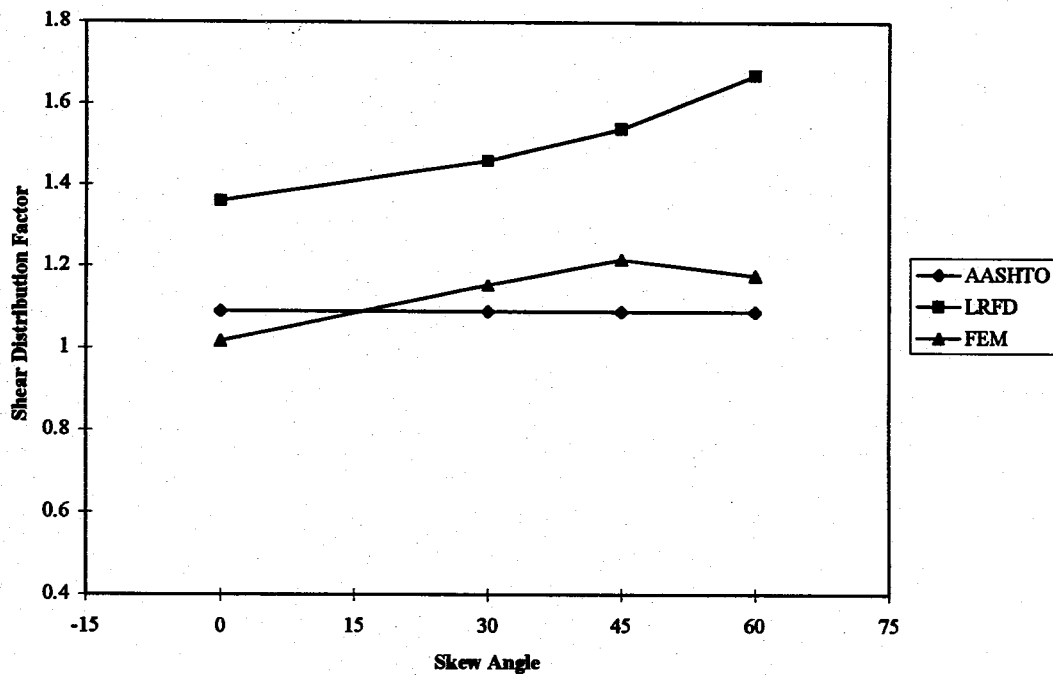


Fig. 4.8 Shear load distribution factors for different skew angles close to the interior support (interior girder)

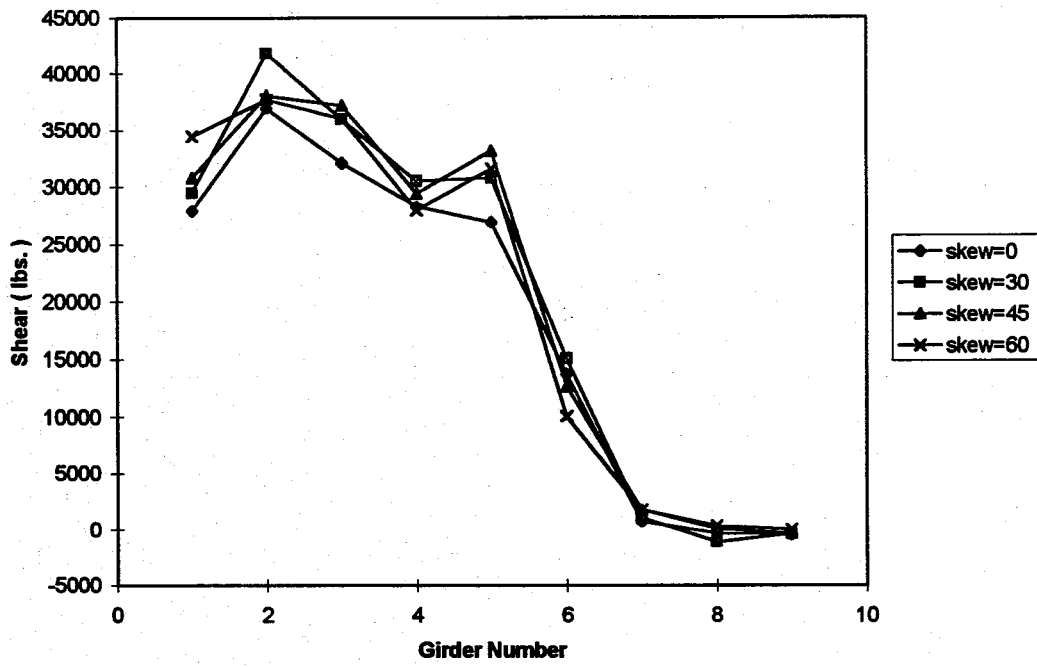


Fig 4.9 shear distributions at exterior support for different skew angles (exterior girder loading)

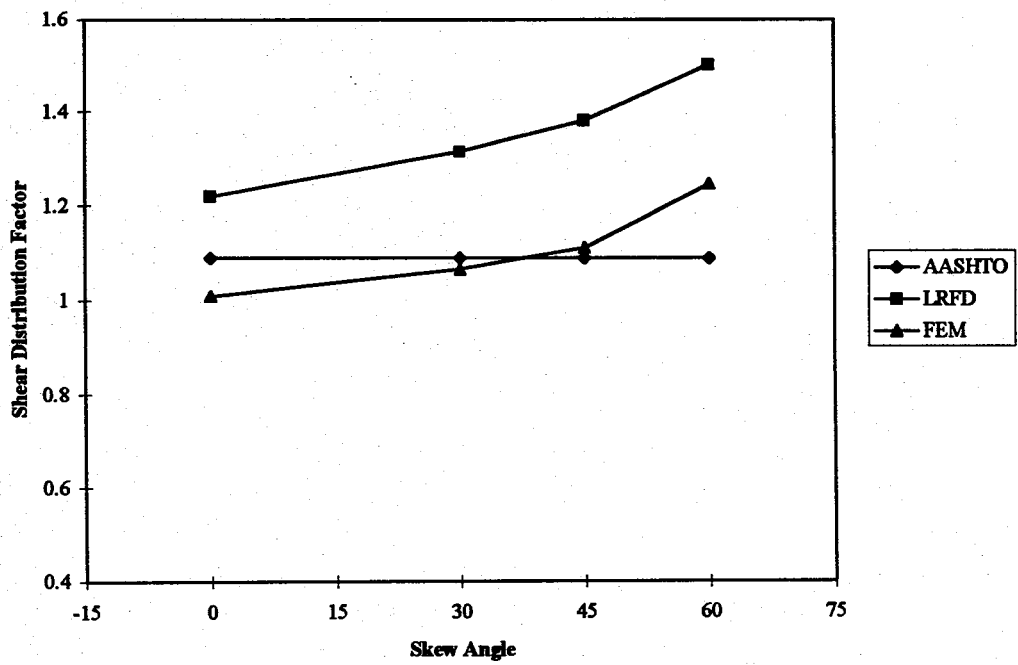


Fig. 4.10 Shear load distribution factors for different skew angles close to the exterior support (exterior girder)

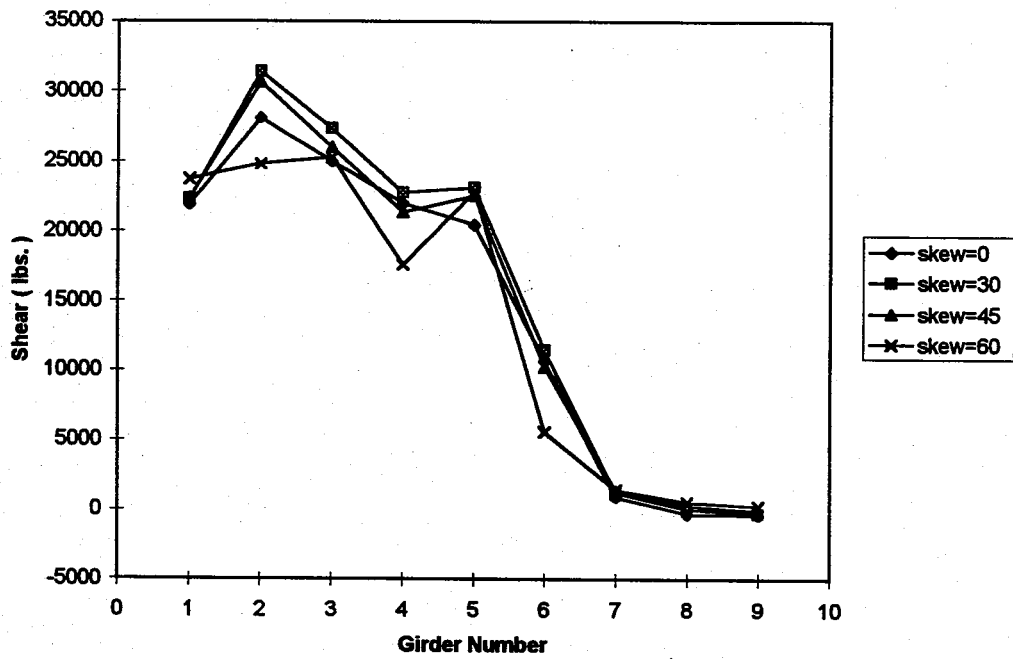


Fig 4.11 Shear distributions at interior support for different skew angles (exterior girder loading)

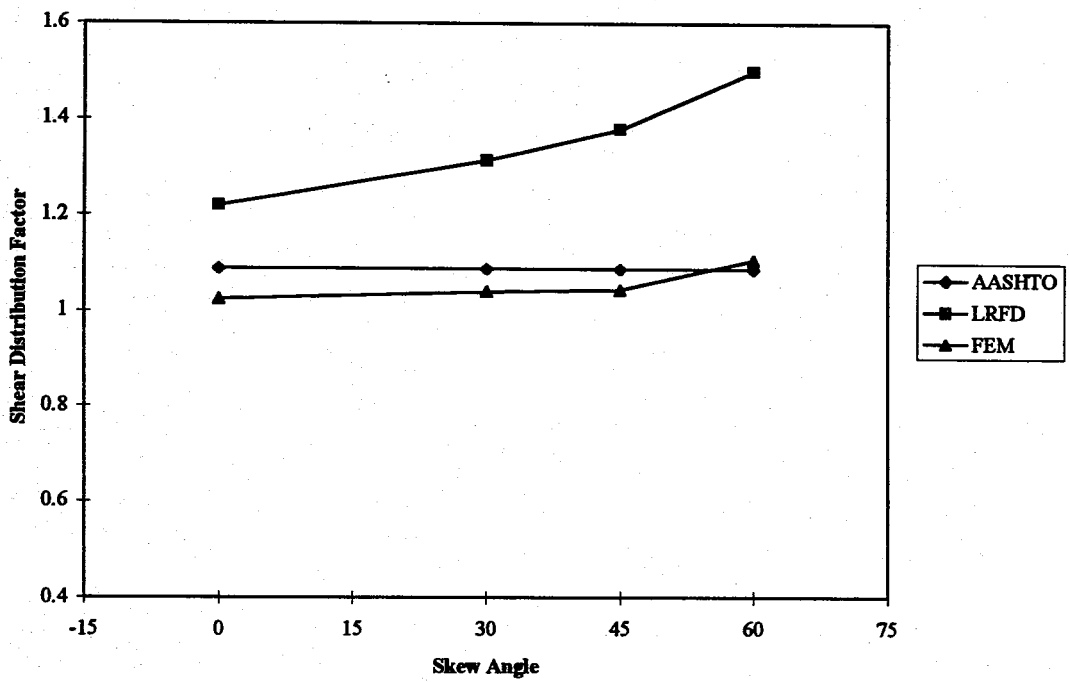


Fig. 4.12 Shear load distribution factors for different skew angles close to the interior support (exterior girder)

4.3.3.2 Number of spans

The effect of the number of spans on the shear load distribution factors is evaluated in this section. The study cases are divided into two sets: straight bridges and skew bridges with a skew angle of thirty degrees. Each bridge set consists of one, two, and three spans for parametric studies. Fig. 4.13 shows the transverse shear distributions for interior girders close to the exterior support of the straight bridges. The shear forces decrease slightly with the increase in number of spans. The shear load distribution factors are shown in Fig 4.14, which shows the factors are constant with the increase in the number of spans and that the AASHTO and LRFD distribution factors are higher than the FEM values. The shear distributions for the interior girders close to the interior support for straight bridges are shown in Fig. 4.15, which also shows a slight decrease in shear with increase in the number of spans. Fig. 4.16 shows the shear load distribution factors for interior girders close to the interior support for straight bridges. The FEM shear load distribution factors are lower than the LRFD and AASHTO values and show no change with increase in the number of spans. Fig. 4.17 shows the shear distribution for exterior girders close to the exterior support for the straight bridges. The change in shear with increase in number of spans is negligible. The shear load distribution factors are shown in Fig. 4.18 for exterior girders in straight bridges close to the exterior support. There is no change in the factors with increase in the numbers of spans and FEM factors are lower than both the LRFD and AASHTO values. The same trend can be seen in Figs. 4.19 and 4.20 for exterior girders close to the interior support.

The transverse shear distributions and the shear load distribution factors for skew bridges were determined for one, two and three spans. It is found that the shear slightly decreases with an increase in the number of spans for both interior and exterior girders close to the interior and exterior supports. The shear load distribution factors based on the FEM are smaller than the LRFD and AASHTO values for interior and exterior girders and remain more or less constant with increase in the number of spans. Typical shear distributions and load distribution factors are shown in Figs 4.21, 4.22, 4.23, and 4.24 for interior and exterior girders close to the interior supports.

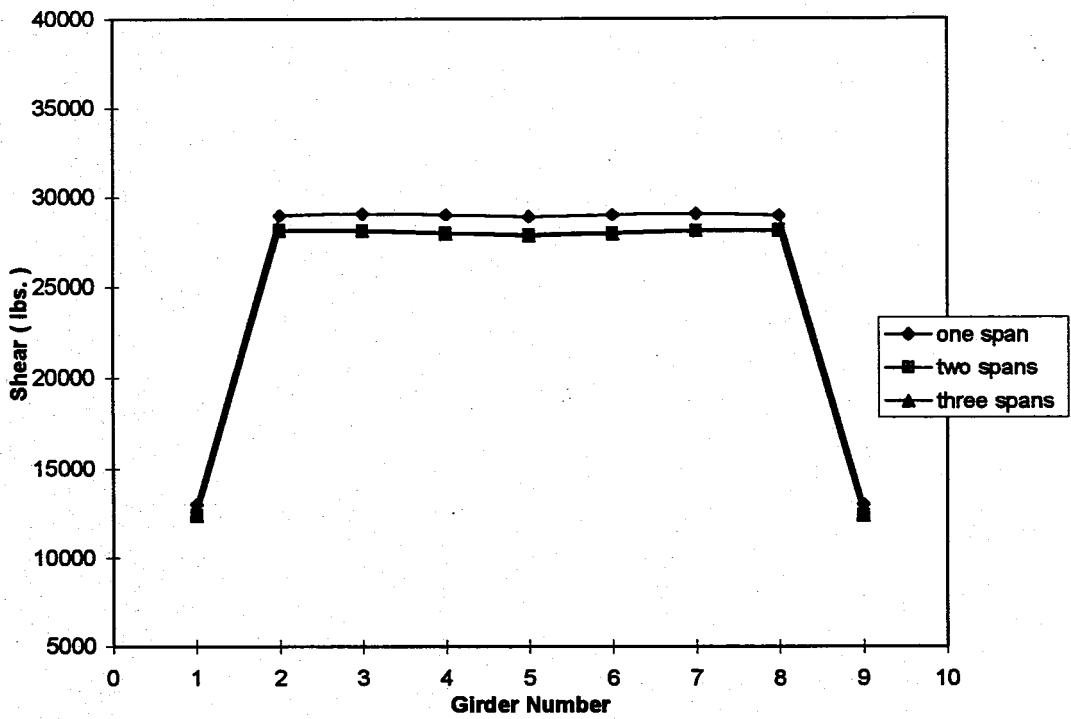


Fig. 4.13 Shear distributions at exterior support for straight bridges with different number of spans (interior girder loading)

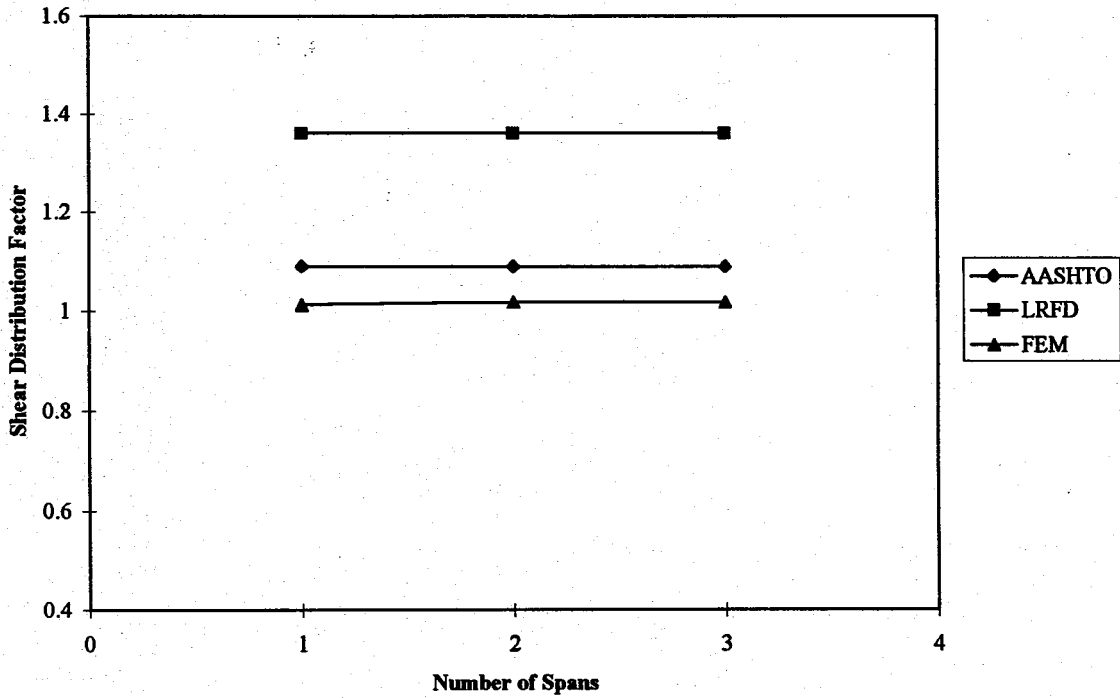


Fig. 4.14 Shear load distribution factors at exterior support for straight bridges with different number of spans (interior girder)

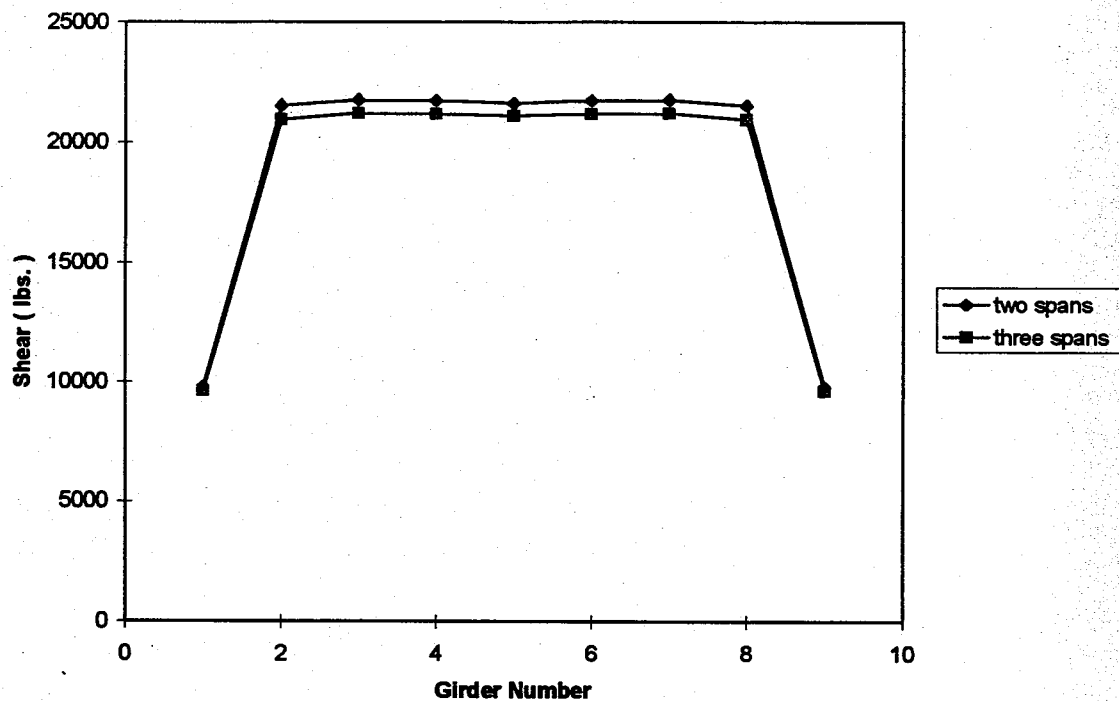


Fig. 4.15 Shear distributions at interior support for straight bridges with different number of spans (interior girder loading)

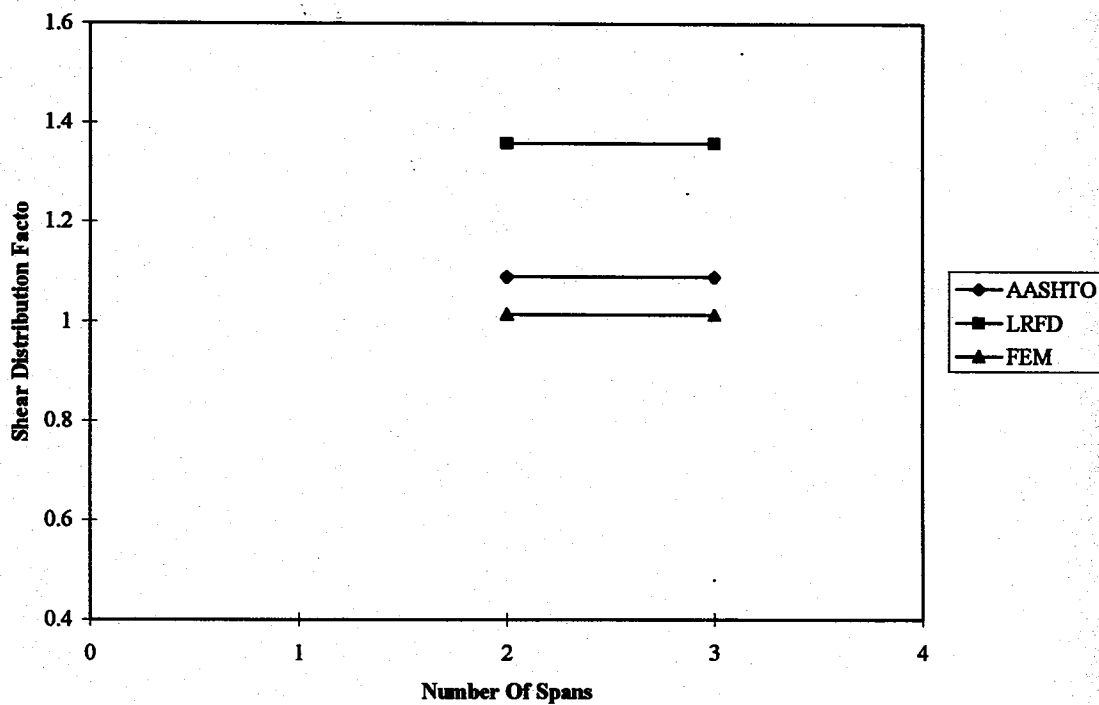


Fig. 4.16 Shear load distribution factors at interior support for straight bridges with different number of spans (interior girder)

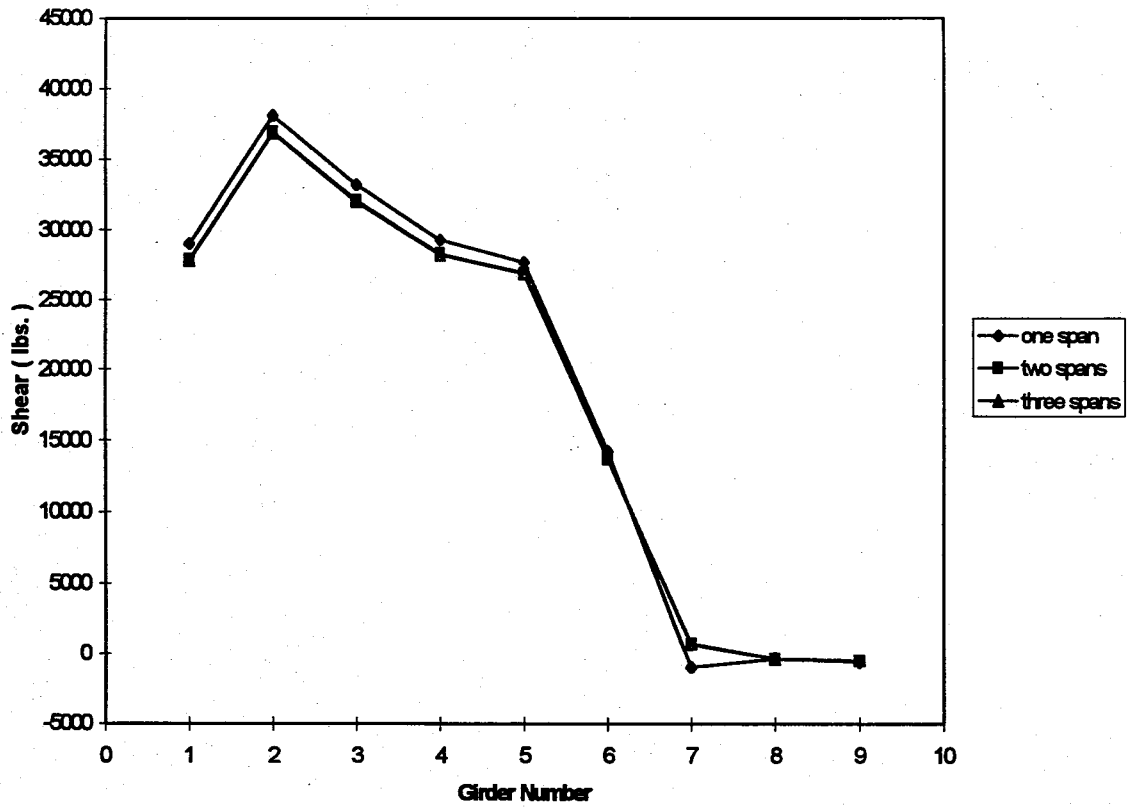


Fig. 4.17 Shear distributions at exterior support for straight bridges with different number of spans (exterior girder loading)

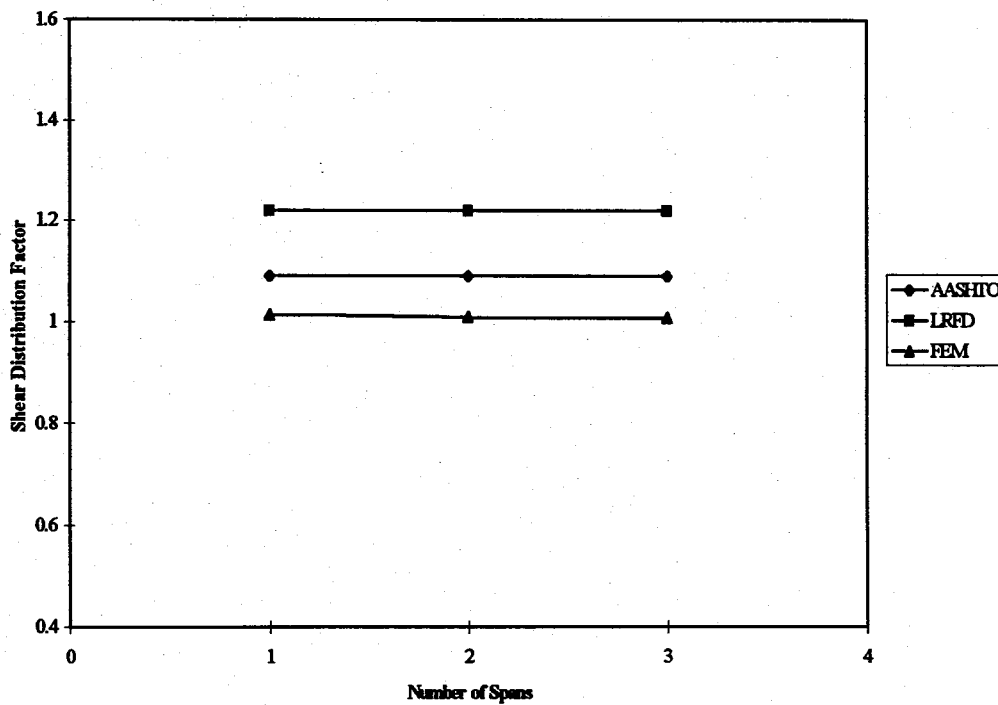


Fig. 4.18 Shear load distribution factors at exterior support for straight bridges with different number of spans (exterior girder)

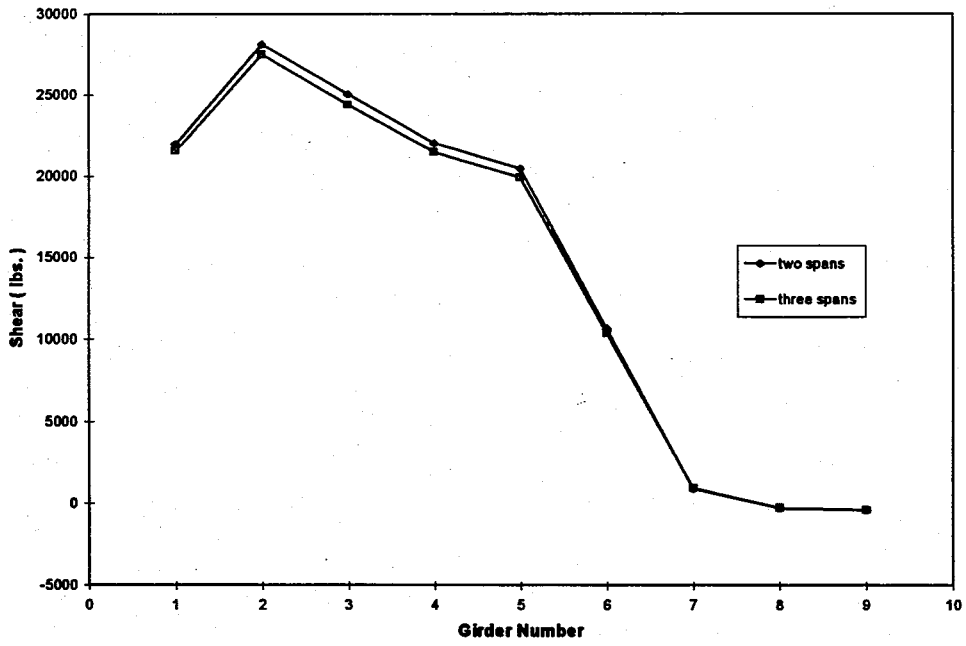


Fig. 4.19 Shear distributions at interior support for straight bridges with different number of spans (exterior girder loading)

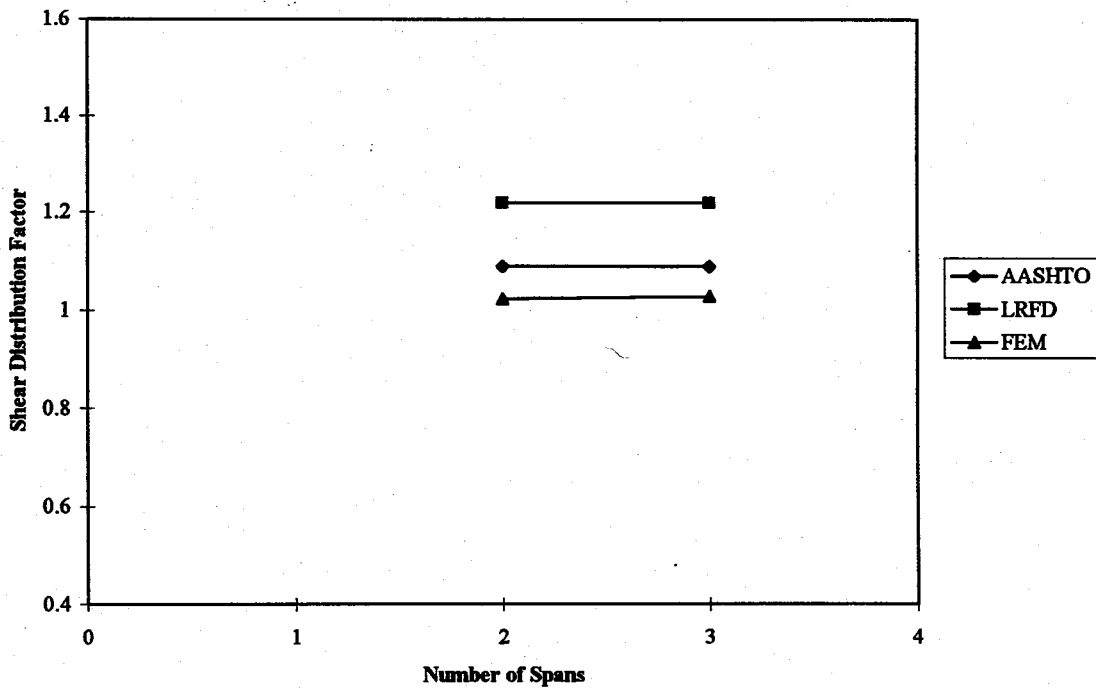


Fig. 4.20 Shear load distribution factors at interior support for straight bridges with different number of spans (exterior girder)

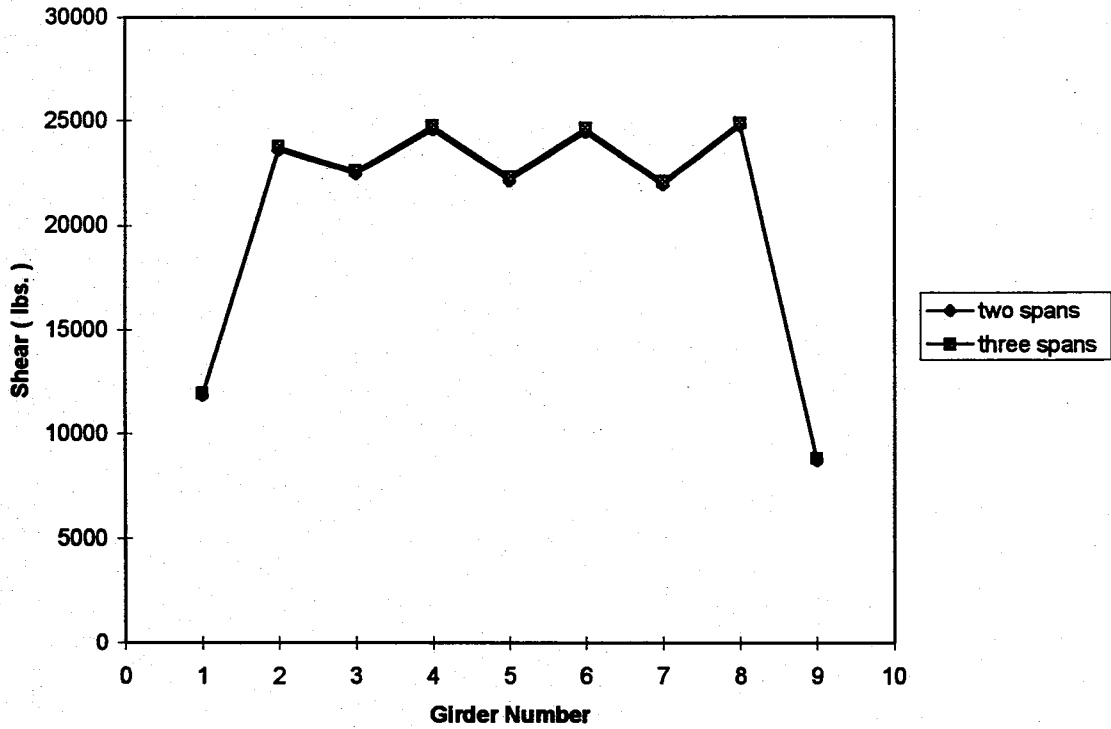


Fig. 4.21 Shear distributions at interior support for skew bridges with different number of spans (interior girder loading)

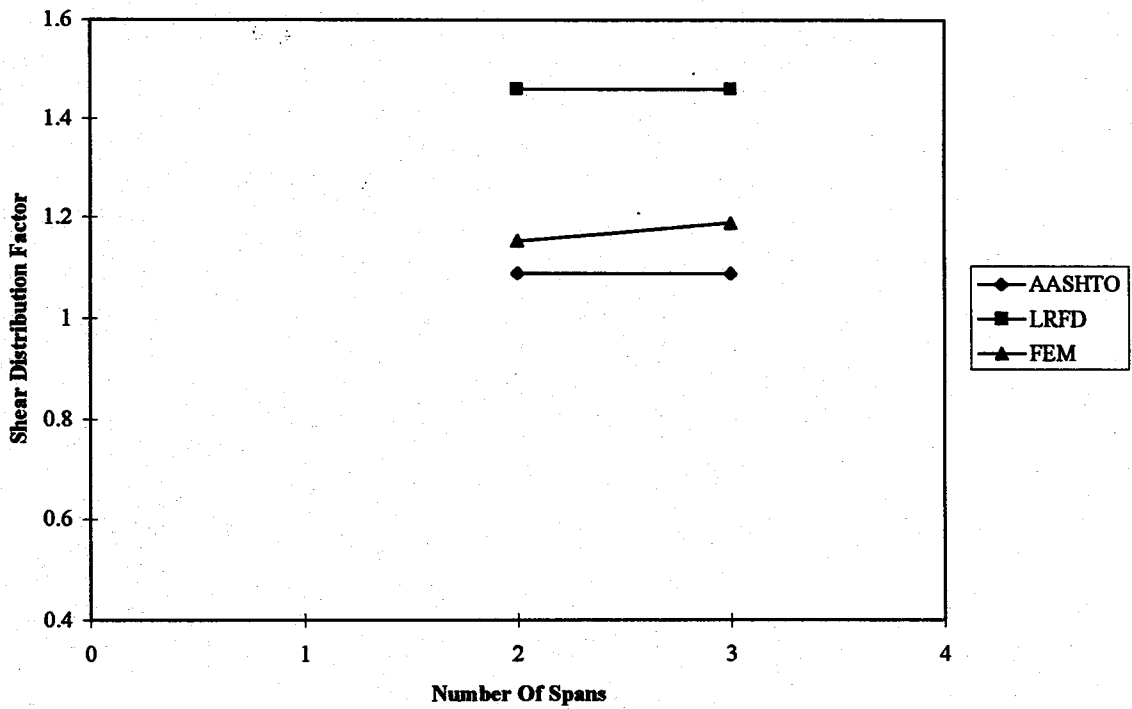


Fig. 4.22 Shear load distribution factors at interior support for skew bridges with different number of spans (interior girder)

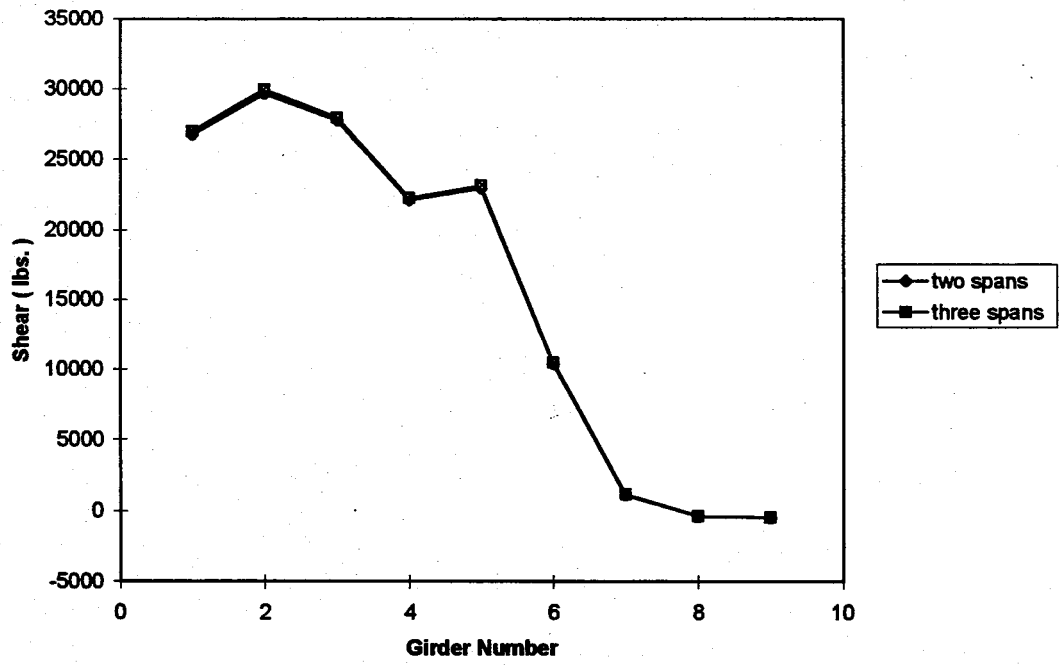


Fig. 4.23 Shear distributions at interior support for skew bridges with different number of spans (exterior girder loading)

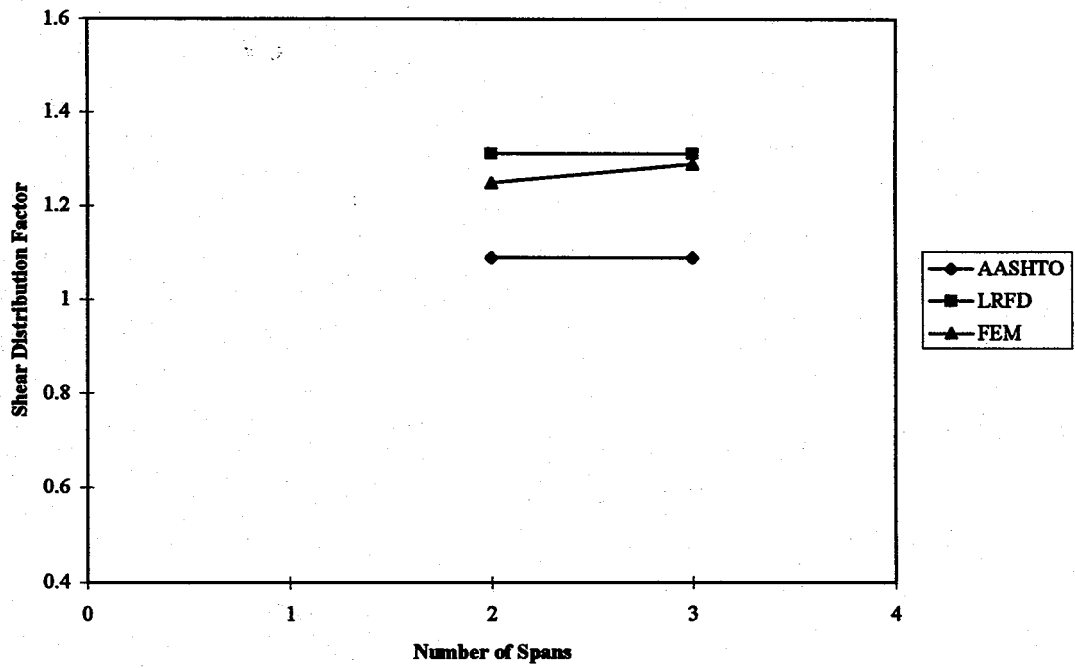


Fig. 4.24 Shear load distribution factors at interior support for skew bridges with different number of spans (exterior girder)

4.3.3.3 Number of Girders per Lane

The shear load distribution factors are dependent on the number of girders per lane (girder spacing) for single span bridges [Arockiasamy and Amer, 1995]. This section focuses on the effect of varying the girder spacing on the shear load distributions of both straight and skew continuous slab-on-girder bridges.

The transverse shear distributions and the shear load distribution factors for straight and skew bridges were determined for different girder spacing. The parametric studies in this section include 24 cases, which consider the interior and exterior girders close to the exterior and interior supports (Table 4.2). It is found that the shear forces in the girders and the shear load distribution factors increase with an increase in the girder spacing for both interior and exterior girders close to the interior and exterior supports. The shear load distribution factors based on the FEM are smaller than the LRFD and AASHTO values for interior and exterior girders. The shear distributions and shear load distribution factors are similar at both sections close to the interior and exterior supports. Typical shear distributions and load distribution factors are shown in Figs. 4.25 to 4.32 for interior and exterior girders close to the interior supports of straight and skew bridges.

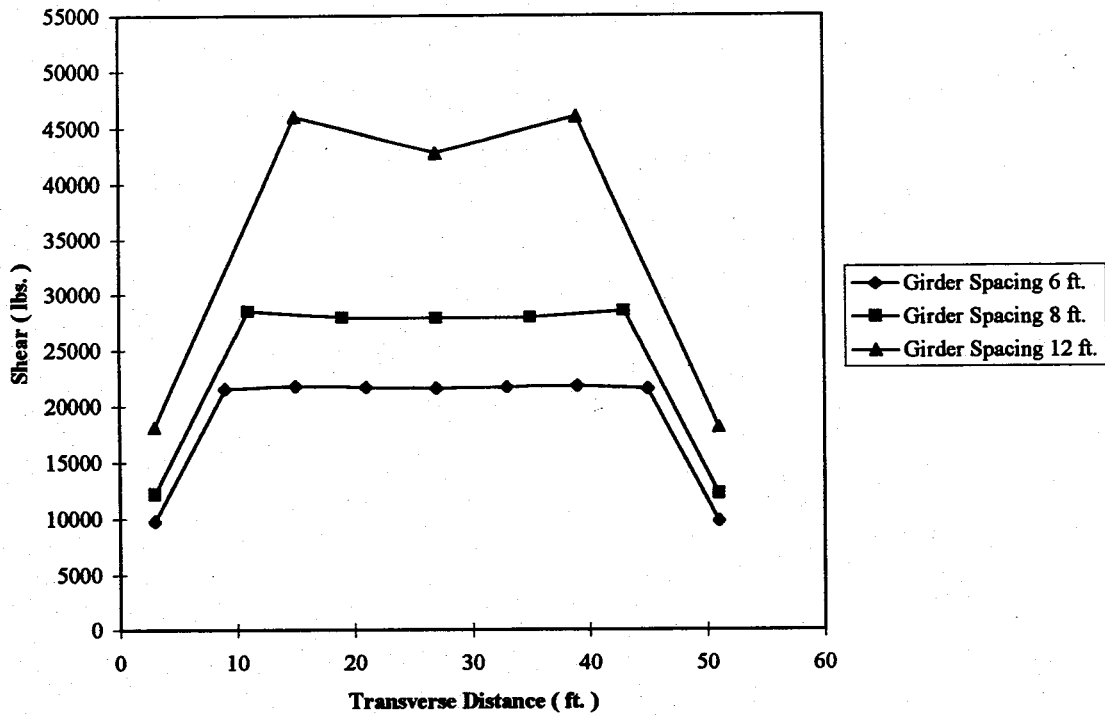


Fig. 4.25 Shear distributions at interior support for straight bridges with different girder spacing (interior girder loading)

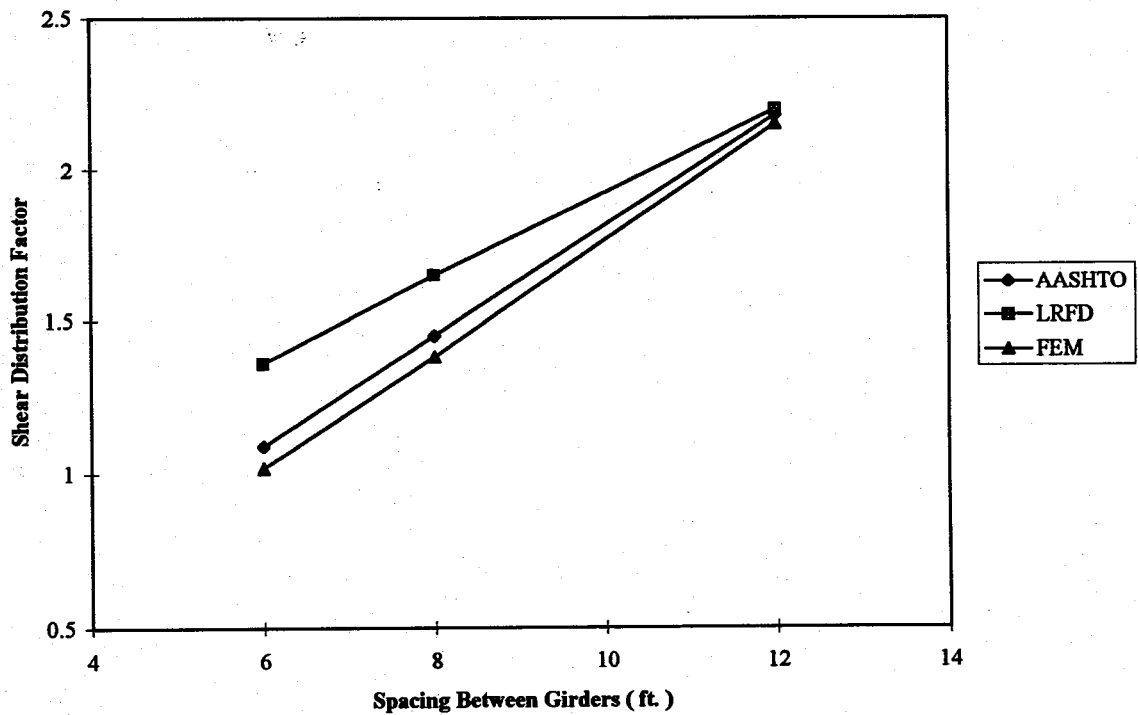


Fig. 4.26 Shear load distribution factors at interior support for straight bridges with different girder spacing (interior girder loading)

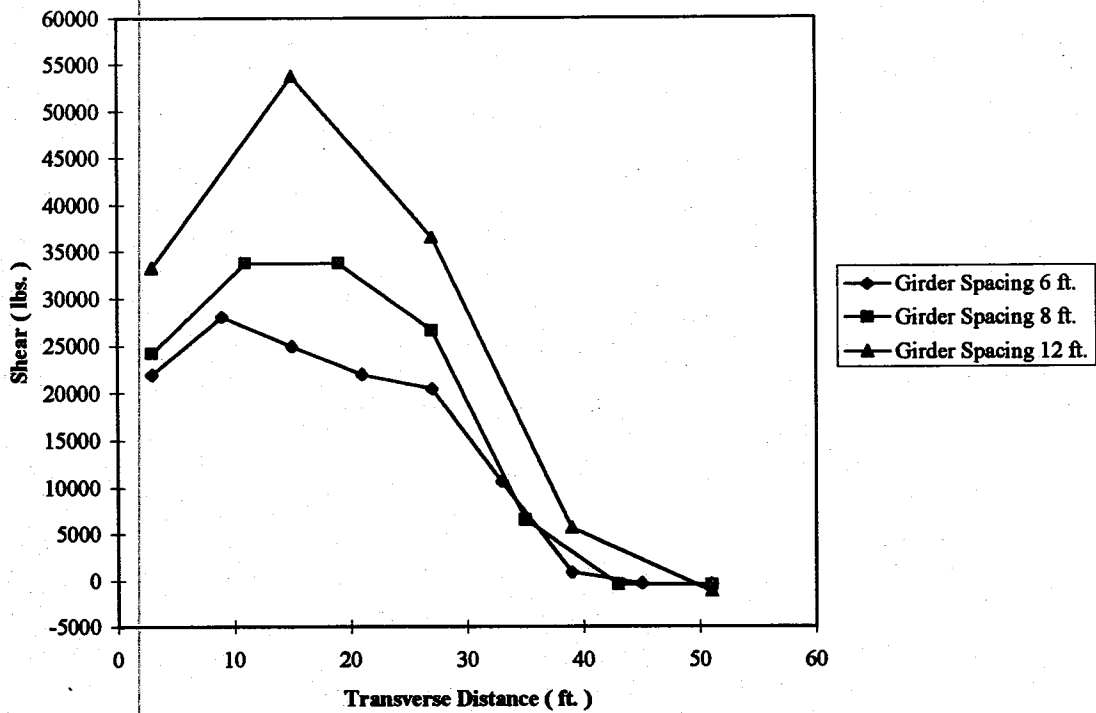


Fig. 4.27 Shear distributions at interior support for straight bridges with different girder spacing (exterior girder loading)

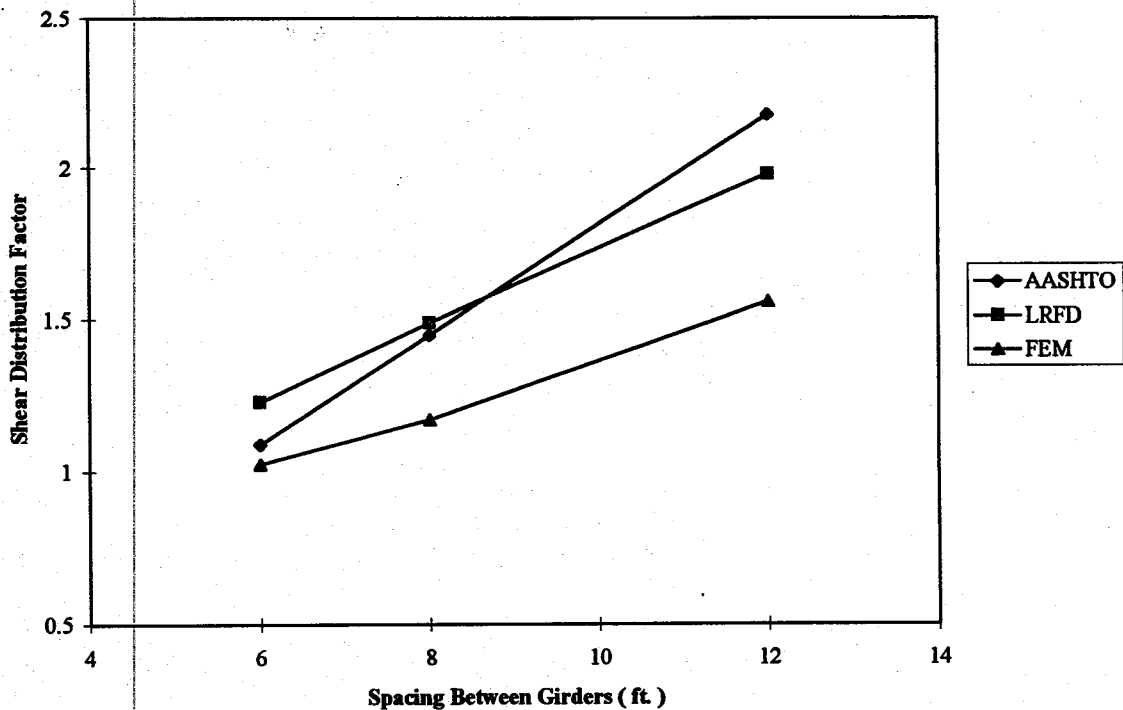


Fig. 4.28 Shear load distribution factors at interior support for straight bridges with different girder spacing (exterior girder loading)

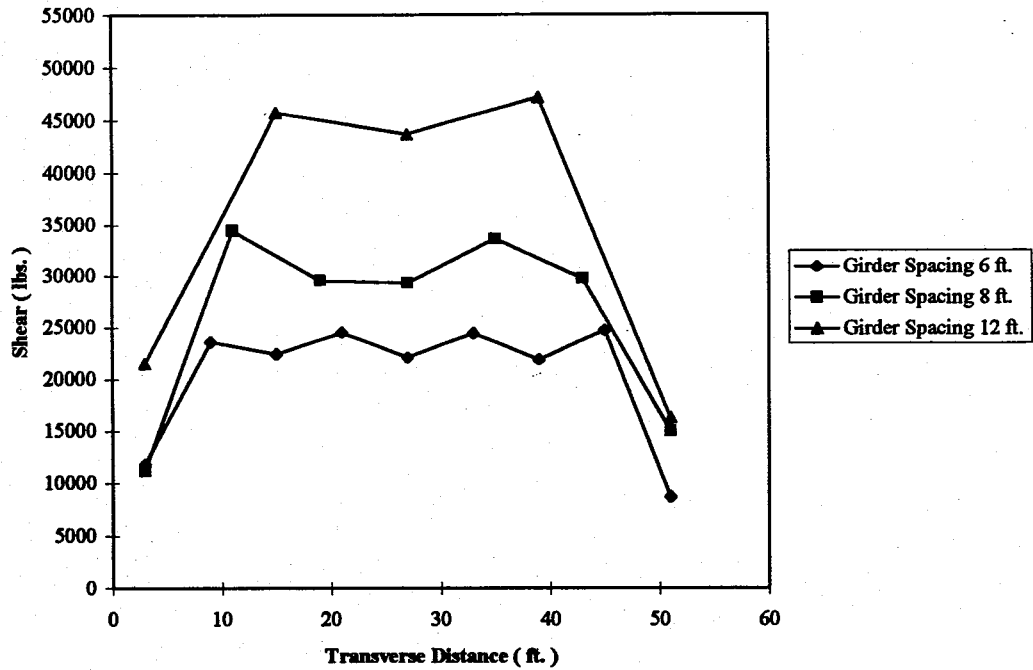


Fig. 4.29 Shear distributions at interior support for skew bridges with different girder spacing (interior girder loading)

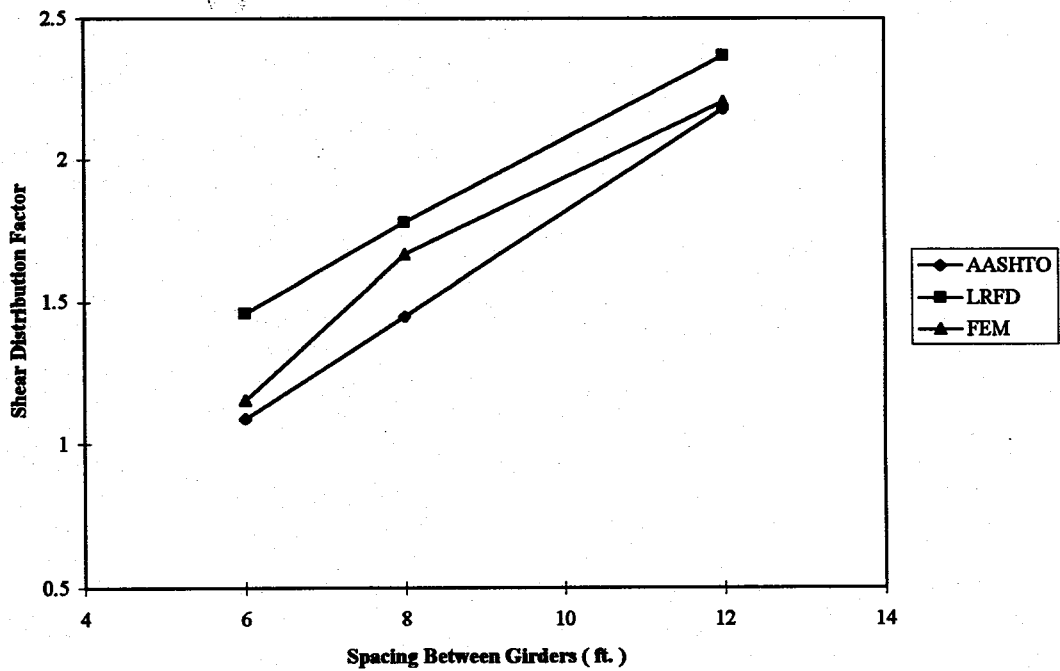


Fig. 4.30 Shear load distribution factors at interior support for skew bridges with different girder spacing (interior girder loading)

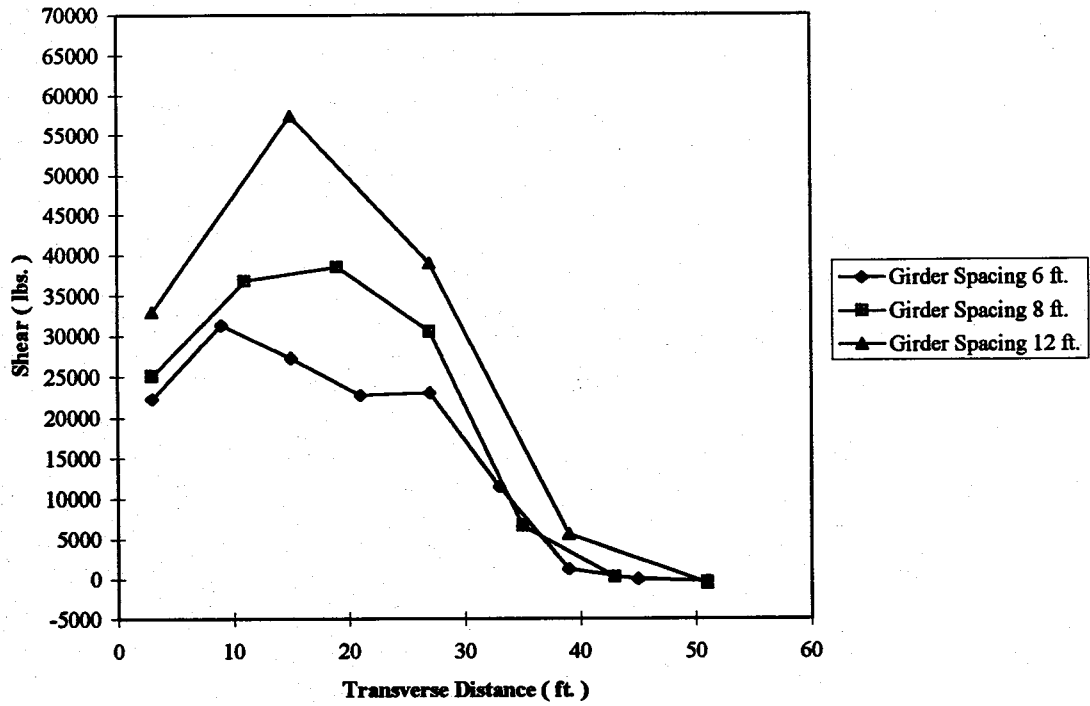


Fig. 4.31 Shear distributions at interior support for skew bridges with different girder spacing (exterior girder loading)

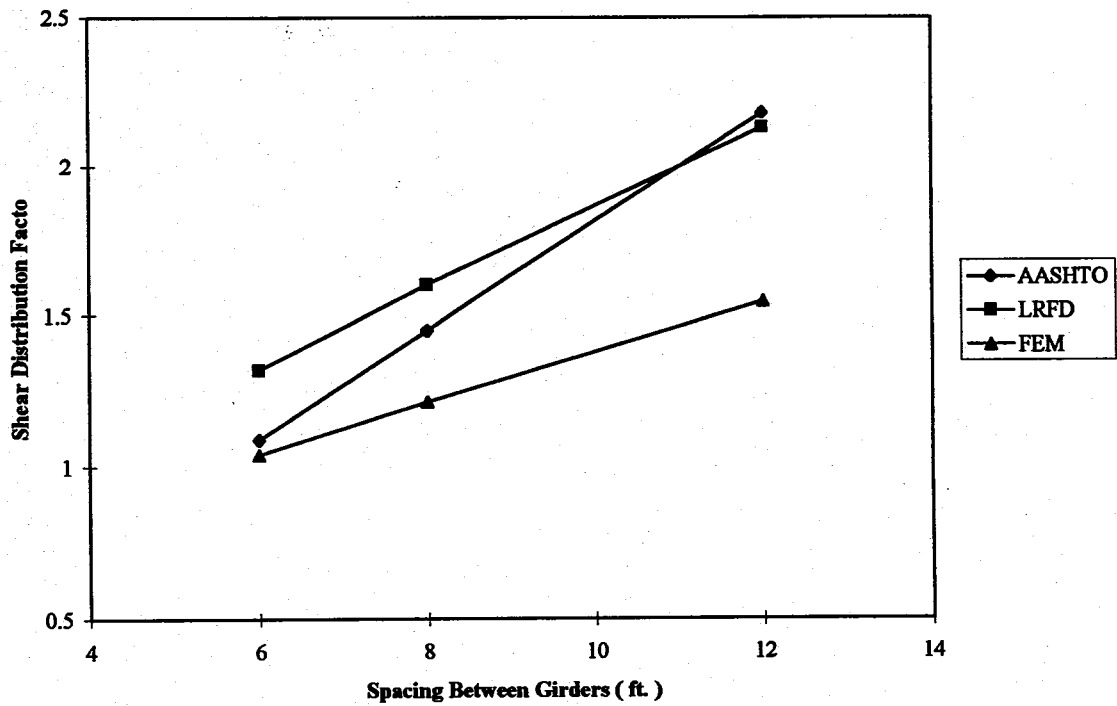


Fig. 4.32 Shear load distribution factors at interior support for skew bridges with different girder spacing (exterior girder loading)

4.3.3.4 Ratio of Adjacent Two Spans

The ratios of the spans for continuous two span bridges were varied to study the effects on the shear load distribution factors. The ratios between the spans used in this study were 1:1, 1:1.5 and 1:2 as shown in Table 4.2. Straight bridges and skew bridges with thirty degrees skew angle were studied in this section. Thirty-six cases were investigated in this study. The shear distributions and shear load distribution factors were determined for the exterior and interior girders close to the first exterior, interior and second exterior supports. The results show that the shear distributions and the shear load distribution factors follow the same trend for both exterior and interior girders close to the supports. Therefore, only typical cases are illustrated in the following.

The interior girder shear distributions of straight bridges close to the interior support is shown in Fig. 4.33. The shears in the interior girders remains nearly the same as the ratios of the spans increase and the shear load distribution factors are also constant as shown in Fig. 4.34. The exterior girder shear distributions of straight bridges close to the interior support are shown in Fig 4.35. The variations in the shear distributions are very small with increase in the ratios of the spans and the corresponding shear load distribution factors are constant as shown in Fig. 4.36. The same trends are observed for skew bridges with varying span ratios (Fig 4.37 - 4.40).

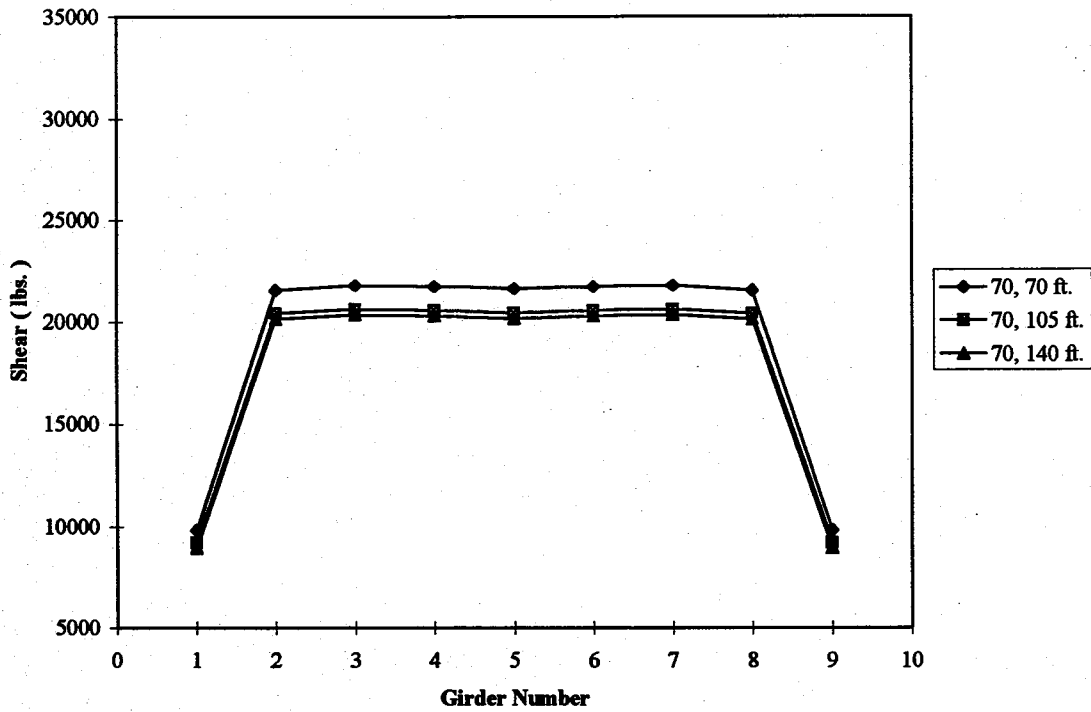


Fig. 4.33 Shear distributions at interior support for straight bridges with different span ratios (interior girder)

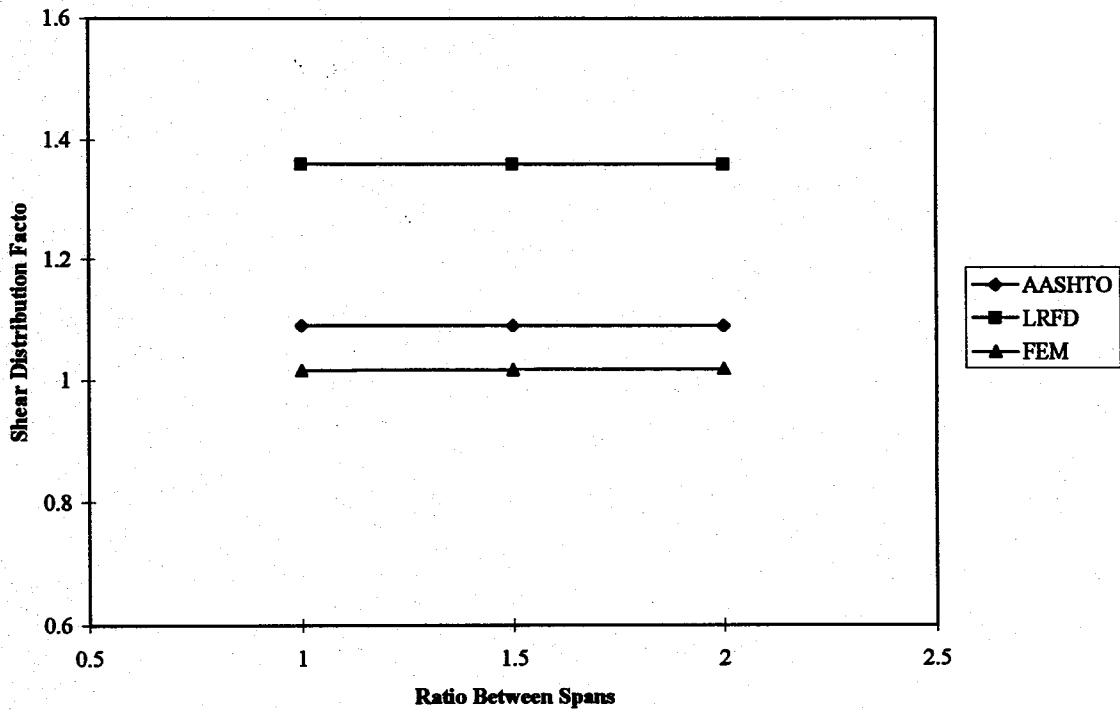


Fig. 4.34 Shear load distribution factors close to the interior support for straight bridges with different span ratios (interior girder)

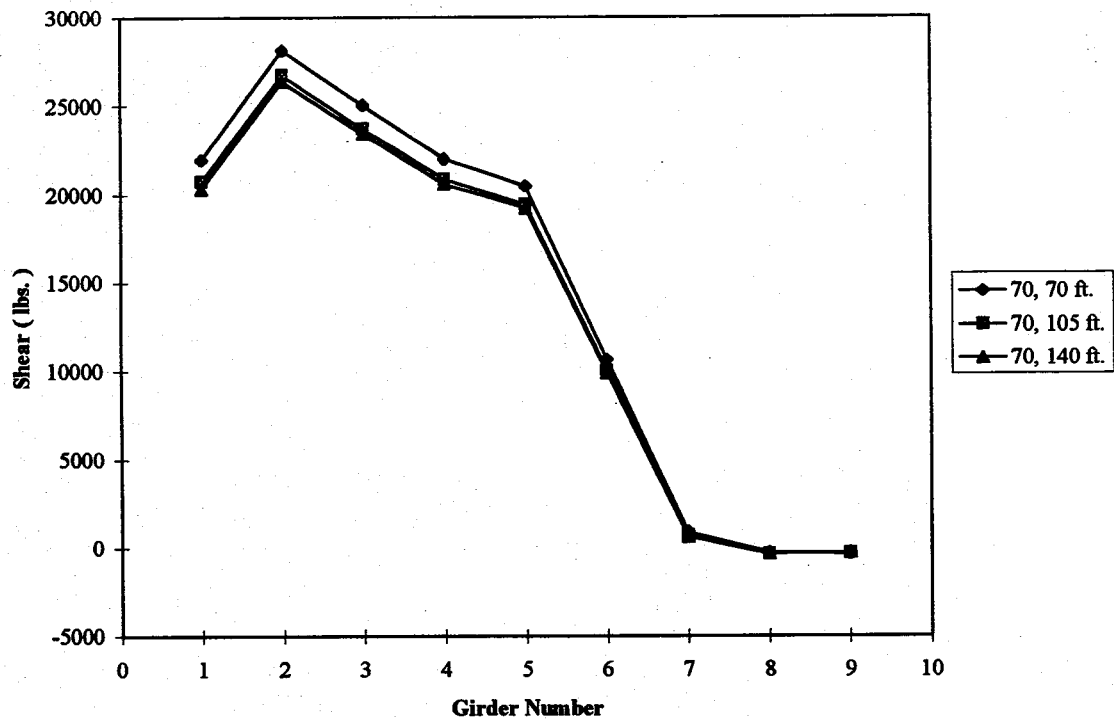


Fig. 4.35 Shear distributions at interior support for straight bridges with different span ratios (exterior girder)

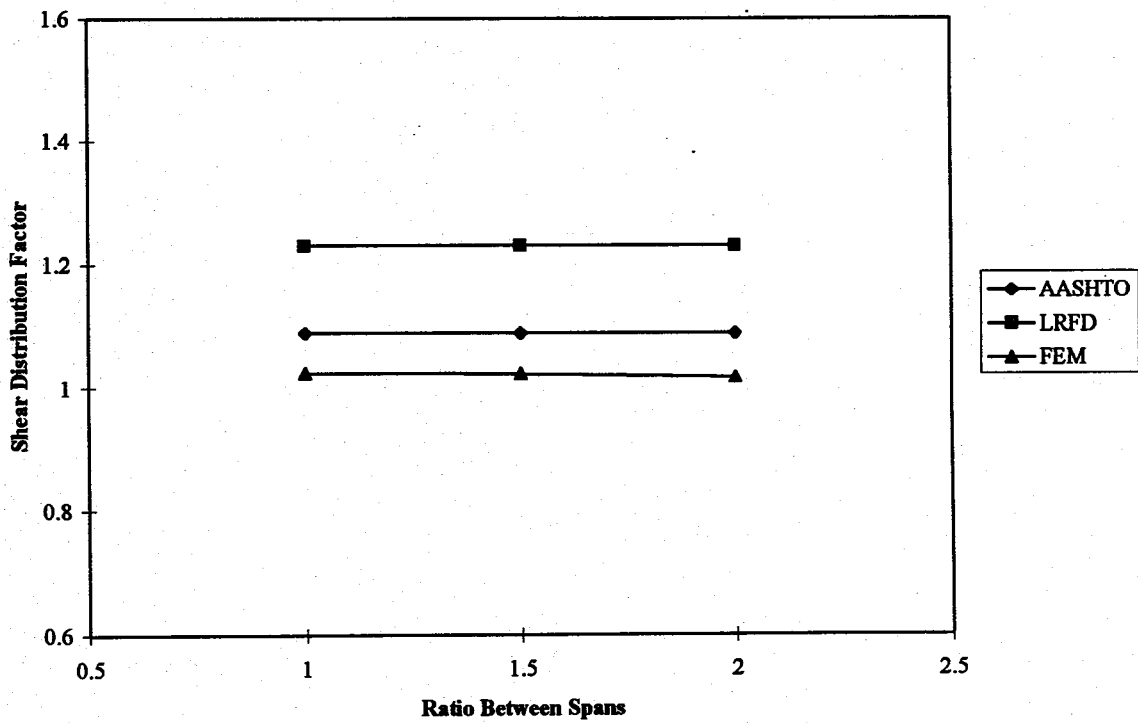


Fig. 4.36 Shear load distribution factors at interior support for straight bridges with different span ratios (exterior girder)

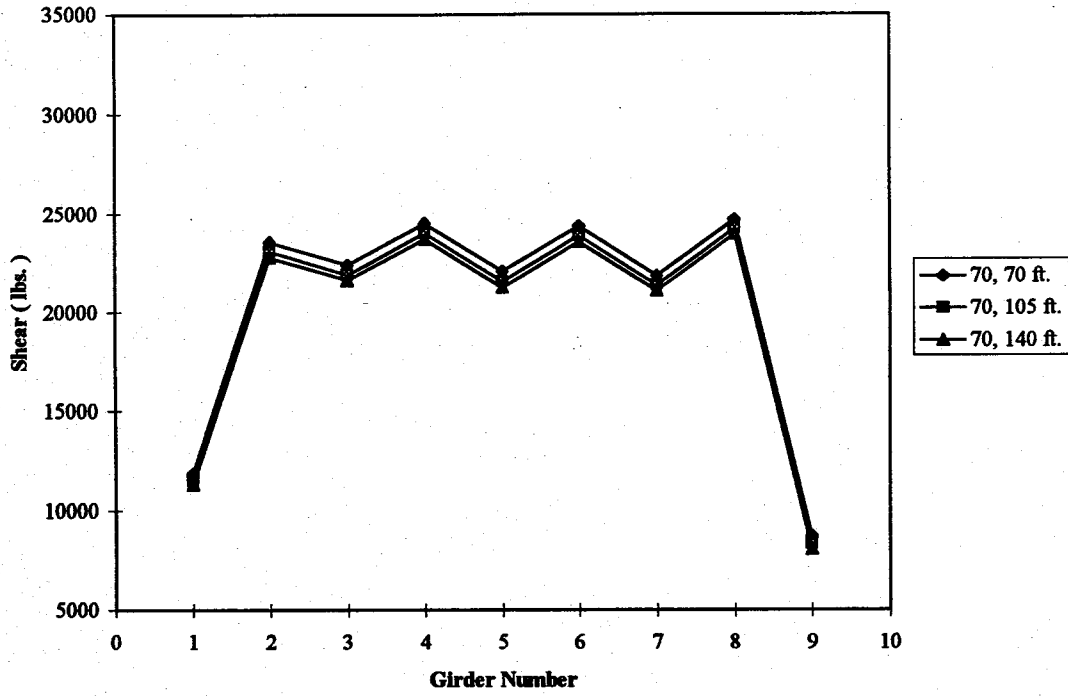


Fig. 4.37 Shear distributions at interior support for skew bridges with different span ratios (interior girder)

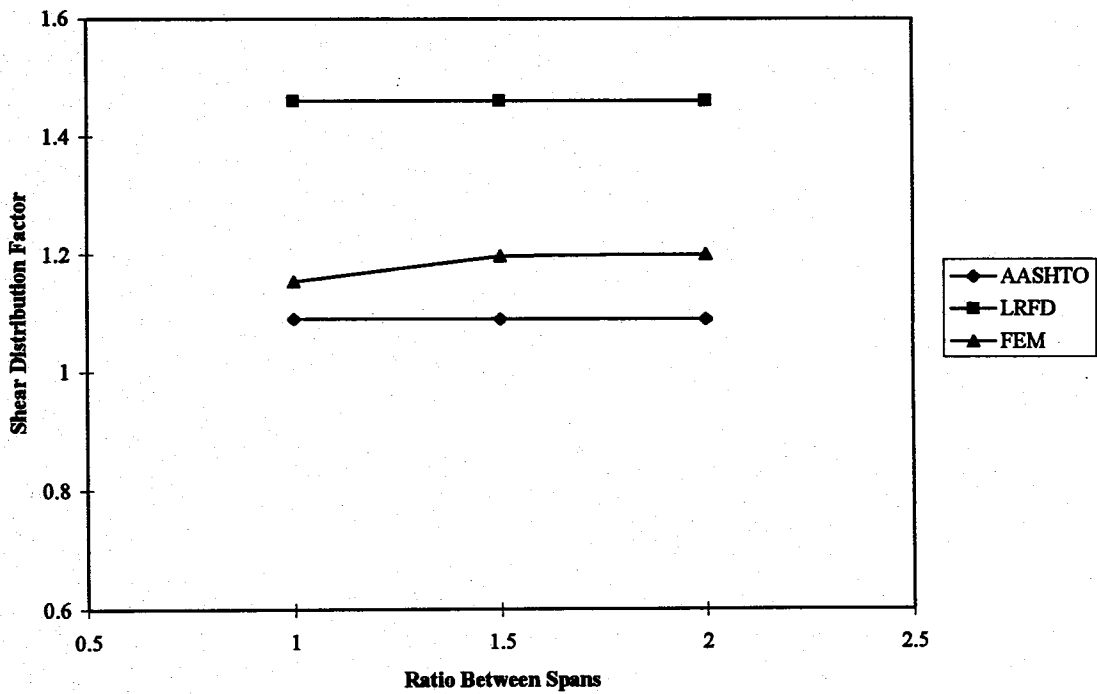


Fig. 4.38 Shear load distribution factors at interior support for skew bridges with different span ratios (interior girder)

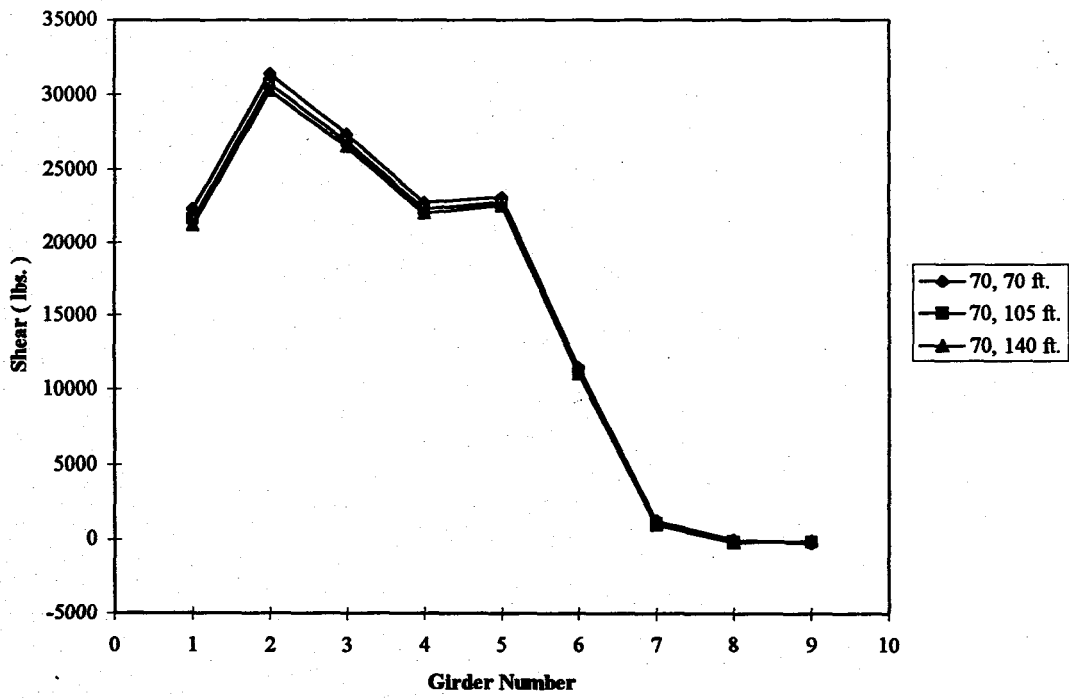


Fig. 4.39 Shear distributions at interior support for skew bridges with different span ratios (exterior girder)

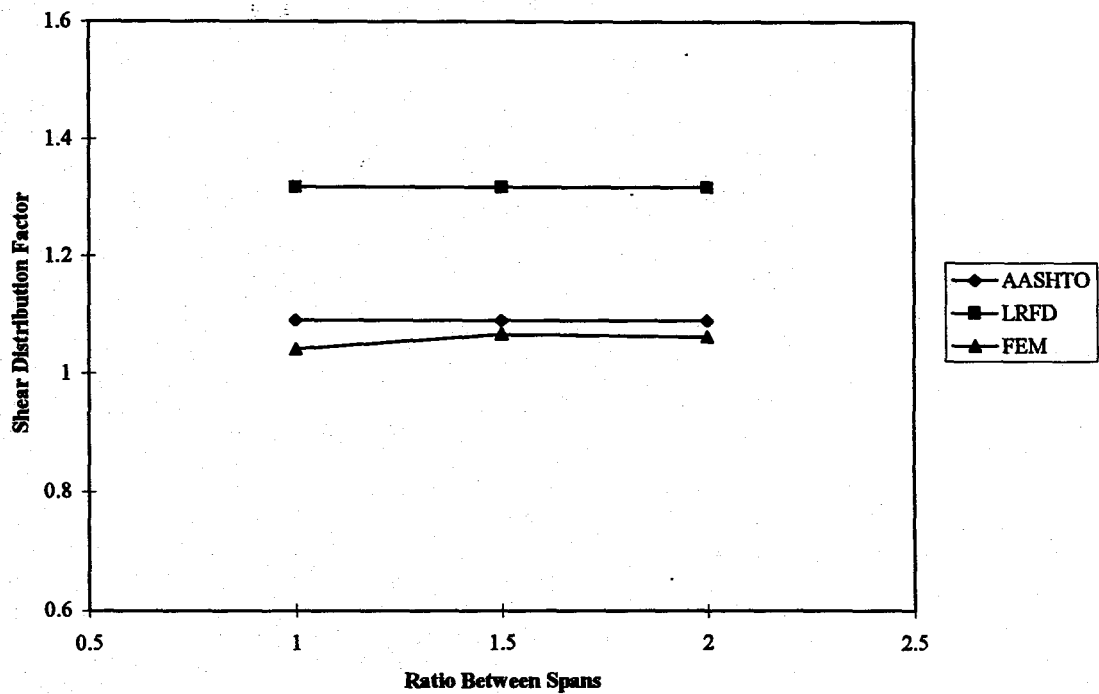


Fig. 4.40 Shear load distribution factors at interior support for skew bridges with different span ratios (exterior girder)

4.3.3.5 Span Lengths

The effect of varying the span length in both straight and skew continuous bridges is studied in this section. Bridges with two equal span lengths of 70ft. and 105ft. were considered in the parametric study. The effects on shear distributions and shear load distribution factors of the interior and exterior girder were examined for both straight and skew bridges. Twenty-four cases have been analyzed to obtain the shear distribution and the corresponding load distribution factors. The analytical results showed that the shear load distribution factors are independent of the span lengths for all the cases. Only typical graphs showing the shear variations and the shear load distribution factors for the interior and exterior girders close to the interior supports are shown in Figs. 4.41- 4.44 for straight bridges and Figs. 4.45 - 4.48 for skew bridges.

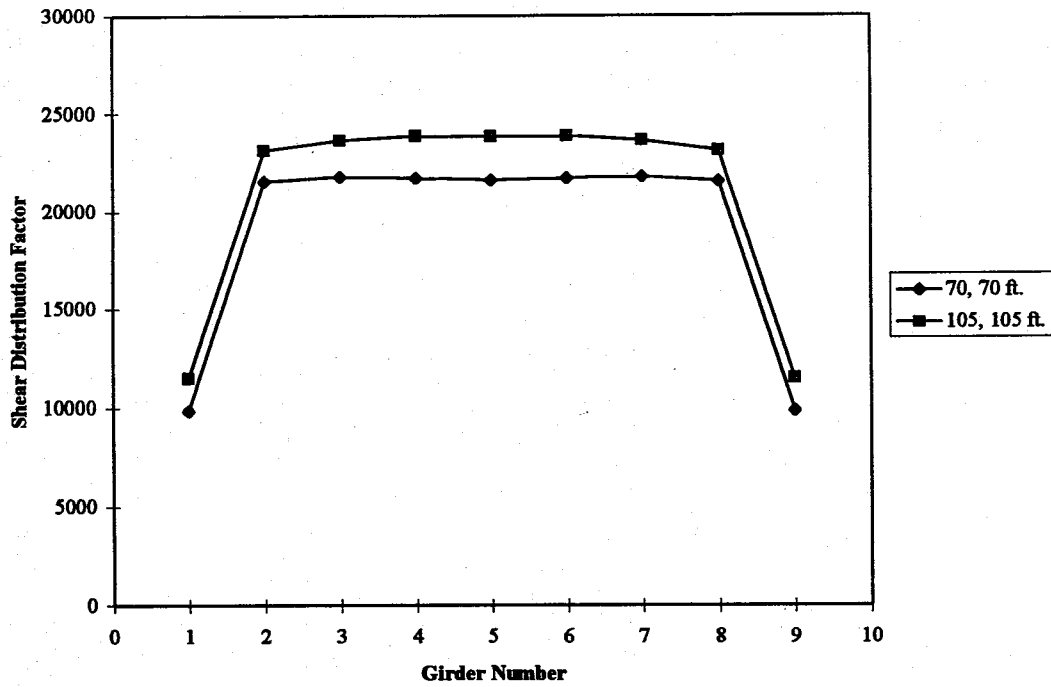


Fig. 4.41 Shear distributions at interior support for straight bridges with different span lengths (interior girder)

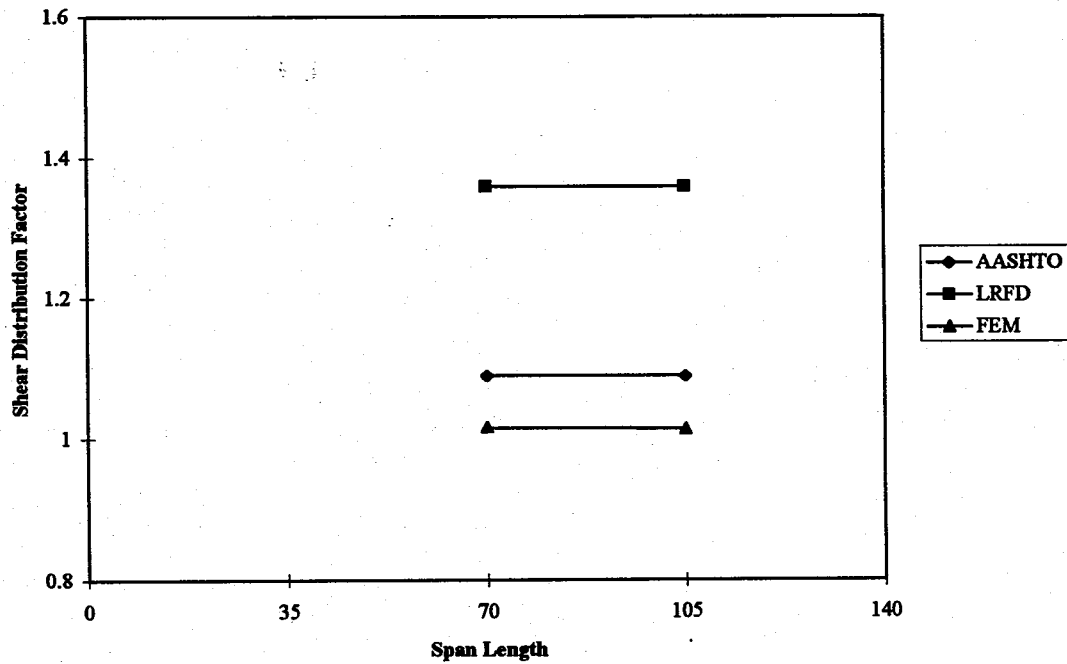


Fig. 4.42 Shear load distribution factors at interior support for straight bridges with different span lengths (interior girder)

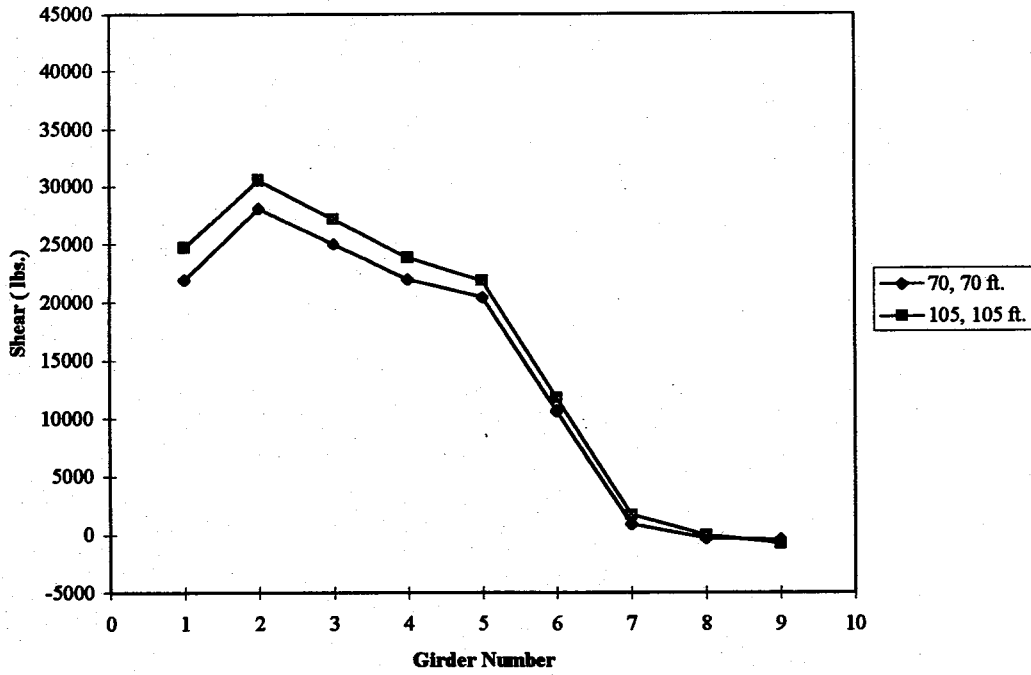


Fig. 4.43 Shear distributions at interior support for straight bridges with different span lengths (exterior girder)

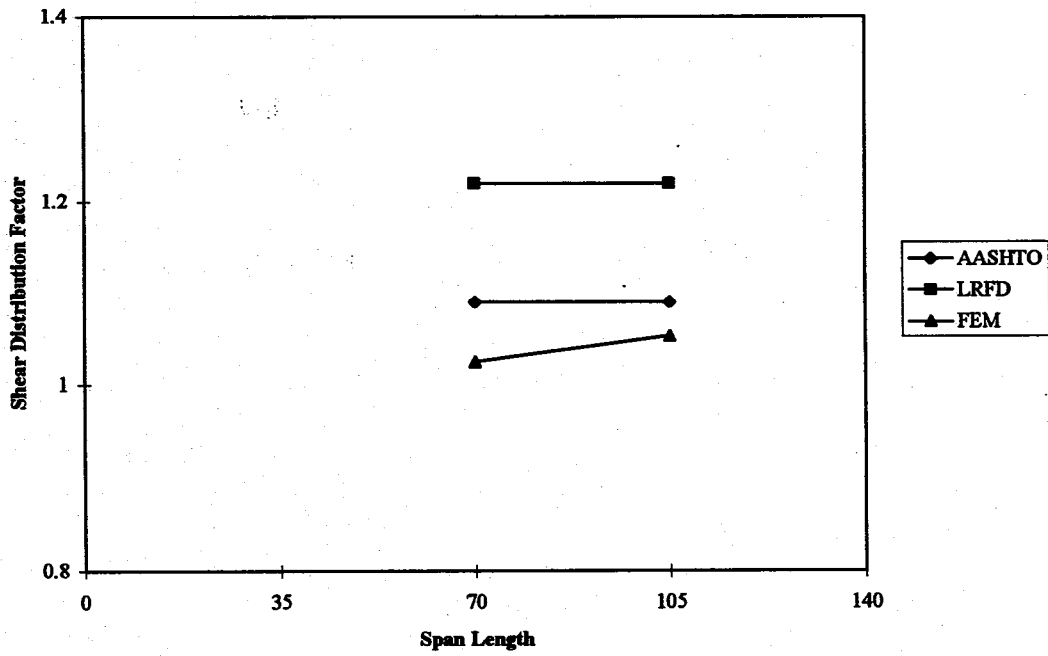


Fig. 4.44 Shear load distribution factors at interior support for straight bridges with different span lengths (exterior girder)

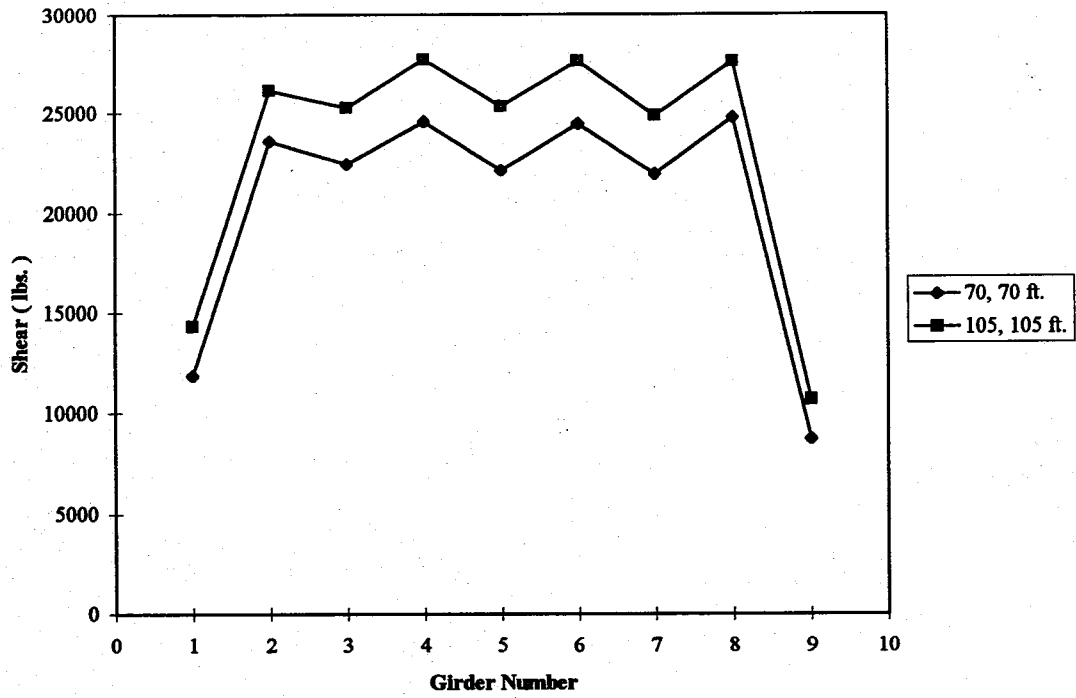


Fig. 4.45 Shear distributions at interior support for skew bridges with different span lengths (interior girder)

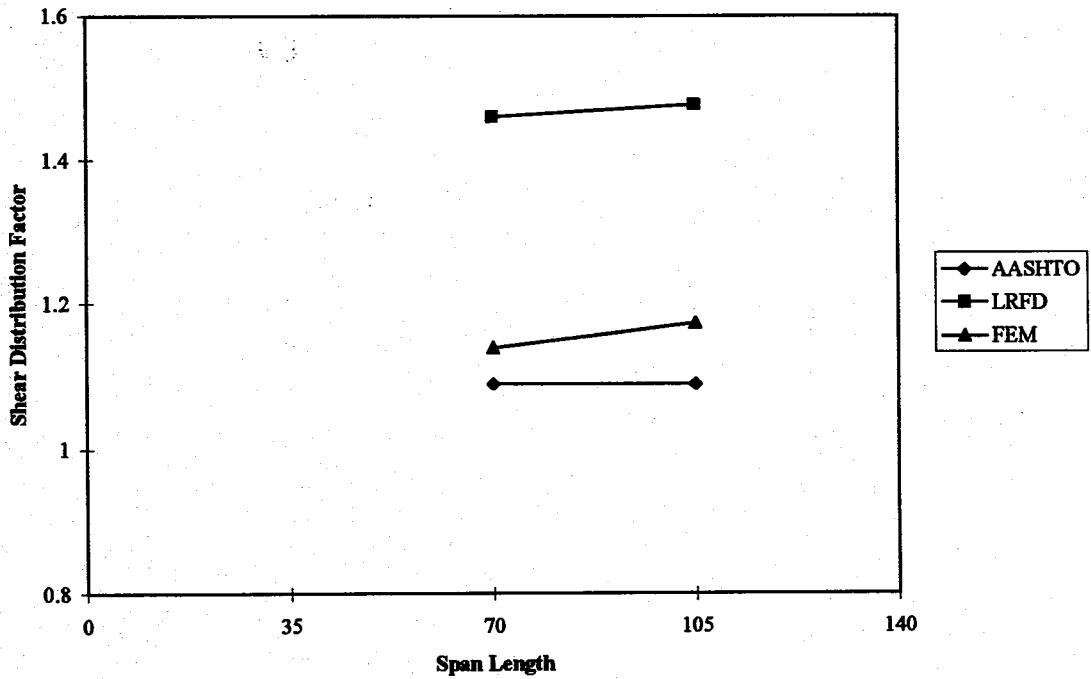


Fig. 4.46 Shear load distribution factors at interior support for skew bridges with different span lengths (interior girder)

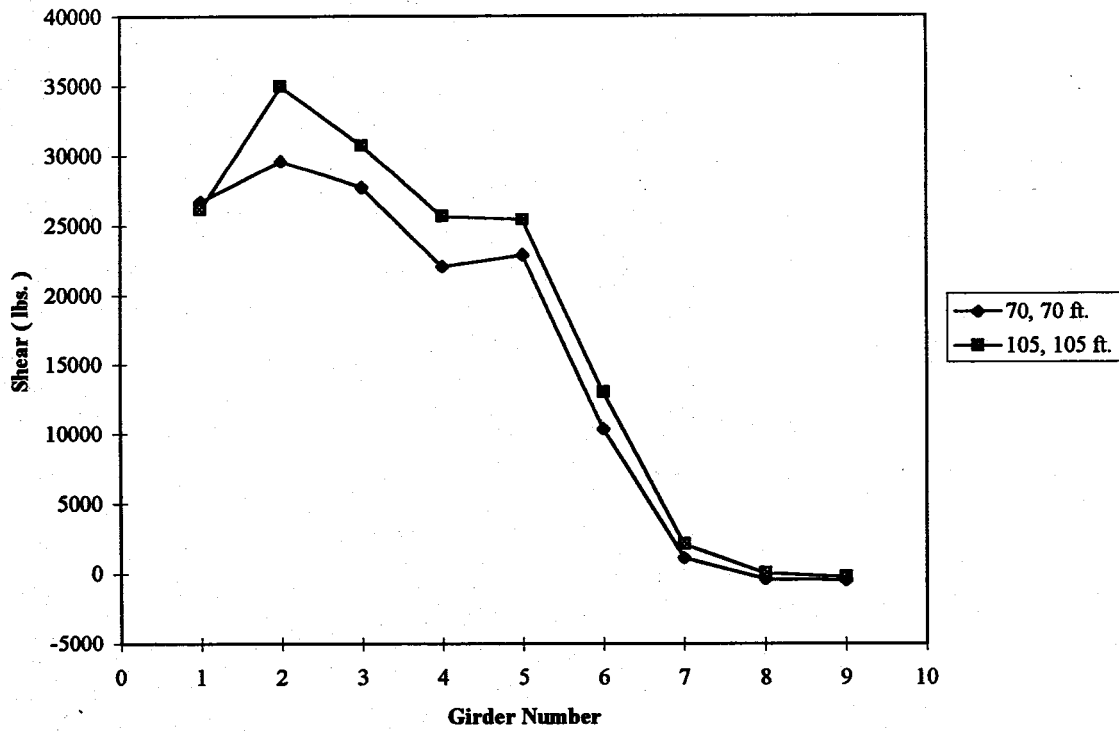


Fig. 4.47 Shear distributions at interior support for skew bridges with different span lengths (exterior girder)

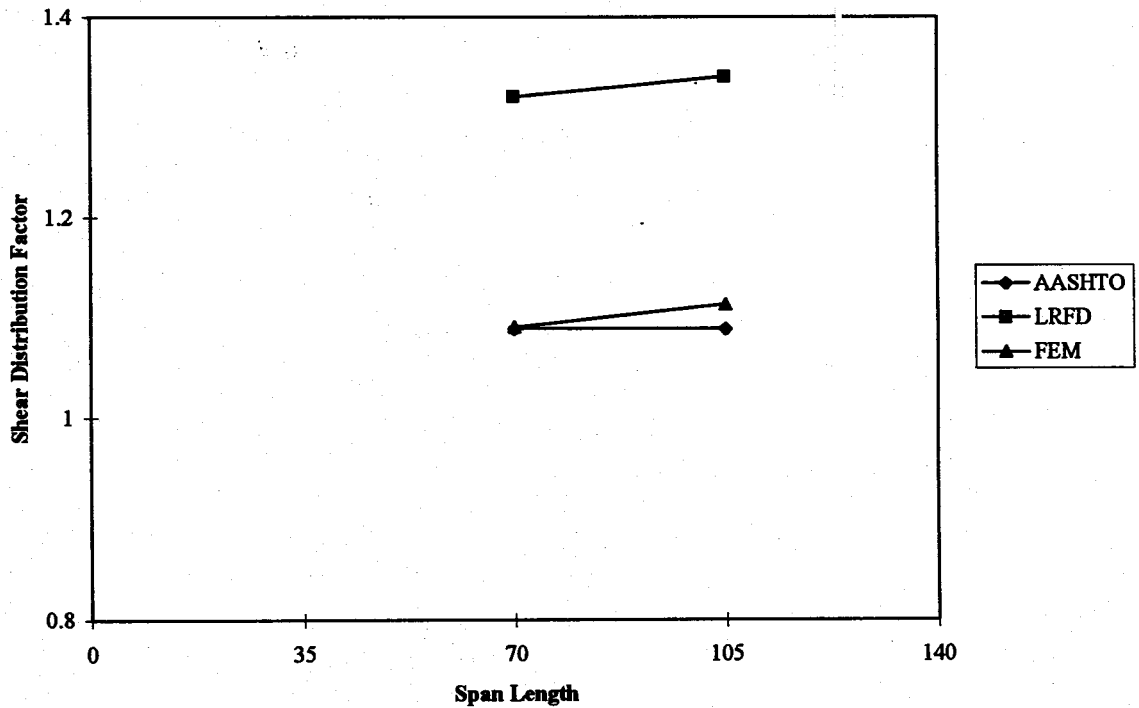


Fig. 4.48 Shear load distribution factors at interior support for skew bridges with different span lengths (exterior girder)

CHAPTER 5

DIAPHRAGM AND SHOULDER EFFECTS ON WHEEL LOAD DISTRIBUTION

5.1 INTRODUCTION

Many parameters affect the wheel load distribution of slab-on-girder bridges. The main parameters considered in the LRFD and AASHTO codes include girder spacing, span length, skew angle, etc. However, the codes do not consider other secondary parameters such as the diaphragms and shoulders, which may affect the wheel load distribution. Diaphragms are either of concrete or steel elements that are placed transversely between girders. Diaphragms provide resistance to live loads and transverse loads from wind or impact from over-height vehicles. Shoulders provide the additional lanes, usually up to 12 ft. wide, placed on either side of the bridge. These lanes are used for emergencies and rerouting traffic when one of the main traffic lanes is shut down. This chapter investigates the effect of diaphragms and shoulders on the wheel load distribution of simply supported slab-on-girder bridges.

5.2 DIAPHRAGMS

A literature review reveals many different opinions on the purpose and function of the intermediate diaphragms in slab-on-girder bridges. Diaphragms provide resistance against the accidental overturning of bridge girders during construction and placement of the deck. Diaphragms serve to some extent to distribute the traffic loads transversely

among the girders. Questions have been raised about the diaphragms effectiveness in resisting the impacts caused by lateral loads. There are different opinions whether the diaphragms are damage limiting or damage-spreading members.

Several studies have been conducted on the effectiveness of diaphragms in the vertical load distribution. Cheung et al. (1986), Sithichaikasem and Gamble (1972) and Wong and - Gamble (1973) noticed that the previous researchers disagree on the effectiveness of the intermediate diaphragms and the best positioning of the diaphragms. Research conducted by Abendroth et al. (1993) through questionnaire to 50 state departments of transportation, seven Canadian provinces and the District of Columbia, shows that 96% of the agencies use cast-in-place intermediate diaphragms when a bridge is over a river or highway. Diaphragms were placed at the mid-span of the bridge by 50% of the agencies in accordance with the AASHTO requirements. The diaphragms were placed at the third points of the span by 30% of the agencies and at one-quarter points by 10% of the agencies.

In the present study, the effect of diaphragms on wheel load distribution was investigated for single span slab-on-girder bridges. The effect of diaphragms on wheel load distribution was first evaluated for a field test bridge and compared with a finite element model of the actual bridge. The diaphragm parameters that affect the wheel load distribution were studied to evaluate the effect of each parameter.

5.2.1 FEM Modeling of Slab-on-Girder Bridge With and Without Diaphragms

The continuous skew slab-on-steel girder bridge presented in Chapter 3 (section 3.2.2) was used in this study to investigate the effect of diaphragm on the wheel load distribution. The bridge is located on I-75 over U.S. 301 in Hillsborough County, Florida (Figs. 3.9-3.12). The bridge consists of four continuous spans with the length of the tested span being 172'-8 13/16" with a skew angle of 45°. Eight A36 steel plate girders are spaced at 7'-7" center-to-center with a deck slab thickness of 7 in. The bridge carries three lanes of traffic with curb-to-curb width of 56.0 ft. The plan view of the bridge is shown in Fig. 3.13. Fig. 3.14 shows the cross section of the bridge with the concrete deck, steel girders, and diaphragms in place. Table 3.6 shows the material and sectional properties of the bridges used in the finite element modeling. The plan view of the finite element model is shown in Fig. 3.16. There are 125 elements of length 4ft. in the longitudinal direction and 16 elements in the transverse direction. Although only span 3 was the tested span in the bridge, the entire bridge was modeled in the finite element analysis, since the bridge is continuous.

The concrete slab-on-steel-plate-girder bridge was modeled using finite element method with and without diaphragms. The transverse strain distribution for the tested bridge is presented in Fig. 3.19. Approximately 11% difference was observed between the measured maximum strain and the calculated value based on finite element model without diaphragms and the difference reduces to 3% with diaphragm. The addition of diaphragms increases the strength and stiffness of the bridge and hence lowers the maximum strains. In this bridge, the addition of the diaphragm to the FEM model

reduces the difference between measured and calculated maximum strain by 8%. This difference indicates the importance of considering the diaphragms in FEM modeling.

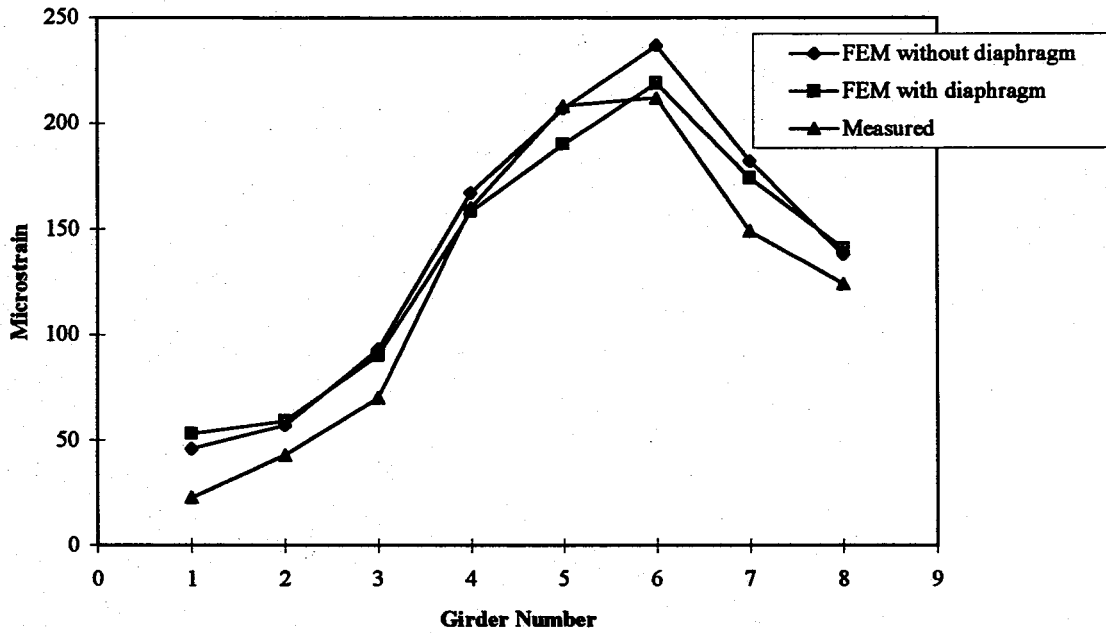


Fig. 3.19 Transverse strain distributions for the tested bridge with and without diaphragms

5.2.2 Diaphragm Parametric Study

The parametric study was focused on determining the effect of the diaphragm locations along the span on the wheel load distribution of skew and straight concrete slabon-girder bridges.

A total of 12 cases have been investigated in this parametric study (Table 5.1). Three different diaphragm locations that are commonly used in bridges were selected in the parametric studies. All the parametric study cases have diaphragms

between the girders at the supports. The first case has no interior diaphragms, whereas the diaphragms at the mid-span are considered in the second case. The diaphragms at the third points were considered in the third case.

The diaphragm was modeled in this study using a two-node beam element BEAM-4 with six degrees of freedom (u_x , u_y , u_z , rot_x , rot_y , rot_z). The diaphragm has the same material properties as the girders and the deck slab. The diaphragms are six inches wide with height equal to the web depth and upper flange and connected to the girders at the upper web node.

Table 5.1 Summary of parametric studies for diaphragms

Parameter	Interior diaphragm locations	Skew angles (degrees)	Cases	Comments
Diaphragm Locations	None	0	2	Cases: Interior girder moment Exterior girder moment
	Mid-span	0	2	
	Third points	0	2	
	None	30	2	
	mid-span	30	2	
	third points	30	2	
Total			12	

(*All cases have a bridge width of 54 ft. and a slab thickness of 7 in. on 9 AASHTO type IV girders)

The typical single span bridge with a span of 70 ft. used in Chapter 4 is considered in this section. Loading patterns to obtain the maximum bending moments are used for interior and exterior girders. Three trucks were loaded transversely across the bridge for maximum moment in the exterior girders and four trucks were positioned transversely for maximum moment in interior girders. The load position in the longitudinal direction was chosen to give the maximum positive moment.

Fig 5.1 shows the transverse strain distributions for straight bridges with no interior diaphragms, diaphragms at the mid-span, and diaphragms at the third points for interior girder loading. The flexural strains slightly decrease with the increase in the number of diaphragms. The wheel load distribution factors of interior girders for straight bridges with different diaphragm locations are shown in Fig. 5.2. The wheel load distribution factors are not dependent on the number of diaphragms and this agrees with AASHTQ and LRFD specifications, which do not consider the diaphragm in wheel load distribution. The transverse strain distributions at the mid-span of straight bridges for exterior girder loading decrease marginally as the number of diaphragms increase (Fig. 5.3). The wheel load distribution factors for exterior girders remain nearly the same with the increased in the number of diaphragms (Fig. 5.4). The skew bridges show similar trends as those of the straight bridges shown in Figs. 5.5-5.8. The transverse strain distributions at the mid-span of skew bridges for interior girders do not show an appreciable decrease as the number of diaphragms increase.

The following few observations can be mentioned from the field test and parametric study on diaphragms. The use of diaphragms increases the strength of the bridge and provides stability for the girders. Realistic modeling of the bridges using FEM should include diaphragms, if the actual bridge has diaphragms. The presence and location of interior diaphragms do not seem to have a major effect on the transverse load distribution at the mid-span for interior and exterior girders and this is valid for straight and skew bridges. This finding agrees with the AASHTO and LRFD codes, which neglect the diaphragm in wheel load distribution.

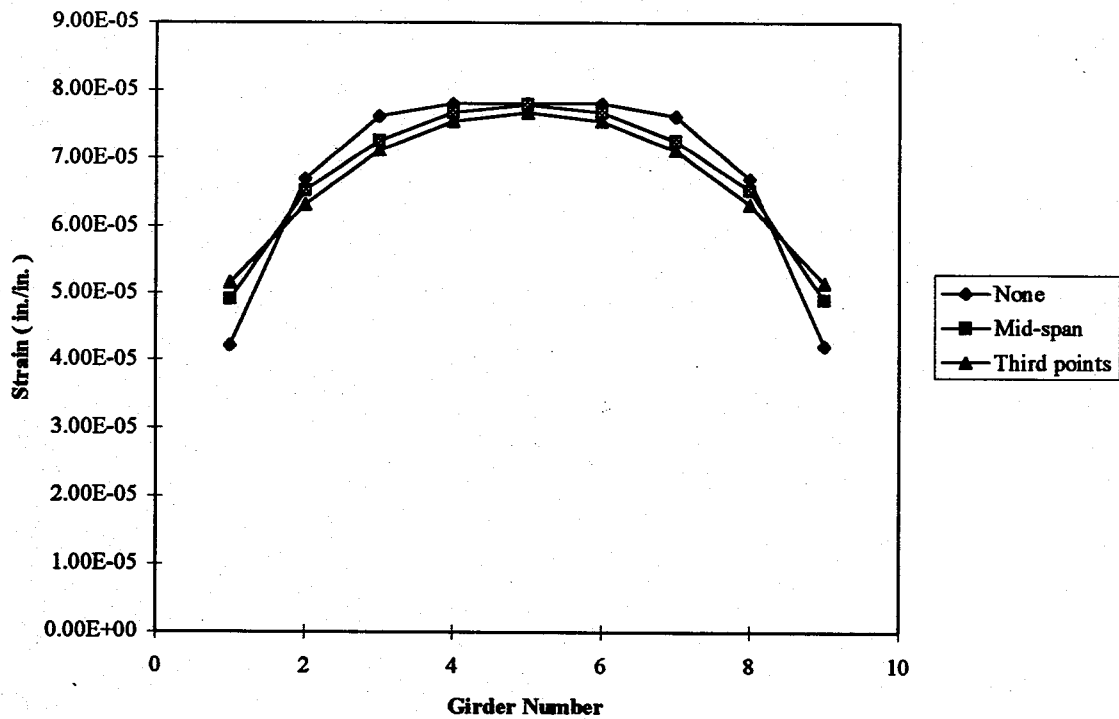


Fig 5.1 Transverse strain distributions at mid-span of straight bridges with different location of diaphragms (interior girder loading)

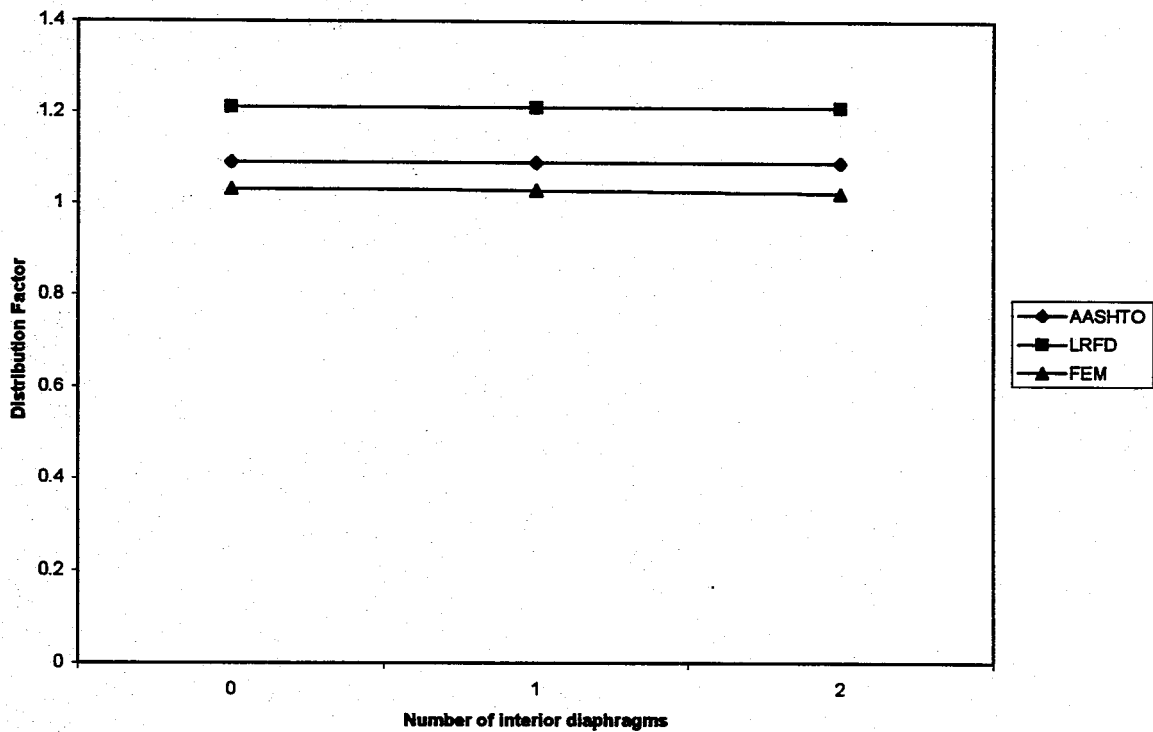


Fig 5.2 Load distribution factors at mid-span of straight bridges with different location of diaphragms (interior girders)

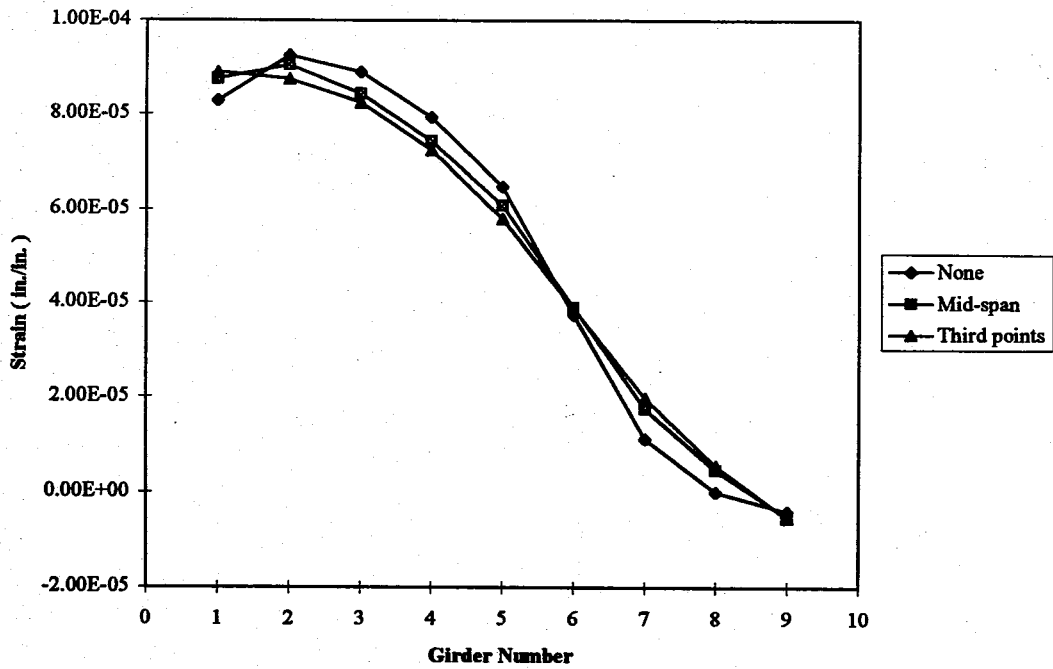


Fig 5.3 Transverse strain distributions at mid-span of straight bridges with different location of diaphragms (exterior girder loading)

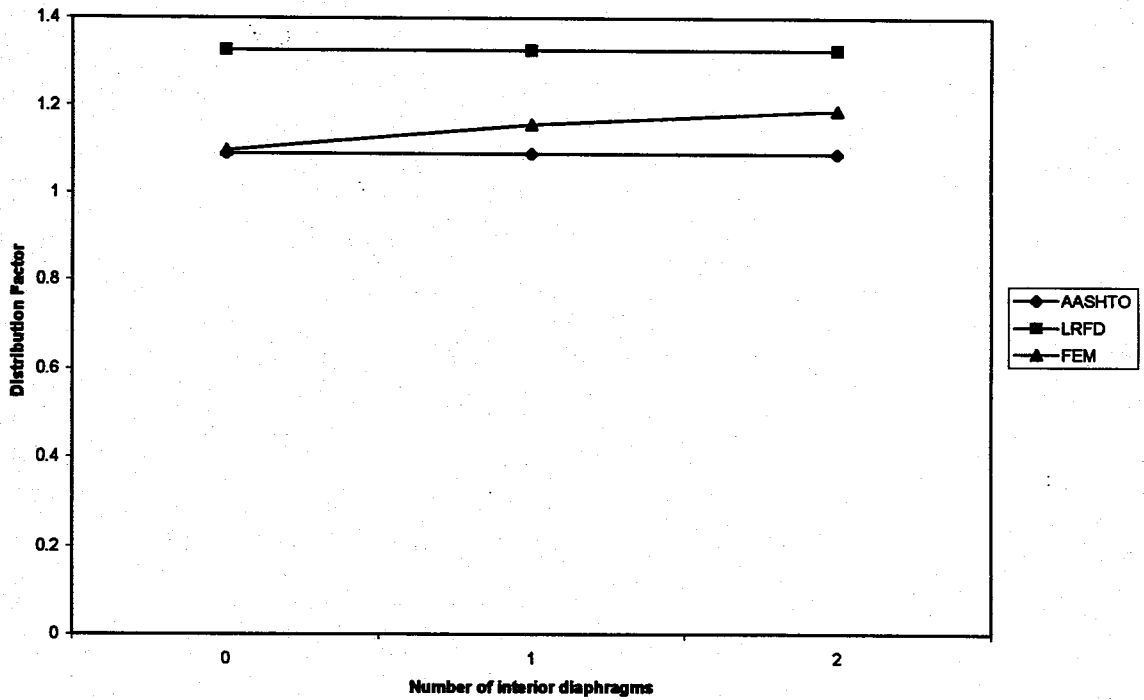


Fig 5.4 Load distribution factors at mid-span of straight bridges with different location of diaphragms (exterior girders)

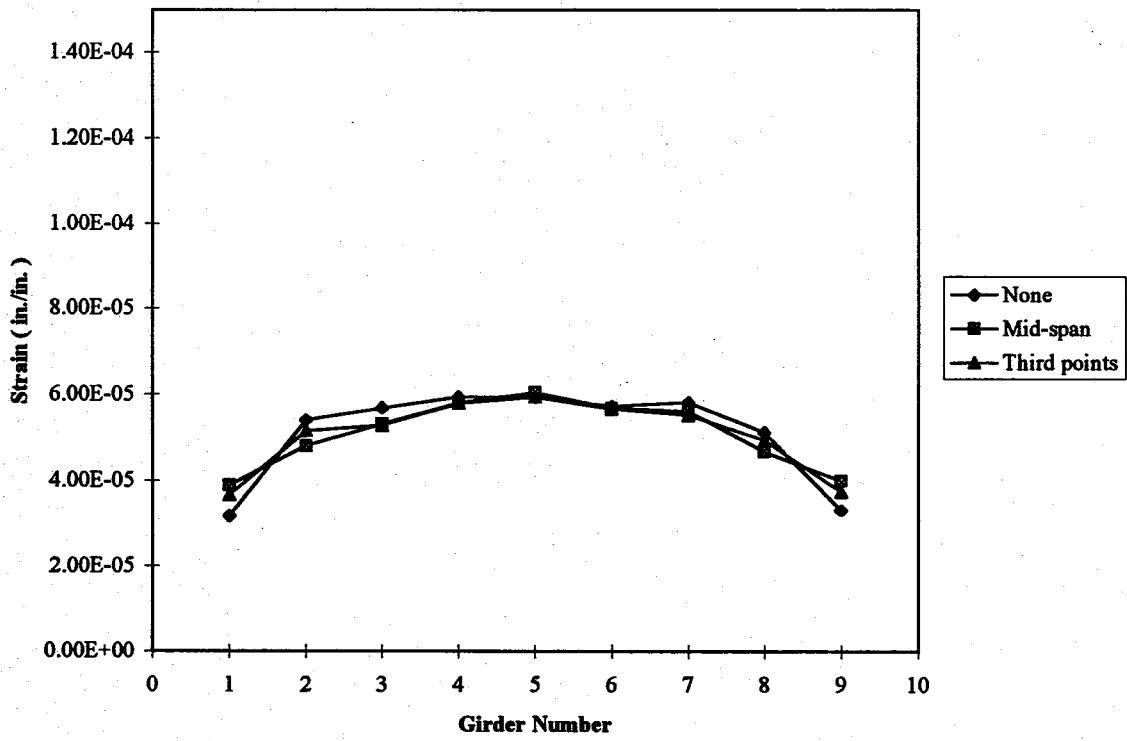


Fig 5.5 Transverse strain distributions at mid-span of skew bridges with different location of diaphragms (interior girder loading)

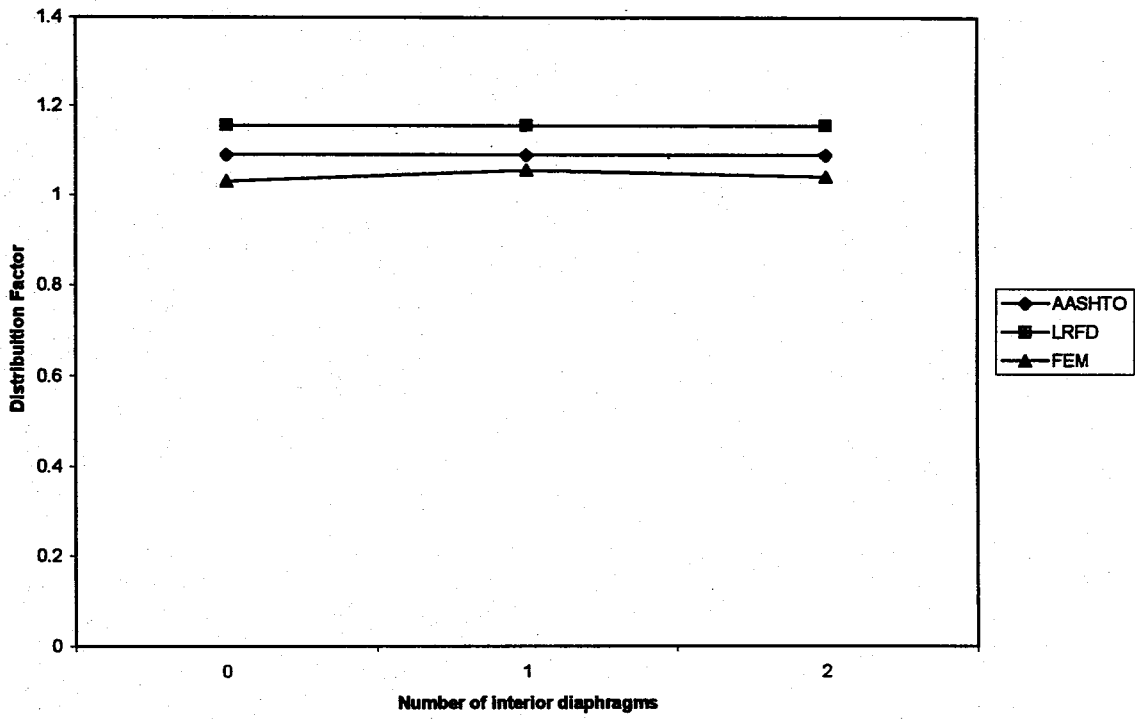


Fig 5.6 Load distribution factors at mid-span of skew bridges with different location of diaphragms (interior girders)

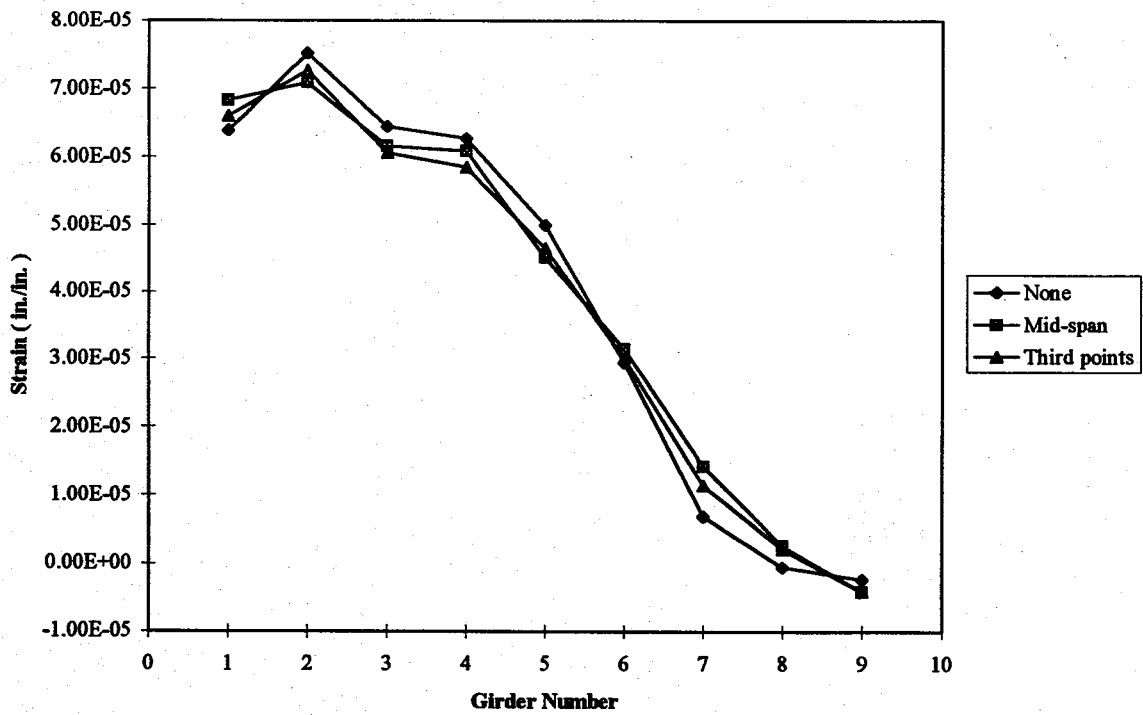


Fig 5.7 Transverse strain distribution at mid-span of skew bridges with different location of diaphragms (exterior girder Loading)

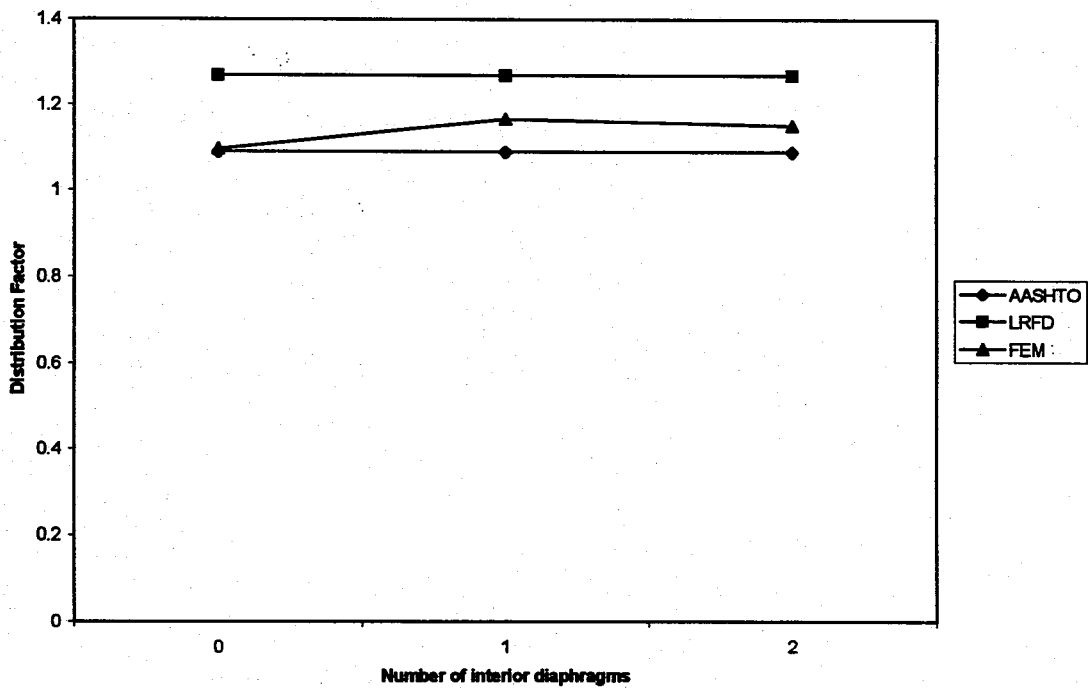
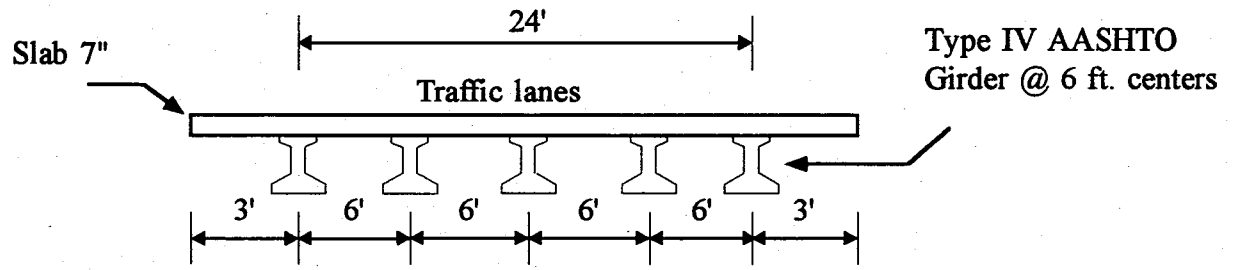


Fig 5.8 Load distribution factors at mid-span of skew bridges with different location of diaphragms (exterior girders)

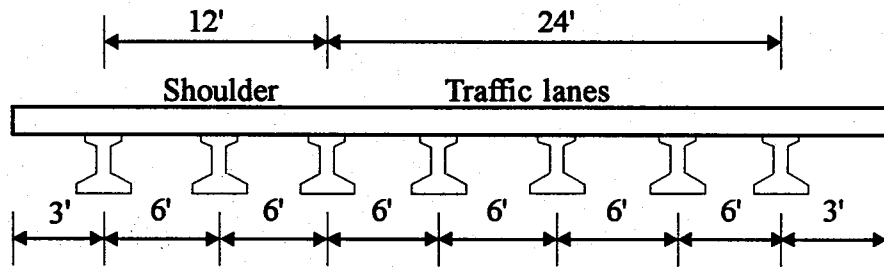
5.3 SHOULDER EFFECT ON LOAD DISTRIBUTION

Bridges in the urban areas are built with or without shoulders based on the traffic volume. The provision of shoulders in a bridge is also dictated by the overall cost considerations. The shoulders can be considered as additional lanes on each side of the bridge. The width of the shoulders can be as wide as the traffic lanes. This study investigates the effect of shoulders on the wheel load distribution of highway concrete slab-on-girder bridges.

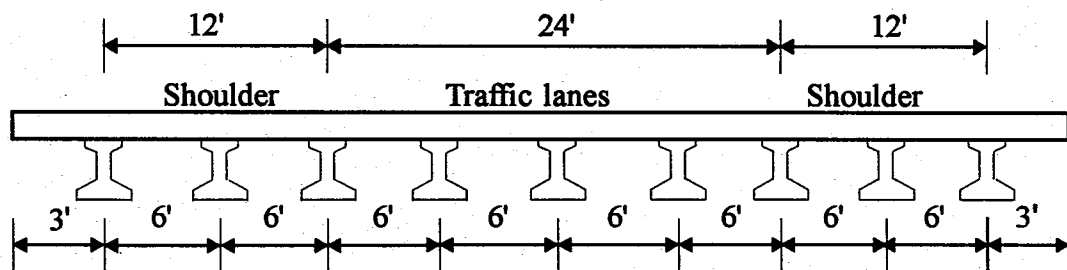
The typical bridge described in Chapter 4 is used for investigating the effect of shoulders on wheel load distribution. Fig. 5.9 shows the typical slab-on-girder bridge used in the analysis. The slab-on-girder bridge has a slab thickness of 7 in. on AASHTO type IV girders spaced at 6 ft. center to center and span length of 70 ft. The width of the bridge between the outside girders is 24 ft. with a 3 ft. overhang on each side when no shoulders are present (total width of 30 ft.). The addition of one 12-ft. shoulder increases the bridge width to 36 ft. (total width of 42 ft.) and the addition of two shoulders increases the width to 48 ft (total width of 54 ft.). The concrete strength of the girder and the slab is taken as 5000 psi in the study. The material properties (Elastic modulus, E , Poisson's ratio and modulus of rigidity, G) used in the FEM analysis are presented in Table 4.1 along with the sectional properties of the AASHTO type IV girder (Area, A and moments of inertia, I_y and I_z).



(a)



(b)



(c)

Fig 5.9 Typical slab-on-girder bridges: (a) without shoulder: (b) with one shoulder and (c) with two shoulders

A total of five cases were investigated in this study (Table 5.2). In the first case study, the bridge is considered with no shoulders and loads only on both the traffic lanes. One shoulder and loads only on both the traffic lanes are taken into account in the second case study. The third case study is similar to that in the second case except that the loads are applied on both the traffic lanes and the shoulder. In the fourth case, the bridge has two shoulders with loads only on the traffic lanes. The fifth case study includes loads on both the traffic lanes and the two shoulders. In all the cases, the bridges were loaded with the AASHTO HS-20 trucks at the location to produce maximum positive moments.

The transverse strain distributions in the bottom of the girder at the location of the maximum bending moment in the bridge are shown in Figs. 5.10-5.14. The transverse strain distributions are shown separately for the five cases since the width of the bridge varies for each case. The wheel load distribution factors for all cases based on the finite element method, AASHTO and LRFD codes are compared in Table 5.2.

The wheel load distribution factors based on AASHTO and LRFD specifications are constant for the five cases, since the codes do not consider the effect of shoulders on the distribution factors. The distribution factors based on FEM are generally smaller than those based on the AASHTO and LRFD codes. When the wheel loads are applied on the shoulders together with the traffic lanes, the load distribution factors tend to be the same for bridges without shoulders. However, when the wheel loads are applied only on the traffic lanes in the bridges with one or two shoulders, the load distribution factors

decrease slightly by about 4 to 8 %. Further studies using field tests could be made for determining the influence of shoulders on the wheel load distribution factors.

Table 5.2 Load distribution factors for bridges with or without shoulders

No. of shoulders	None	One	One	Two	Two
Wheel loads	2 Lanes	2 Lanes	2 Lanes and one shoulder	2 Lanes	2 Lanes and two shoulders
AASHTO	1.09	1.09	1.09	1.09	1.09
LRFD	1.211	1.211	1.211	1.211	1.211
FEM	1.016	0.966	1.054	0.997	1.035

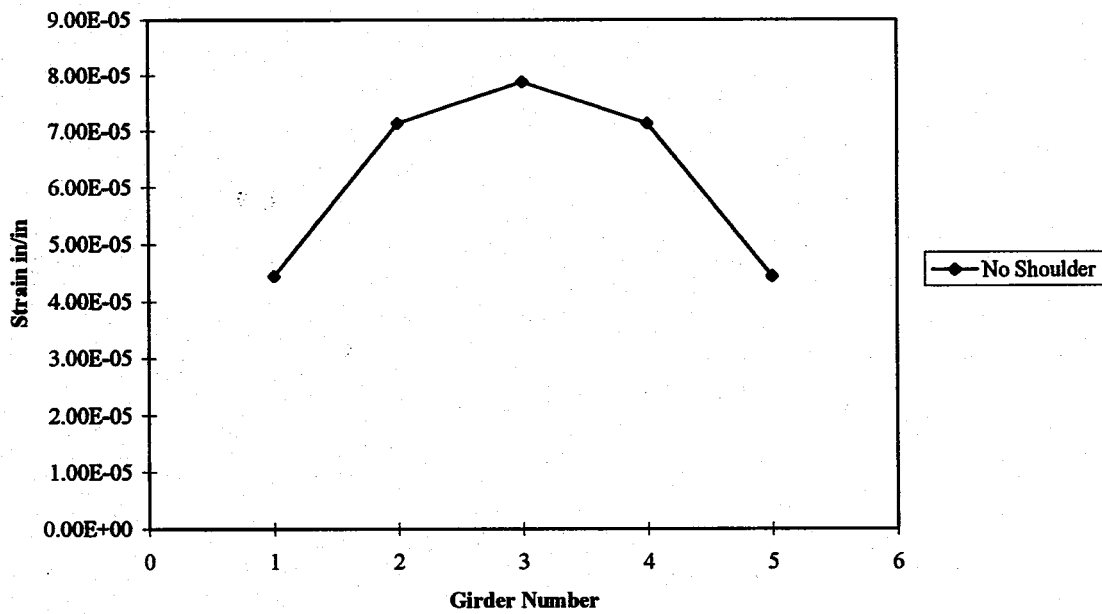


Fig. 5.10 Transverse strain distributions at mid-span for bridge with both traffic lanes loaded (no shoulders)

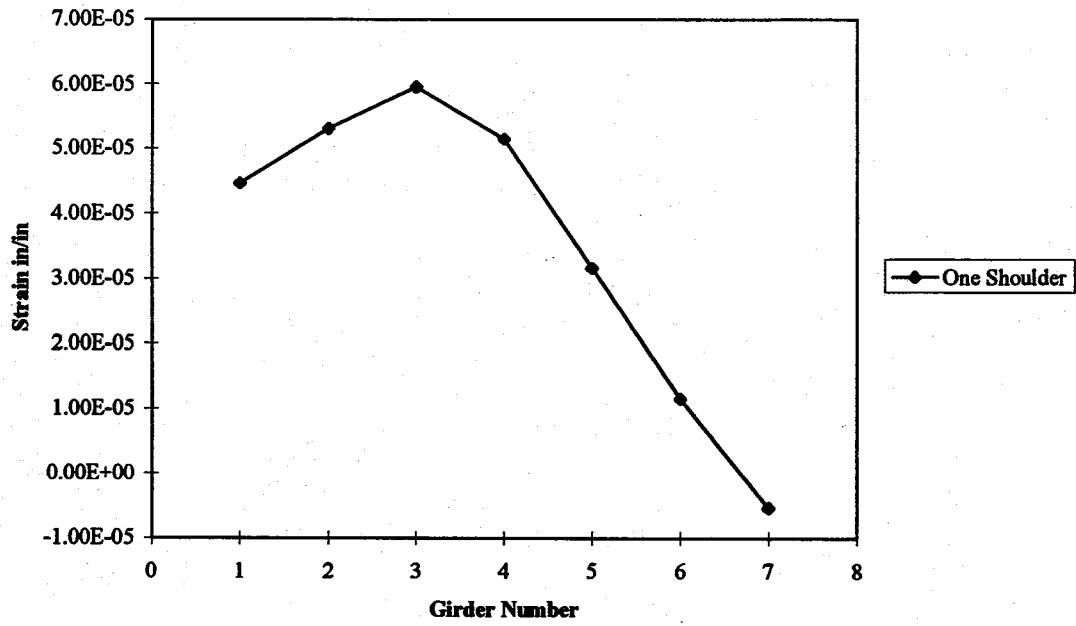


Fig. 5.11 Transverse strain distributions at mid-span for bridge with both traffic lanes loaded (one shoulder)

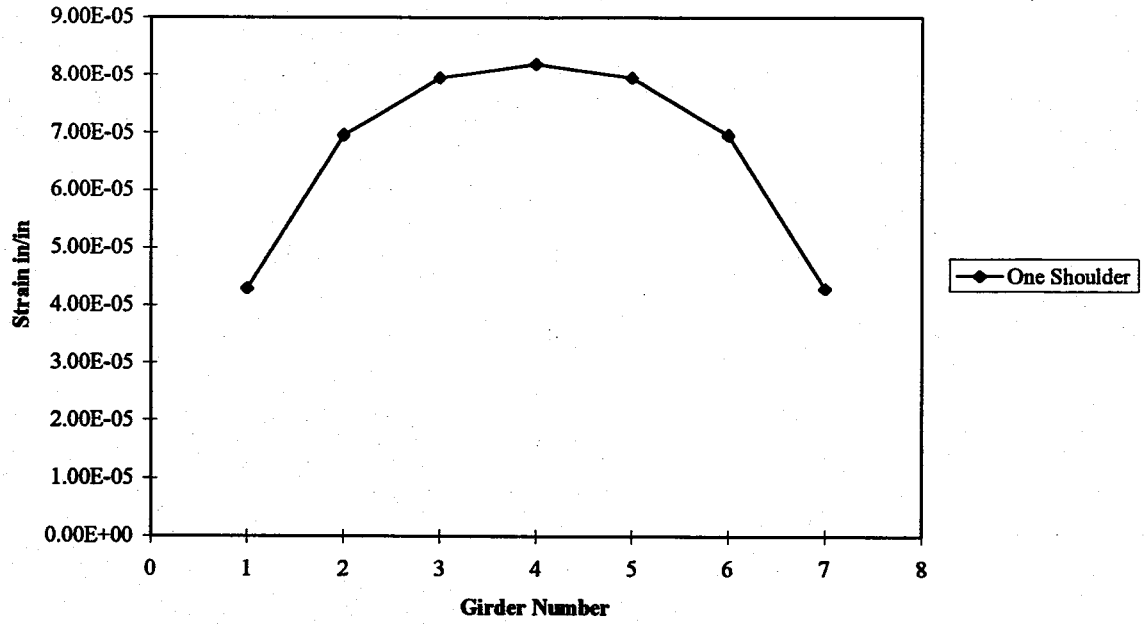


Fig. 5.12 Transverse strain distributions at mid-span for bridge with both traffic lanes and shoulder loaded (one shoulder)

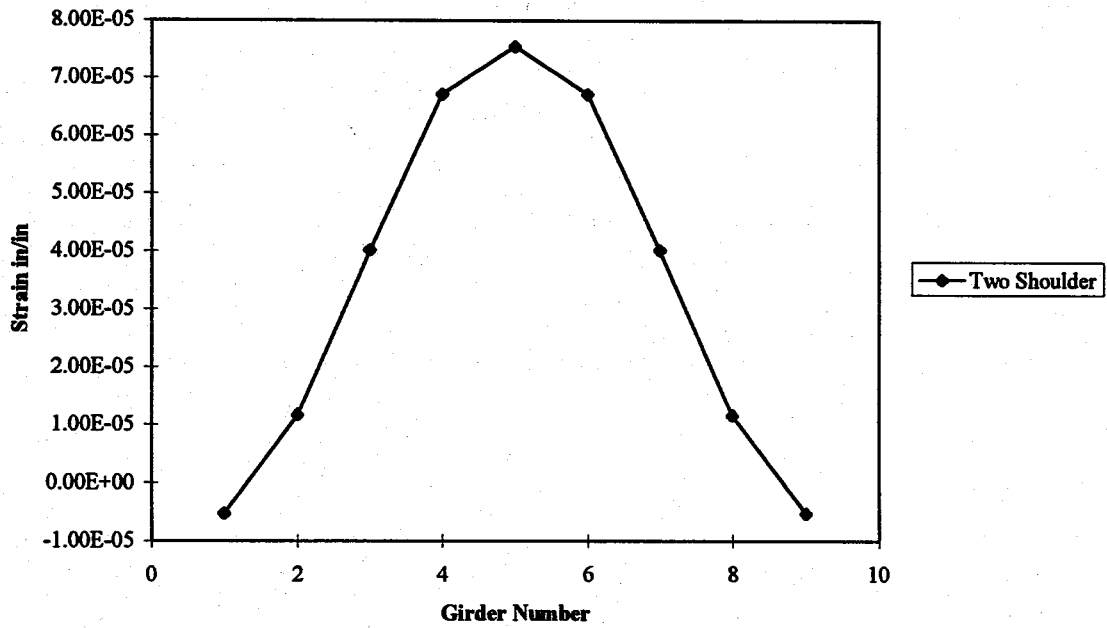


Fig. 5.13 Transverse strain distribution at mid-span for bridge with both traffic lanes loaded (two shoulders)

Two Shoulder (Lanes and Shoulders Loaded)

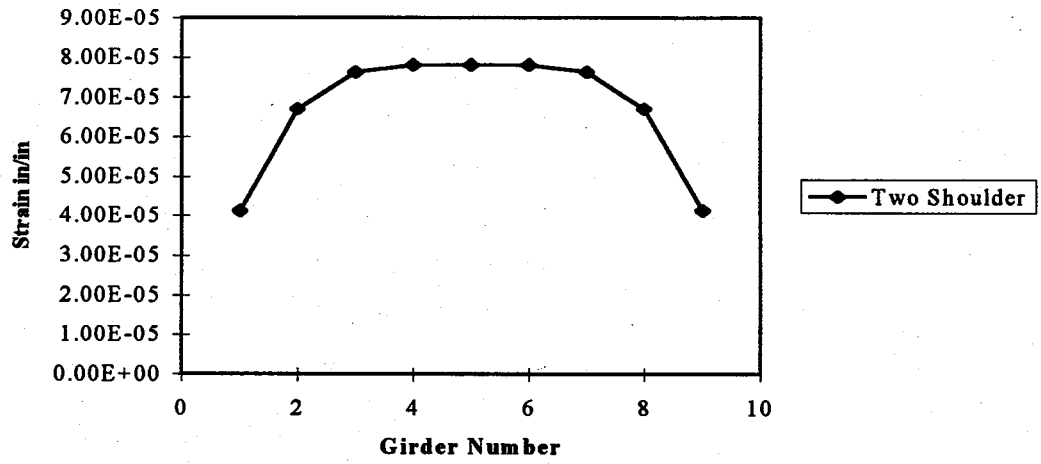


Fig. 5.14 Transverse strain distribution at mid-span for bridge with both traffic lanes and shoulders loaded (two shoulders)

CHAPTER 6

DISCUSSIONS ON WHEEL LOAD DISTRIBUTIONS OF SKEW SLABON-I-GIRDER BRIDGES BASED ON FIELD TESTS AND BRIDGE RATING

6.1 INTRODUCTION

Skew bridges are usually adopted to overcome complex intersections and space limitations. The AASHTO specifications (1992) provide the designer with load distribution factors for normal bridges (skew angle = 0°). The LRFD (Load and Resistance Factor Design) specifications (1994) allow for the girder bending moment to be reduced when the supports are skewed. Both the specifications are mainly based on laboratory tests and analyses of bridges with various bridge parameters such as span length, girder spacing, skew angle, etc. However, Departments of Transportation in certain states allow the use of load distribution factor based on bridge field-testing for the rating of existing bridges.

The purpose of this chapter is to provide the practicing engineer with a rational procedure to determine the load distribution factor from skew bridge field testing data and evaluate the specifications based on field tests and finite element analyses.

6.2 SKEW SLAB-ON-I-GIRDER BRIDGE FIELD TESTS

Florida Department of Transportation (FDOT) has tested many bridges for strength determinations. Prior to the actual load testing, the strain or deflection gages are installed at the critical locations along the girders. The test vehicles are then driven and placed on the critical locations of the bridge. The bridge is then loaded incrementally to induce the maximum bending moments. Incremental loading is achieved by adding concrete blocks with a self-contained hydraulic crane mounted on the test trucks. The measured strains and deflections are later analyzed and used to establish the strength of each component as well as the load distribution factors. Field test data from four slab-on I girder skew bridges are used in this study (Table 6.1). Three of the bridges are simply supported (Figs. 6.1-6.3) and one is continuous over two spans (Fig. 6.4).

TABLE 6.1 Skew slab-on-I girder bridge field tests

Field test	Location (Florida)	Span length (ft.)	Total width (ft.)	No. of lanes	Girder type ¹	Girder spacing (ft.)	Slab thickness (ft.)	Skew angle (deg.)	Span type
1	Duval County	104.15	42.9	Two	IV	5.3	7.0	17.5	Simple support
2	S.R.17	85.5	37.75	Two	III	5.17	7.5	45	Simple support
3	Turnpike	151.5	70.75	Four	V	5.92	7.0	20	Simple support
4	Palm Beach County	143.6	46.75	Two	V	7.79	7.0	30	Contin. (two spans)

Note: (1) All the girders are of AASHTO type

The Duval County (Jacksonville, Florida) bridge consists of 7 simply supported spans with span lengths ranging from 56 ft. to 104.15 ft. The length of the test span is

104.15 ft. with a skew angle of 17.48. The span consists of eight AASHTO Type IV prestressed concrete girders, spaced at 5.30 ft. center to center. The bridge carries two lanes of *traffic* with curb-to-curb width of 40.0 ft. The State Road 17 bridge consists of three simply supported spans with the test span of 85.5 ft. The span consists of seven AASHTO Type III prestressed concrete girders, spaced at 5.17 ft. center to center with the skew angle of 45 degrees. The bridge carries two lanes of traffic with curb-to-curb width of 26 ft.

The Florida Turnpike bridge is located over Interstate 595, which consists of five simply supported spans with the test span of 151.5 ft. The bridge consists of twelve simply supported AASHTO Type V girders spaced at 5.92 ft. center to center. The bridge is 68 ft. wide from curb to curb and carries four lanes and two 10 ft. shoulders with typical crash barriers on either side. The slab is 7 in. thick and the bridge is skewed 20 degrees. The bridge was constructed using an innovative shoring system to ensure composite action for both dead as well as live loads. The Palm Beach County bridge is located over I-95, which has four spans, two of which are continuous. The intermediate continuous spans are 143.6 ft. long with a bridge width of 46.75 ft. The 7 in. thick deck slab is supported on six AASHTO type V girders spaced at 7.79 ft. centers.

The bridge decks and girders of all the four bridges were in good condition. The bridges were loaded incrementally with 36, 48, 60 and 72 concrete blocks per truck. The strains and or deflection readings were taken at each load increment to establish the behavior of the bridge. The truck wheel loads for different number of blocks are

summarized in Table 6.2 and Figs. 2.4 and 2.5. Figs. 6.5, 6.6 and 6.8 show the strain distributions along the transverse sections for the field tests # 1, # 2 and # 4, whereas Fig. 6.7 shows the girder deflections for field test # 3.

TABLE 6.2 Truck Wheel Loads for the Skew Bridge Field Tests

Field test	Maximum number of blocks	Applied loads (kips)					Number of trucks
		P1	P2	P3	P4	P5	
1	60	12.00	33.01	33.01	42.84	42.84	Two
2	60	12.00	33.01	33.01	42.84	42.84	One
3	72	12.17	37.80	37.80	49.66	49.66	Two
4	48	11.83	28.23	28.23	36.03	36.03	One and two

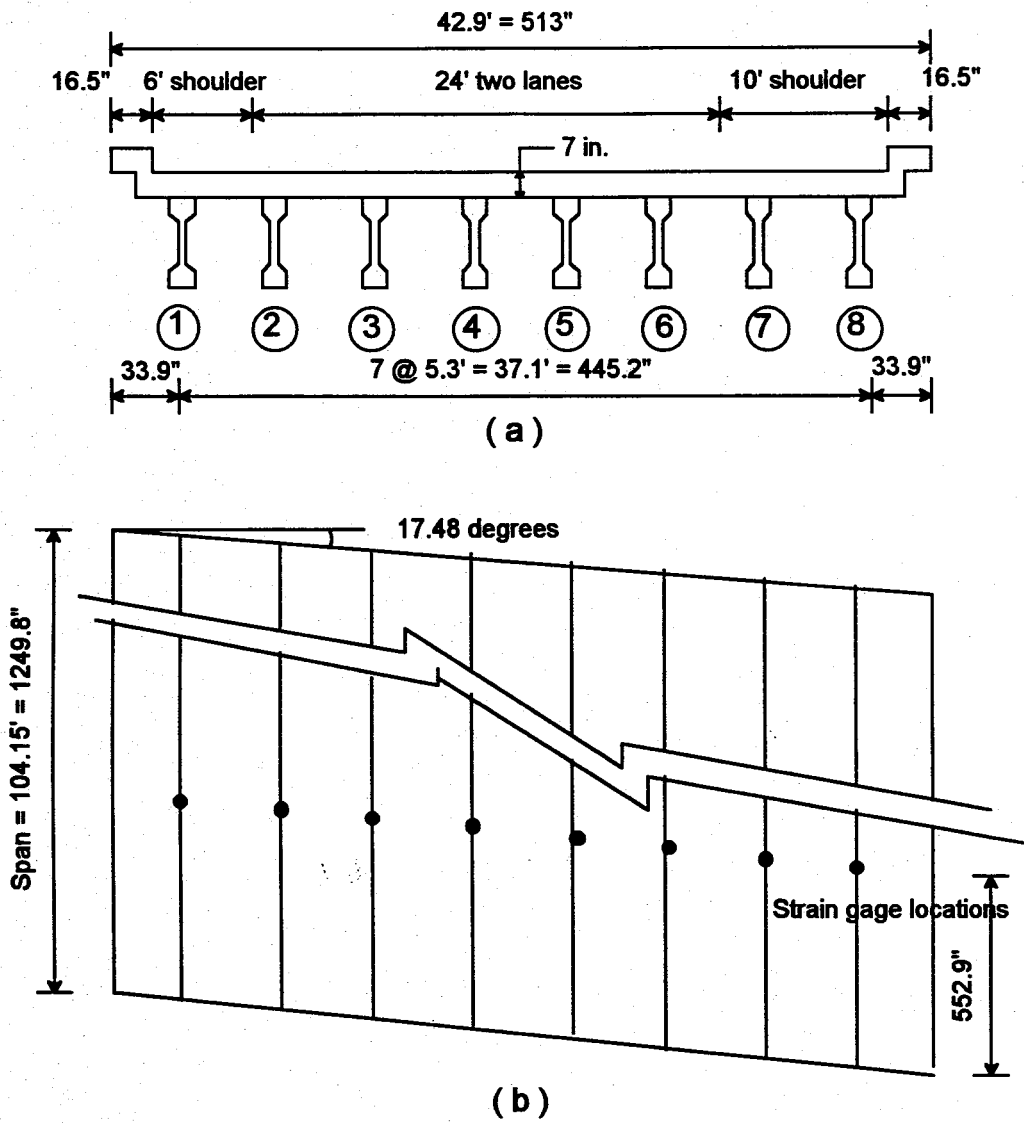
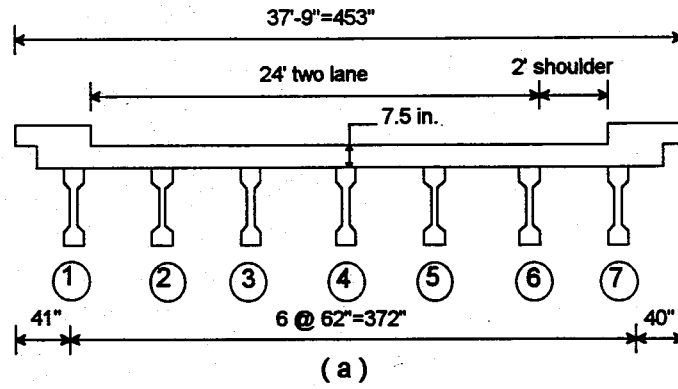
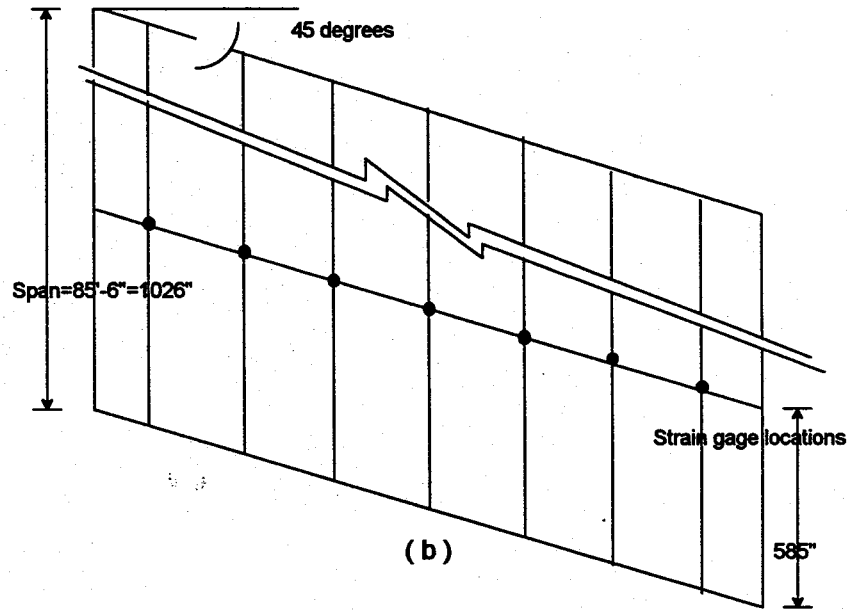


Fig. 6.1 Details of bridge – field test # 1



(a)



(b)

Fig. 6.2 Details of bridge – field test # 2

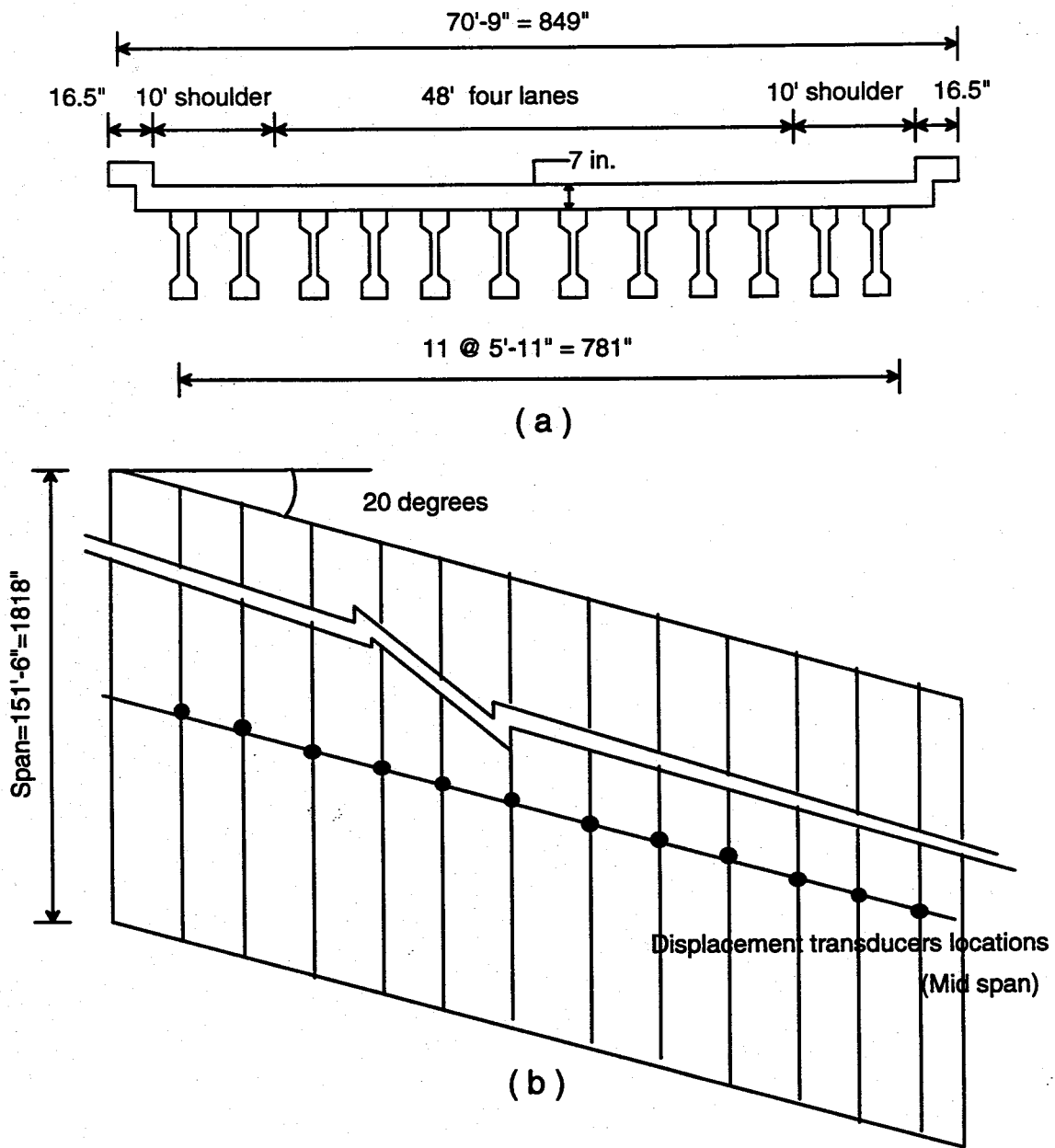


Fig.4.32 Details of Turnpike bridge

Fig. 6.3 Details of bridge – field test # 3

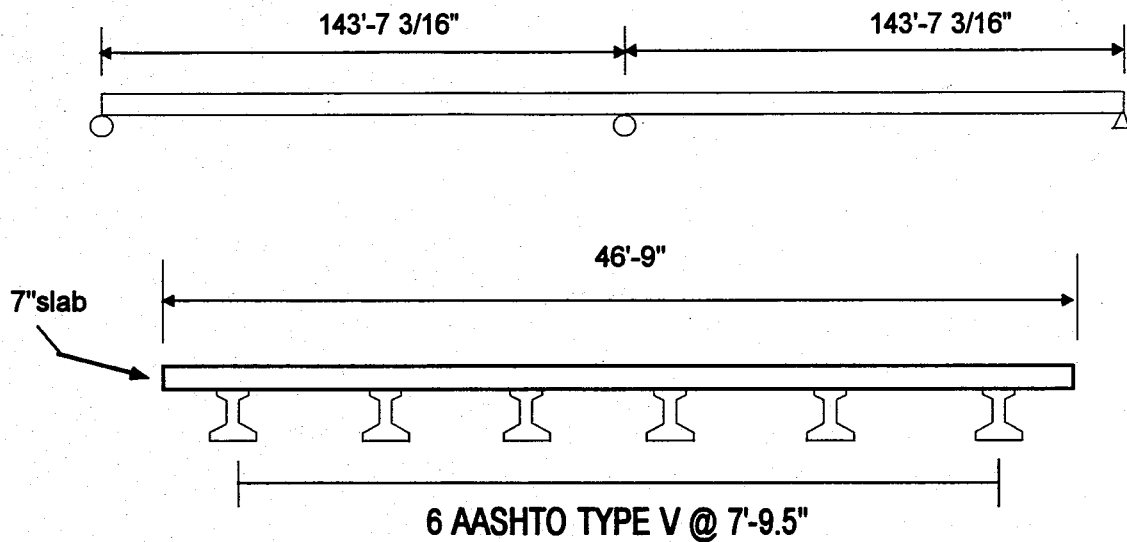


Fig. 6.4 Details of bridge – field test # 4

6.3 FINITE ELEMENT ANALYSES OF LAB-ON-1-GIRDER BRIDGES

Linear elastic material properties are used in the modeling. The reinforced concrete slab is modeled using shell elements with eight or four mid-surface nodes. Each I-girder is divided into three parts: the bottom and top flanges and the web (Fig. 2.2). Each flange was modeled by a beam element with its properties lumped at the centroid of the flange. The web was modeled by shell elements with four or eight mid-surface nodes. Each mid-surface node has six degrees of freedom. To satisfy the compatibility of composite behavior, a rigid element was assumed between the top beam elements and the centroids of the top deck slab shell elements. Each bearing support was assumed to be located at the centroid of the beam element representing the bottom flange of the girder. Under linear elastic conditions, strains are proportional to the bending moments in the girders. Hence, maximum strains at the extreme fiber of the bottom flanges obtained from finite element results were used to compute the wheel load distribution factors of the girders, which are compared with those of AASHTO and LRFD specifications.

6.4 LOAD DISTRIBUTION FACTORS OF SLAB-ON-1-GIRDER BRIDGES BASED ON STRAIN AND DEFLECTION MEASUREMENTS

Two methods for determining the load distribution factors from the measured and computed strains or deflections are presented, evaluated and compared with AASHTO and LRFD specifications in this section. The specifications define the load distribution factor as the fraction of maximum moment in a girder to the maximum moment in the bridge idealized as one-dimensional beam subjected to a loading of one line of wheels (AASHTO) or a loading of two lines of wheels, i.e. a truck (LRFD). This basic definition of the load distribution factor is the basis for the first method (Method I) of calculating load distribution. The load distribution factor in method I is calculated using the following Eqn. 6.1:

$$DF_{Method\ I} = \frac{M_{Girder}}{M_{Bridge}} \quad (6.1)$$

The girder maximum bending moment (M_{Girder}) can be obtained by multiplying the maximum strain measured at the bottom flange by the section modulus and the concrete modulus of elasticity as shown below:

$$M_{Girder} = \epsilon ES \quad (6.2)$$

Where

ϵ = the strain at the extreme fibers of the bottom flange, E = the concrete modulus of elasticity, and S = the section modulus. The elastic modulus of concrete was calculated based on concrete strength, f'_c (5000 psi). Many bridges exhibit some degree of composite action even when they are not constructed with shear studs or other devices for transferring shear between the girders and deck slab. The composite and non-composite

section moduli were used to calculate the measured bending moments. The use of composite section modulus yields a higher measured bending moment.

The second method (Method II) is based on the fact that the sum of internal bending moments in the girders is equal to the externally applied bending moment due to the wheel loads for a straight bridge. For the field load tests, where all traffic lanes are loaded with equal-weight trucks, the measured wheel load distribution factor is given below [Stallings and Yoo(1993)]

$$DF_{method\ II} = \frac{n\epsilon_{max}}{\sum_{i=1 \rightarrow k} \epsilon_i w_i} \quad (6.3)$$

Where

ϵ_{max} = maximum bottom flange strain at any girder,

ϵ_i = bottom flange strain at the i th girder

w_i = the ratio of the section modulus of the i th girder to the section modulus of a typical interior girder

k = number of girders,

n = number of wheel lines of applied loading

The parameter, n is required to make the measured wheel load distribution factor compatible with AASHTO definition.

Eqn. 6.3 is based on the assumption that the sum of the internal moments or the total area under the moment distribution curve should be equal to the externally applied moment. This assumption is valid for straight bridges. However, this assumption is not accurate for bridges with large skew angles, which exhibit larger torsional moments.

Therefore, the sum of the girder strains in a straight bridge will be used to take into account the total external load effects in skew bridges and Eqn. 6.3 can be modified as follows:

$$DF_{\max \theta} = \frac{n \varepsilon_{\max \theta}}{\left(\sum_{i=1 \rightarrow k} \varepsilon_i W_i \right)_{\theta=0}} \quad (6.4)$$

The skew angle for all the tests were less than 30° except for field test # 2 and therefore, Eqn. 6.3 was used instead of Eqn. 6.4 in the load distribution calculations. The measured load distribution factors were compared with those based on AASHTO, LRFD and finite element analyses.

6.5 FIELD TEST RESULTS AND DISCUSSIONS

The measured strains and deflections corresponding to the maximum bending moment location during the field tests are shown in Figs. 6.5 to 6.8. The measured strains and deflections corresponding to the loading cases (Table 6.2) and the finite element analysis are presented in the above graphs. Generally the measured strains and deflections in the field tests show good agreement with the computed values using FEM. The finite element modeling presented in section 6.3 thus appears to realistically take into account the behavior of the test bridges. Table 6.3 summarizes and presents the comparison of the load distribution factors for interior girders of the test bridges based on the measured strains and deflections, FEM AASHTO, and LRFD.

The load distribution factors determined using method I are based on noncomposite and composite section moduli of the slab-on-1-girder bridges. The girder

moments as well as the load distribution factors based on composite section modulus are always greater than that based on non-composite section modulus. The wheel load distribution factors based on method II are generally higher than those from method I and closer to the values from the AASHTO and LRFD methods. Thus, it appears that the method II presented in section 6.4 can be used in computing realistic wheel load distribution factors for slab on girder bridges. Method II requires only the bottom flange strains or girder deflections in the computations of load distribution factors, whereas method I requires the estimation of the section modulus (composite or non-composite) and concrete modulus of elasticity besides the strains for an existing bridge. The wheel load distribution factors based on AASHTO and LRFD codes are generally higher than those based on measured and computed strains.

For field test # 2 and one loading case in field test # 4, only one traffic lane was loaded, whereas the AASHTO and LRFD methods always assume that all the traffic lanes to be loaded in the calculation of the load distribution factors of interior girders. Hence, the load distribution factors determined based on the measured and computed strains are not compared with the AASHTO and LRFD values. In the case of field test # 3, the measured deflections were used to determine the load distribution factors using method II. The method I could not be used since the estimation of the girder moments based on the measured deflections in the bridge is rather complex. The measured deflections in the bridge are a function of the overall geometry, boundary conditions, effective moment of inertia of the girders and the structural configuration.

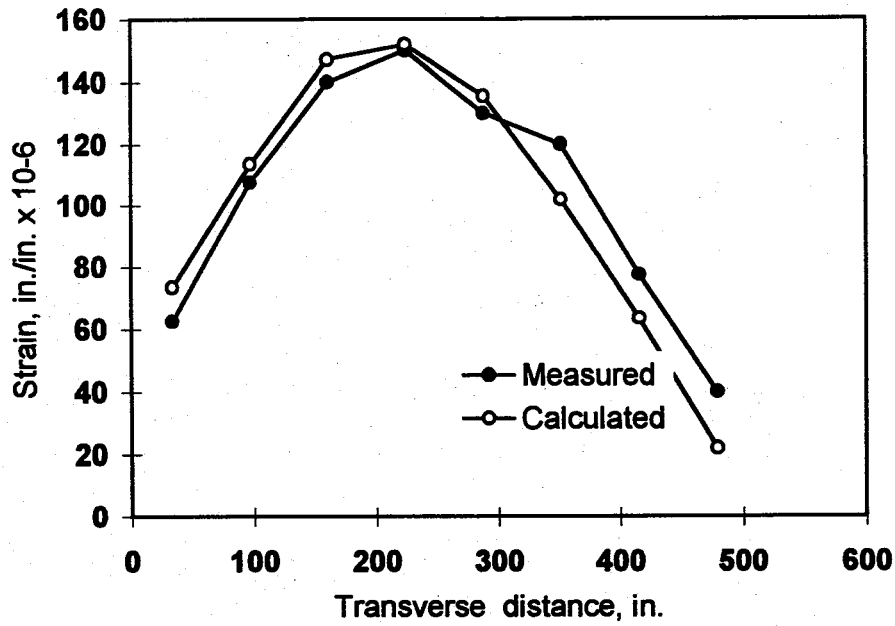


Fig 6.5 Transverse strain variations (field test # 1)

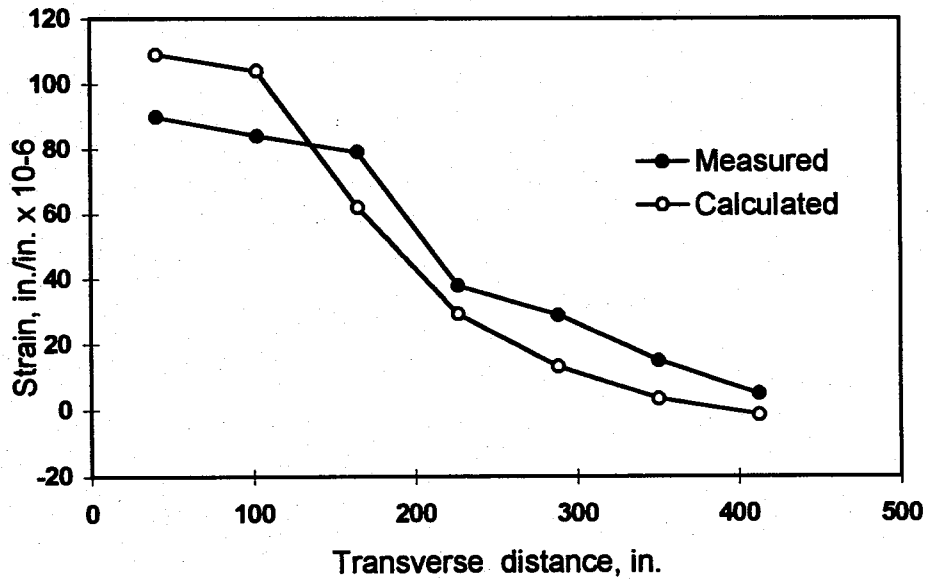


Fig. 6.6 Tranverse strain variations (field test # 2)

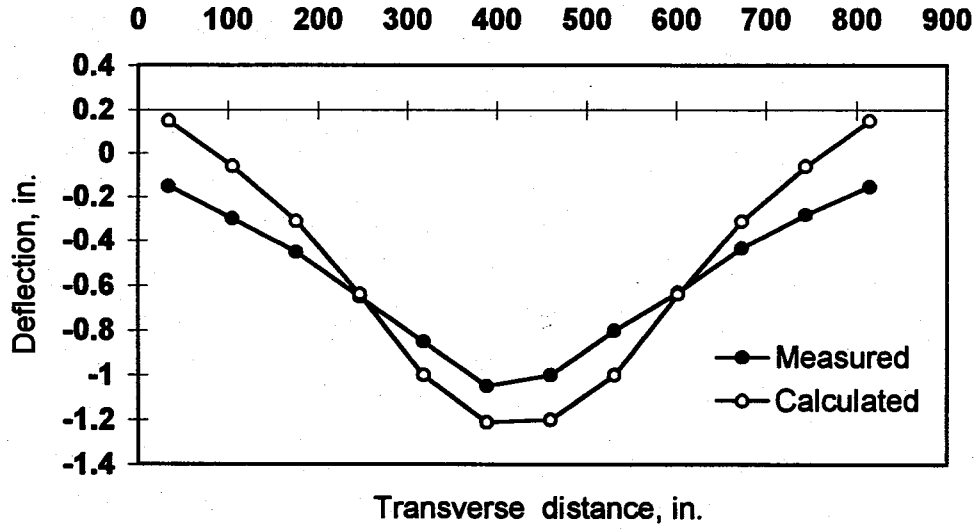


Fig. 6.7 Transverse deflection variations (field test # 3)

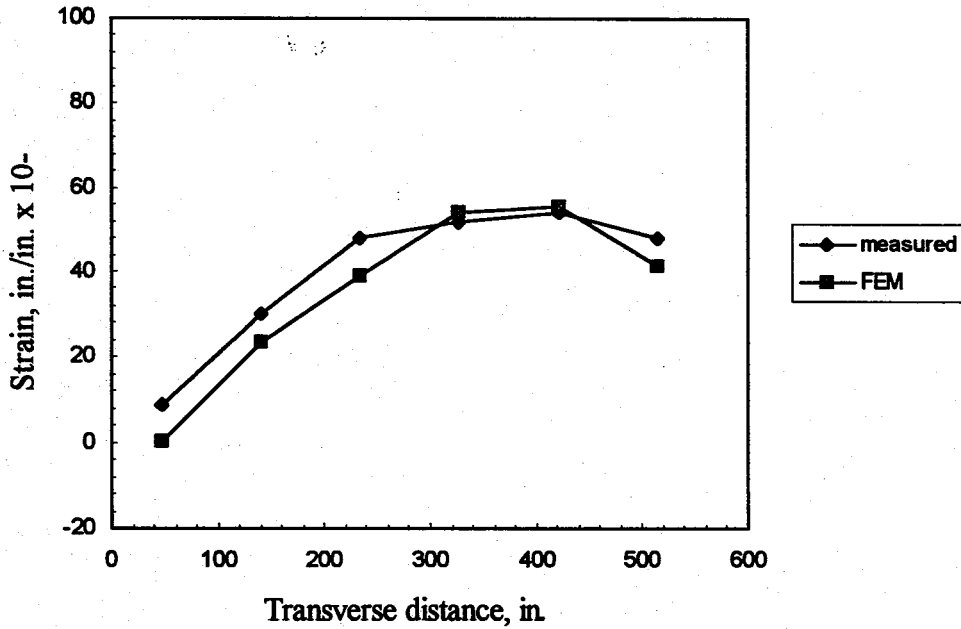


Fig. 6.8 Transverse strain variations (one truck) (field test # 4)

TABLE 6.3 Summary of load distribution factors (interior girders)

Field test	Measured strains			F.E.M.			AASHTO	LRFD
	Method I		Method II	Method I		Method II		
	Non-comp.	Comp.		Non-comp.	Comp.			
# 1	0.614	0.906	0.725	0.622	0.918	0.752	0.964	0.988
# 2 (one lane loaded)	0.279	0.453	0.494	0.344	0.560	0.650	N.A.	N.A.
# 3	-----	-----	0.623	-----	-----	0.790	1.076	1.003
# 4 (one truck)	0.300	0.406	0.900	0.309	0.420	1.042	N.A.	N.A.
# 4 (two trucks)	0.603	0.810	0.840	0.871	1.170	0.967	1.42	1.21

6.6 SLAB-ON-1-GIRDER BRIDGE. RATING BASED ON DIFFERENT WHEEL LOAD DISTRIBUTION FACTORS

Wheel load distribution factors based on measured strains, finite element method, AASHTO and LRFD codes are used in calculating the operating rating for slab-on-I-girder bridges. The following expressions are used to determine the operating ratings (Manual for Maintenance Inspection of Bridges, 1982).

The operating strength analysis:

$$RF = \frac{\phi R_n - 1.3D}{1.3L(1+I)} \quad (6.5)$$

where

RF = the rating factor

Φ = the capacity reduction factor

D = the nominal dead load effect

L = the nominal live load effect

I = the impact factor

R_n = the nominal strength of the member

The bridges (field test # 1 and # 4 with two traffic lanes loaded) are used as illustrative examples for the bridge rating based on different methods of wheel load distributions. The nominal moment strengths are actually dependent on the concrete strength, steel properties and amount of prestressing and untensioned reinforcement. For the sake of illustrations, realistic values of nominal strengths are assumed, which could be different from the actual values for the two existing bridges.

Table 6.4 summarizes the results of the rating calculations for the two bridges. The calculations for the bridge (field test # 1) are based on girder nominal moment, M_n equal to 65,000 kips-in. and the girder dead load moment MD equal to 22,573 kips-in. For the FDOT test vehicle, the maximum live load moment per truck is equal to 20,760 kips-in. The girder nominal moment, M_n for the second bridge (field test # 4) was assumed to be equal to 94,000 kips-in. and the girder dead load moment MD equal to 29,122 kips-in. The maximum live load moment per truck in the second bridge (field test # 4) was equal to 23,530 kips-in.

The operating rating factors based on measured strains and finite element method, are generally much higher than those calculated based on AASHTO and LRFD specifications. These rating factors give more realistic assessment of the bridge strength than the codes. However, the values of rating factors presented in Table 6.4 may vary depending on the actual amount of reinforcement and the properties of concrete and steel in the existing bridges.

Table 6.4 Summary of slab-on-I-girder bridge rating factors

Load distribution based on	Field test # 1			Field test # 4		
	Load distribution factor	Live load moment per girder (kips-in.)	Operating rating factor	Load distribution factor	Live load moment per girder (kips-in.)	Operating rating factor
Measured strain	0.725	7522	2.29	0.84	9883	2.80
FEM	0.752	7802	2.21	0.967	11377	2.43
AASHTO	0.964	10002	1.725	1.42	16707	1.65
LRFD	0.988	10251	1.68	1.21	14236	1.94

CHAPTER 7

SUMMARY AND CONCLUSIONS

7.1 SUMMARY

The studies on wheel load distribution are carried out in three phases. Studies in Phase I were focused on straight slab-on-girder, solid slab, voided slab and double Tee bridges. The existing analytical and field load distribution methods were reviewed for different bridge types. The grillage analogy concepts were presented together with the cross sectional properties of different bridge types for grillage analogy idealization, field test procedures and methodologies. Several parameters such as span length, bridge width, slab thickness, edge beam and number of lanes are considered in the parametric studies of solid and voided slab bridges. One hundred and sixty study cases were carried out to evaluate the various parameters affecting load distribution of slab-on-girder bridges. The load distribution factors from the analysis of double Tee simply supported bridges are compared with those based on the AASHTO and LRFD codes. The studies in Phase II were focused on wheel load distribution of the skew slab-on-girder and skew solid slab bridges. The various parameters affecting load distribution of skew simply supported slab-on-girder bridges were studied using finite element method and data from the field tests are used to verify the analytical results. Analytical and field studies on the wheel load distribution of skew simply supported solid slab bridges are presented and compared with those

based on the AASHTO and LRFD codes. The finite element method and field test data were used to investigate the continuous skew and straight slab-on-I girder bridges and compute the corresponding wheel load distribution factors.

The present studies in Phase III were mainly directed towards the analyses of comprehensive field test data, shear load distribution of continuous slab-on-girder bridges, and effects of diaphragms and shoulders on the wheel load distribution factors. The main parameters that affect shear load distribution are compared for single and multiple span bridges. The study on shear load distribution focuses on five main parameters: spacing between the girders, variation of skew angle, variation in the number of spans, ratio between adjacent two spans, and span length. The effect of diaphragms on wheel load distribution was first evaluated for a field test bridge and compared with a finite element model of the actual bridge. The diaphragm parameters that affect the wheel load distribution were studied to evaluate the effect of each parameter. The main conclusions based on the studies in Phases I, II and III are presented in the following sections.

7.2 CONCLUSIONS

7.2.1 Straight Solid and Voided Slab Bridges

- i) The effective widths calculated using grillage analogy are larger than those based on AASHTO and LRFD codes, which indicate that both the codes give conservative estimate of effective width, E for solid slab bridges.

- ii) Based on this limited study, the bridge width can be neglected as a parameter in calculating the effective widths of solid slab bridges.
- iii) The variation of slab thickness has very little effect in the effective width, which confirms the approaches specified by AASHTO and LRFD codes in neglecting the thickness as a parameter.
- iv) The edge beam moment increases with increase in moment of inertia, i.e. increase in edge beam depth or width. Slab bridges without edge beams or with hidden edge beams have greater maximum moment than similar slab bridges with edge beam and hence the resulting effective width is smaller. These results suggest that the edge beam size should be taken into account in wheel load distribution.
- v) Based on the solid slab parametric studies, the span length and the edge beam depth are the main parameters affecting the effective width calculations. Effective width equations are proposed for solid slab bridges without edge beams and with edge beams.
- vi) The maximum bending moment for solid slab is smaller than that for voided slab bridges, which means the solid slab has larger effective width than voided slab bridges. The larger moment in existing voided slab bridges may be attributed to the relative vertical movements between the voided slab precast units.

7.2.2 Straight Slab-on-Girder Bridges

- i) Girder spacing is an important factor in determining both flexural and shear wheel load distributions of slab-on-girder bridges.
- ii) The flexural load distribution factors based on LRFD are slightly smaller than those calculated using grillage analogy for larger girder spacing. However, the load distribution factors based on LRFD code are in better agreement with those for smaller girder spacing, which are more commonly used.
- iii) The calculated flexural load distribution factors are slightly larger than those based on AASHTO and LRFD codes particularly for shorter spans. However, the AASHTO and LRFD load distribution factors are more accurate for longer spans (90 and 100 ft), which are commonly used in bridges.
- iv) The flexural load distribution factor for the 54 ft. wide bridge is slightly higher than that for the 36 ft. wide bridge (2% to 4%) and this can be considered to be insignificant. This establishes that AASHTO and LRFD codes are realistic in neglecting the bridge width as a parameter in wheel load distribution.
- v) For a given girder spacing, the LRFD load distribution equation overestimates the effect of longitudinal stiffness parameter, K_g on wheel load distribution and this is more evident for exterior girders.

- vi) The detailed parametric studies on shear load distribution indicate that the spacing between girders is a dominant parameter in shear load distribution. Parameters such as span length, bridge width and girder stiffness have little effect on shear load distribution for AASHTO girders.
- vii) Simplified equation for shear load distribution of slab-on-AASHTO girders is suggested for interior and exterior girders.
- viii) In general, the flexural load distribution factor decreases with increasing span for interior and exterior bulb-tee girders; but this decrease is more than that for AASHTO girders. The girder stiffness effect was insignificant in bulb-Tee flexural load distribution.

7.2.3 Straight Double-Tee Bridges

- i) The load distribution factors for the interior girders decrease whereas those for exterior girders increase with increase in span. The load distribution in exterior girders is more dependent on the span, which is consistent with that of the slab-on-AASHTO girders.
- ii) The calculated distribution factors based on grillage analogy are smaller than those based on LRFD and AASHTO codes.

7.2.4 Skew Solid Slab Bridges

- i) The effective widths calculated using finite element method are larger than those based on AASHTO and LRFD codes, which indicate that the codes give conservative estimate of effective width, E for skew solid slab bridges.
- ii) The effective width increases with increase in the skew angle for solid slab bridges. This confirms the LRFD code in considering the skew angle as a parameter in effective width calculation. The finite element results show that for skew angles higher than 30° , the effective width is governed by the lane width.
- iii) The span length is an important factor in effective width calculation of skew solid slab bridges. The effective width tends to increase as the span length increases.
- iv) The effect of edge beams has been studied in this investigation and found to be significant. The effective widths of skew solid slab bridges with edge beams are smaller than those without edge beams and follow the same trend for the straight solid slab bridges.
- v) Based on the skew solid slab parametric studies, the skew angle, span length and the edge beam depth are the main parameters, which significantly affect the effective widths. The effective width equations proposed for straight solid slab bridges are modified for skew bridges with a skew angle factor.

- vi) Effective width calculations based on the measured strains are higher than the AASHTO and LRFD values. The AASHTO and LRFD effective width equations do not take into account the additional stiffness due to edge beams, shoulder widths and parapets.

7.2.5 Skew Slab-on-Girder Bridges

- i) Based on the parametric studies using finite element method, it is observed the skew angle increase reduces load distribution factors for the interior girders and that the LRFD code accurately estimates the skew angle effect particularly for skew angles higher than 30 degrees.
- ii) Skew angle effect on load distribution for exterior girders is similar to that of the interior girders.
- iii) Girder spacing is a very important factor in determining flexural wheel load distributions of skew slab-on-girder bridges.
- iv) The flexural distribution factors based on LRFD are slightly smaller than those calculated using finite element method particularly for larger girder spacing. It is shown that the distribution factors based on LRFD code are in better agreement with those calculated using finite element method for smaller girder spacing, which is more commonly used.

- v) The interior girder distribution factor based on finite element method shows much- smaller decreases with increasing span length similar to the LRFD code. However, the load distribution factors for exterior girders based on finite element analyses increase with increasing span length.
- vi) For a given skew angle, girder spacing and span length, the LRFD load distribution equation overestimates the effect of slab thickness on wheel load distribution. The finite element results show little effect on load distribution for variation of slab thickness between 3.85 in to 7 in., which corresponds to a variation of stiffness ratio, H between 5 to 30.
- vi) The load distribution factors based on finite element analyses were close to those based on the measured strains (less than 30 % difference) and this difference may be attributed to the variations in concrete strength and section modulus, which are used in calculating the measured distribution factor. Both load distribution factors based on AASHTO and LRFD were higher than those calculated using the measured strains and finite element method. This may be attributed to the fact that AASHTO code and to a lesser extent, the LRFD code do not take into account the additional stiffness contribution to the bridge from the shoulder and parapets.

7.2.6 Continuous Slab-on-Girder Bridges

The parametric studies of continuous bridges were carried out to investigate the effects of number of spans, the skew angle, and the ratio between two spans.

7.2.6.1 Parametric Study on Flexural Load Distribution Factors

- i) In continuous bridges, the strains are generally higher at the interior supports than at midspans. The strain distributions in the transverse direction are similar for both positive and negative moment load cases. The FEM analyses show that strain distributions become less uniform as skew angle increases.
- ii) Based on the parametric studies, the effect of the number of spans on the load distribution factors is small and can be neglected. In general, the FEM load distribution factors are smaller than those based on LRFD code.
- iii) The interior girder load distribution factors show little variation as the ratios between the spans increase for both positive and negative moments. However, the exterior girder load distribution factors show a small increase (10%- 13%) as the ratios between the spans increase,
- iv) Comparisons between continuous and single span slab-on-girder bridges have shown that there is little change in the distribution factor with increase in the number of spans.

7.2.6.2 Parametric Study on Shear Load Distribution Factors

- i) The shears for interior and exterior girders increase with increase in skew angles at the exterior and interior supports. The skew angle results in non-uniform transverse shear distributions in the girders. The shear load distribution factors based on FEM analysis are smaller than those based on LRFD code.
- ii) The shear forces for interior and exterior girders close to the exterior and interior supports of the straight bridges decrease slightly with the increase in number of spans. The shear load distribution factors are constant with the increase in the number of spans and that the AASHTO and LRFD distribution factors are higher than the values based on FEM.
- iii) The shear forces in the girders and the shear load distribution factors increase with an increase in the girder spacing for both interior and exterior girders close to the interior and exterior supports. The shear load distribution factors based on the FEM are smaller than the LRFD and AASHTO values for interior and exterior girders.
- iv) The shears in the interior girders remain nearly the same as the ratios of the spans increase and the shear load distribution factors are constant. The variations in the shear distributions of exterior girders are very small with increase in the ratios of the span and

the corresponding shear load distribution factors are also constant. The same trends are observed for both straight and skew bridges with varying span ratios.

- v) Based on the parametric studies of twenty four cases considering span length, the shear load distribution factors are found to be independent of the span lengths for all the cases.

7.2.6 Diaphragm and Shoulder Effects on Wheel Load Distribution

7.2.7.1 Diaphragms

The parametric study was focused on determining the effect of the diaphragm locations along the span on the wheel load distribution of skew and straight bridges. Three different diaphragm locations that are commonly used in bridges were selected in the parametric studies. All the parametric study cases have diaphragms between the girders at the supports. The first case has no interior diaphragms, whereas the diaphragms at the mid-span are considered in the second case. The diaphragms at the third points were considered, in the third case.

- i) The flexural strains of interior girders slightly decrease with the increase in the number of diaphragms. The wheel load distribution factors of interior girders are not dependent on the number of diaphragms and this agrees with AASHTO and LRFD specifications, which do not consider the diaphragm in wheel load distribution.

- ii) The transverse strain distributions at the mid-span for exterior girder loading decrease marginally as the number of diaphragms increase. The wheel load distribution factors for exterior girders slightly increase with the increase in the number of diaphragms.
- iii) It can be concluded that the presence and location of diaphragms do not seem to have a major effect on the transverse load distribution at the mid-span for interior and exterior girders and this is valid for straight and skew bridges. This finding agrees with the AASHTO and LRFD codes, which neglect the diaphragm in wheel load distribution.

7.2.7.2 Shoulders

A typical slab-on-girder bridge is used for investigating the effect of shoulders on wheel load distribution. A total of five cases were investigated in this study. In the first case study, the bridge is considered with no shoulders and loads only on both the traffic lanes. One shoulder and loads only on both the traffic lanes are taken into account in the second case study. The third case study is similar to that in the second case except that the loads are applied on both the traffic lanes and the shoulder. In the fourth case, the bridge has two shoulders with loads only on the traffic lanes. The fifth case study includes loads on both the traffic lanes and the two shoulders. In all the cases, the bridges were loaded with the AASHTO HS-20 trucks at the locations to produce the maximum positive moments.

The wheel load distribution factors based on AASHTO and LRFD specifications are constant for the five cases, since the codes do not consider the effect of shoulders on the load distribution factors. The load distribution factors based on FEM are generally smaller than those based on the AASHTO and LRFD codes. When the wheel loads are applied on the shoulders and the traffic lanes, the load distribution factors tend to be the same for bridges without shoulders. However, when the wheel loads are applied only on the traffic lanes, the load distribution factors decrease slightly by about 4 to 8 %.

7.2.8 Field Tests

The typical bridge types for load testing in Phase III include i) skew slab-on-girder and ii) continuous skew slab-on-steel -girder. The instrumentation was designed to measure strains and deflections at critical sections of the test bridges. The members of the research team from the Center for Infrastructure and Constructed Facilities participated in the comprehensive field-testing carried out by the Structural Research Center, Florida Department of Transportation, Tallahassee.

The finite element model was used to analyze the test bridges. In general, the calculated deflections are larger (about 24%) than the measured values in the skew slab-on-girder bridge. The measured and calculated strains show better agreement than the corresponding deflections. This indicates that the finite element model used in the analysis is more accurate in predicting the

strains. The load distribution factors based on measured and calculated strains are smaller than those based on AASHTO and LRFD codes.

The difference between the measured and computed maximum strains at mid-span of the continuous skew slab-on-steel girder bridge is in the range of 11%, when diaphragms are not considered in the FEM analysis. However, this difference reduces to only 3% when diaphragms are taken into account in the FEM analysis. The AASHTO and LRFD load distribution factors are higher than the FEM values and the FEM results are closer to the measured load distribution factors.

7.2.9 Comments on the Load Distribution Factors Based on Measured Strains

The purpose of this section is to provide the practicing engineer with a rational procedure to determine the load distribution factor from test data of skew bridges and evaluate the specifications based on field tests and finite element analyses. Two methods for determining the load distribution factors from the measured and computed strains or deflections are presented, evaluated and compared with AASHTO and LRFD specifications.

The specifications define the load distribution factor as the fraction of maximum moment in a girder to the maximum moment in the bridge idealized as one-dimensional beam subjected to a loading of one line of wheels (AASHTO) or a loading of two lines of wheels, i.e. a truck (LRFD). This basic definition of the load distribution factor is the basis for the first method

(Method I) for calculating load distribution factor. The load distribution factor in method I is calculated using Eqn. 6.1. The girder maximum bending moment (M_{girder}) can be obtained by multiplying the maximum strain measured at the bottom flange by the section modulus and the concrete modulus of elasticity (Eqn. 6.2). Many bridges exhibit some degree of composite action even when they are not constructed with shear studs or other devices for transferring shear between girders and deck slab. The composite and non-composite section moduli were used to calculate the measured bending moments. The use of composite section modulus yields a higher measured bending moment.

The second method (Method II) is based on the assumption that the sum of internal bending moments in the girders is equal to the externally applied bending moment due to the wheel loads. When all traffic lanes are loaded with equal-weight trucks, the measured wheel load distribution factor can be calculated by Eqn. 6.3. This assumption is valid for straight bridges. However, this assumption is not accurate for bridges with large skew angles, which exhibit larger torsional moments. Therefore, the sum of the girder strains in a straight bridge of the same span can be used to take into account the total external load effects in skew bridges (Eqn. 6.4).

The load distribution factors determined using method I are based on non-composite and composite section moduli of the slab-on-I-girder bridges (Table 6.3). The girder moments as well as the load distribution factors based on composite section modulus, are always greater than those based on non-composite section modulus. The wheel load distribution factors based on

method II are generally higher than those from method I and closer to the values based on the AASHTO and LRFD methods. Thus, it appears that the method II presented in section 6.4 can be used in computing realistic wheel load distribution factors for slab-on-girder bridges. Method II requires only the bottom flange strains or girder deflections in the computations of load distribution factors, whereas method I requires the estimation of the section modulus (composite or non-composite) and concrete modulus of elasticity besides the strains for an existing bridge. The wheel load distribution factors based on AASHTO and LRFD codes are generally higher than those based on measured and computed strains.

REFERENCES

1. Abendroth, R. E., Klaiber, F. W., and Shafer, M. W., "Diaphragm effectiveness in prestressed-concrete girder bridges", *Journal of Structural Engineering*, ASCE, Vol. 121, No. 9, September 1995, pp. 1362-1369.
2. ANSYS, Swanson Analysis System, Inc., Houston, PA 15342-0065, 1992. 3. Arockiasamy, M. and Amer, A., " Load distribution on highway bridges based on field test data", Final Report, HPR Study No. 0668, Submitted to Florida Department of Transportation, April 1995.
4. Arockiasamy, M. and Amer, A., " Load distribution on highway bridges based on field test data", Final Report, HPR Study No. 0668, Submitted to Florida Department of Transportation, April 1995.
5. Cheung, M.S., Jategaonkar, R., and Jaeger, L.G., "Effects of intermediate diaphragms in distributing live loads in beam-and-slab bridges", *Can. J. Civil Engineering*, Ottawa, Canada, Vol. 13, no. 8, pp 278-292, 1986.
6. Heins, C. P. and Lawrie, R. A.; "Design of modern concrete highway bridges", John Wiley & Sons, Inc., 1984.
7. Khaleel, M.A. and Itani, R.Y., "Live-load moments for continuous skew bridges", *J. of Structural Engineering*, Vol. 116, No. 9, Sept. 1990.

8. Sithichaikasem, S., and Gamble, W.L., "Effects of diaphragms in bridges with prestressed concrete I-section girders", Civil Engineering Studies No. 383, Univ. of Illinois at Urbana-Champagin, Urbana, Ill., 1972.
9. Stallings, J.M. and Yoo, CH.," Tests and ratings of short span steel bridges", Journal of Structural Engineering, Vol. 119, No. 7, July, 1993.
10. Wong, A Y. C., Gamble, W. L., " Effects of diaphragms in continuous slab and girder highway bridges" Civil Engineering Studies, Structural Research Series no. 391, University of Illinois at Urbana-Champaign, Urbana, Ill., 1973.
11. "Distribution of wheel loads on highway bridges" National Cooperative Highway Research Program (NCHRP), Transportation Research Board (TRB) No. 187(5), pp 1-31, 1992.
12. "Guide specifications for strength evaluation of existing steel and concrete bridges", American Association of State Highways and Transportation Officials, (AASHTO), Washington, D.C., 1989.
13. "Standard specifications for highway bridges", 14th Ed., American Association of State Highways and Transportation Officials, (AASHTO), Washington, D.C., 1992,
14. "AASHTO LRFD bridge design specifications", American Association of State Highways and Transportation Officials, Washington, D.C., First Edition, 1994.
15. "Guide specifications for strength evaluation of existing steel and concrete bridges", AASHTO, Washington, D.C., 1989.
16. "Manual for maintenance inspection of bridges", AASHTO, Washington, D.C., 1982